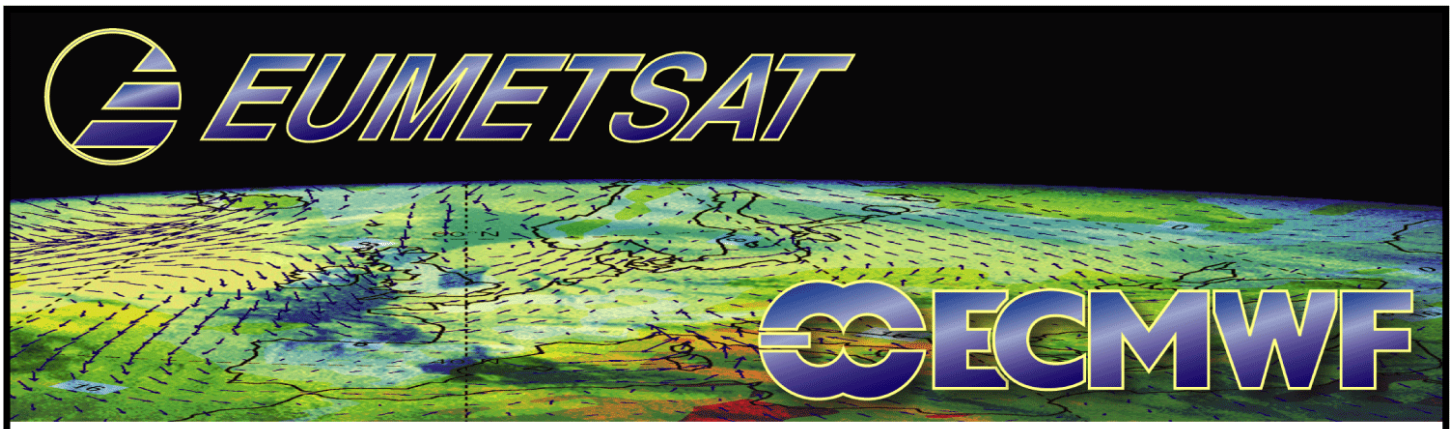

EUMETSAT / ECMWF Report Series
Final report SOW EUM.MET.SOW.04.0290

Evaluation of the impact of the space component of the Global Observing System through Observing System Experiments

Graeme Kelly and Jean-Noël Thépaut

October 2007

Series: EUMETSAT/ECMWF Reports

A full list of ECMWF Publications can be found on our web site under:
http://www.ecmwf.int/publications/

For additional copies please contact: library@ecmwf.int

European Centre for Medium Range Weather Forecasts
Shinfield Park, Reading, RG2 9AX, England

Table of contents

1. Introduction

As many more satellite instruments (both active and passive) became operational the challenge was, and still is, how to assimilate these space measurements together with all the conventional measurements. Figure 1 shows most of the current and near future satellite sensors used or soon to be used. Since 2001 the number of satellite sensors being used has increased by a factor of four and now is in excess of forty sensors. A recent example of the number of observations, mostly satellite radiances, used in the operational data assimilation at ECMWF during a 12-hour period is given in Table 1. Complex data processing techniques are employed to assimilate all these observations in a timely manner.

A study, sponsored by EUMETSAT, has been carried out to evaluate the impact of the space component of the Global Observing System through Observing System Experiments. In this study the relative contributions of the various space observing systems have been assessed within the context of the ECMWF data assimilation system. It is found that all the space based sensors generally contribute in a positive way to the overall improvement of the ECMWF forecast system.

	Screening		Used in Analysis	
SYNOP	421,000	0.43%	64,000	1.94%
Aircraft reports	519,000	0.53%	247,000	7.53%
DRIBU	24,000	0.02%	6,000	0.18%
TEMP	152,000	0.16%	75,000	2.28%
PILOT	119,000	0.12%	57,000	1.75%
AMVs	4,272,000	4.37%	131,000	3.99%
Radiance data	91,786,000	93.91%	2,508,000	76.46%
Scatterometer winds	274,000	0.28%	118,000	3.61%
GPS radio occultation	167,000	0.17%	73,000	2.24%
TOTAL	97,734,000	100.00%	3,280,000	100.00%

Table 1: Observation data count for one 12 hour 4D-Var cycle for 0900–2100 UTC on 24 April 2007. 'Screening' refers to the actual amount of data presented to 4D-Var and the 'Used in Analysis' indicates the amount of data used during the analysis minimization.

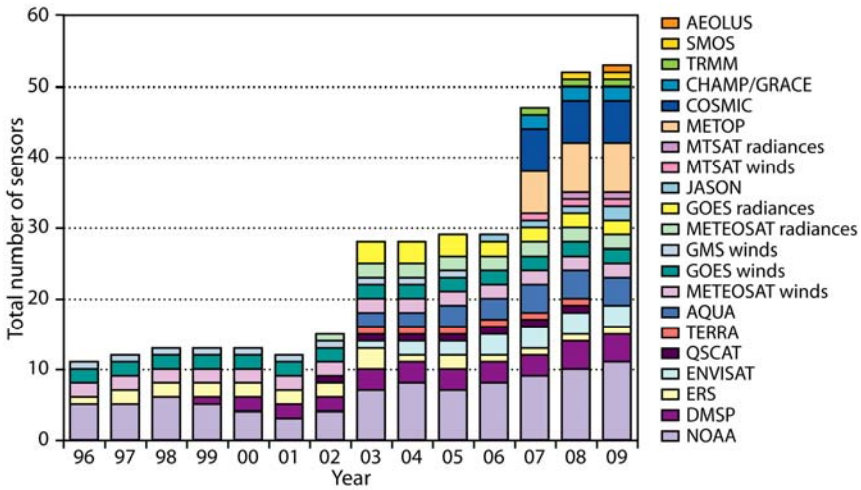

Figure 1: Number of satellite sensors that are or will be soon assimilated in the ECMWF operational data assimilation.

2. Requirement for Observing System Studies

At its meeting at ECMWF on 3 May 2003, the EUCOS Scientific Advisory Team discussed the need to investigate the interdependencies between the space-based and terrestrial components of the observing system. It was suggested that such an investigation could be based on a set of carefully designed Observing System Experiments (OSEs). These studies would be designed to provide guidance on the future development of the terrestrial observing system in view of the increasing capabilities of the satellite observing systems provided by the meteorological space agencies.

In recent years, several NWP centres have demonstrated substantial benefit from the assimilation of, for example, ATOVS radiances and scatterometer winds (referred to hereafter as SCAT). Since 2003 data has become available from second-generation radiometers (AIRS on Aqua in 2003 and IASI on MetOp in 2007) providing significantly enhanced temperature and humidity sounding capabilities – to be followed (in the five to ten year time frame) by similar instruments on the operational NPOESS series of satellites.

It was agreed that, as far as EUCOS is concerned, the primary issues were:

- What are the relative contributions of various components of the terrestrial observing system within the current overall composite observing system?
- How should the terrestrial systems evolve over the next five to ten years and beyond to complement the projected evolution of the space-based observing systems?

This led to a proposal from Andersson et al. (2004) to carry out a set of OSEs specifically designed to evaluate the role of the terrestrial component of the Global Observing System.

Following a number of discussions between EUMETSAT, ECMWF and EUCOS, it was agreed that specific OSEs dedicated to examining the various contributions of the different components of the space observing system were necessary to complement the original proposal about the terrestrial components. Taking this approach would provide a comprehensive assessment of the space/terrestrial links. It was also agreed that the robustness of this combined assessment would be strengthened by the adoption of similar strategies for experimentation and validation of the two studies.

These studies also take onboard one of the outcomes of the Third WMO Workshop on the Impact of Various Observing Systems on NWP. This suggested that, due to a large degree of redundancy of the Global Observing System (GOS), performing impact studies by removing one element of the GOS can show very limited impact and does not necessarily highlight the intrinsic benefit of the element in question. It was therefore decided that the scenarios in which the contributions of different elements of the GOS are investigated would be based on adding datasets or combination of datasets to a reference.

This article will deal with the relative contributions of the various space observing systems which have been assessed within the context of the ECMWF data assimilation system. The results of the complementary study concerning the contributions from various terrestrial observing systems are summarised in Appendix 1.

3. Past OSEs (1996–2003) with satellite data

Three sets of OSEs were run at ECMWF soon after the introduction of 3D-Var in 1996 (Kelly, 1997), after the operational implementation of 4D-Var in 2000 (Bouttier & Kelly, 2001), and later in 2003 (Kelly et al., 2004). For each set of OSEs there were four scenarios considered.

- CONTROL: For each set of OSEs the model cycle closest to the operational system at that time was used.
- NOAIREP: All aircraft measurements (wind and temperature) removed.
- NOUPPER: All TEMP, PILOT and PROFILER reports removed.
- NOSAT: All satellite data removed (the terrestrial network used in operations).

As well as conventional observations (TEMP, PILOT, PROFILER, AIREPS, SYNOP, PAOBS and BUOY reports), the 2003 OSEs included data from:

- Three AMSU-A/B and two HIRS instruments from the NOAA satellites.
- Five geostationary satellites and one polar orbiter (Terra) providing Atmospheric Motion Vectors.
- Three geostationary satellites providing clear-sky water-vapour radiances (CSRs).
- Three SSMI instruments from the DMSP platforms.
- Seawinds instrument from Quikscat.

The results from the three sets of OSEs are summarized in Figures 2 and 3. In a nutshell, they show that satellite data has progressively become the most important data source in both hemispheres, transcending even the conventional upper-air network in the northern hemisphere in the last set of OSEs.

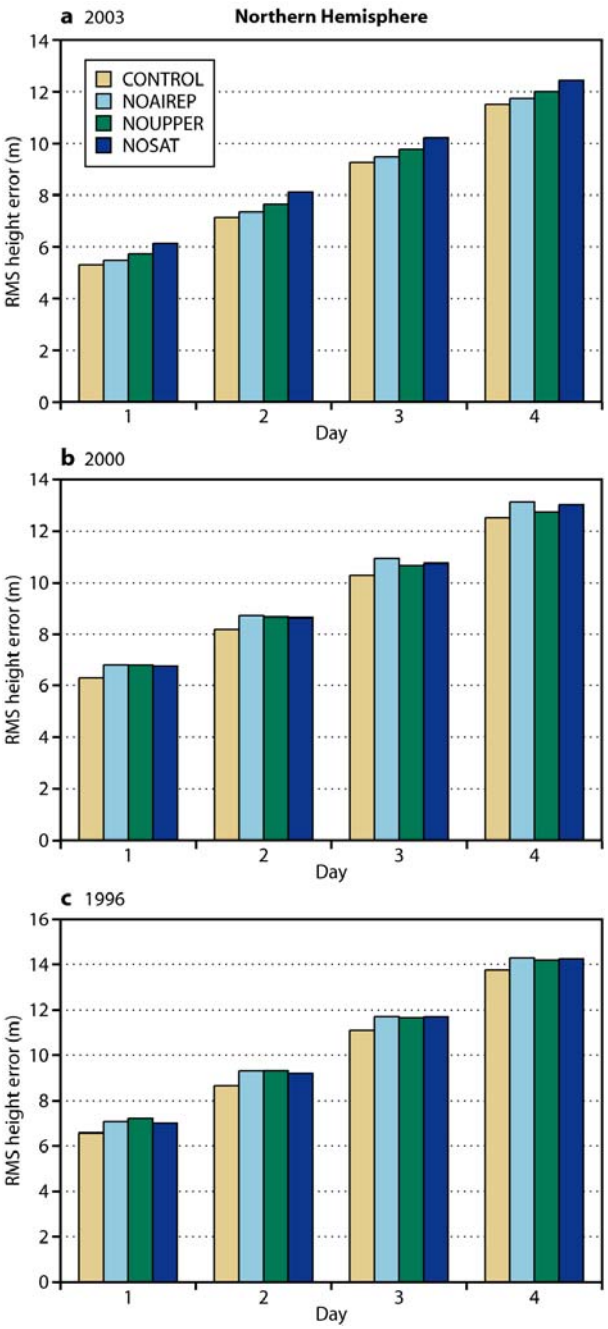

Figure 2: Comparison of three OSEs in the northern hemisphere for the rms error of the 500 hPa geopotential height for (a) 2003, (b) 2000 and (c) 1996.

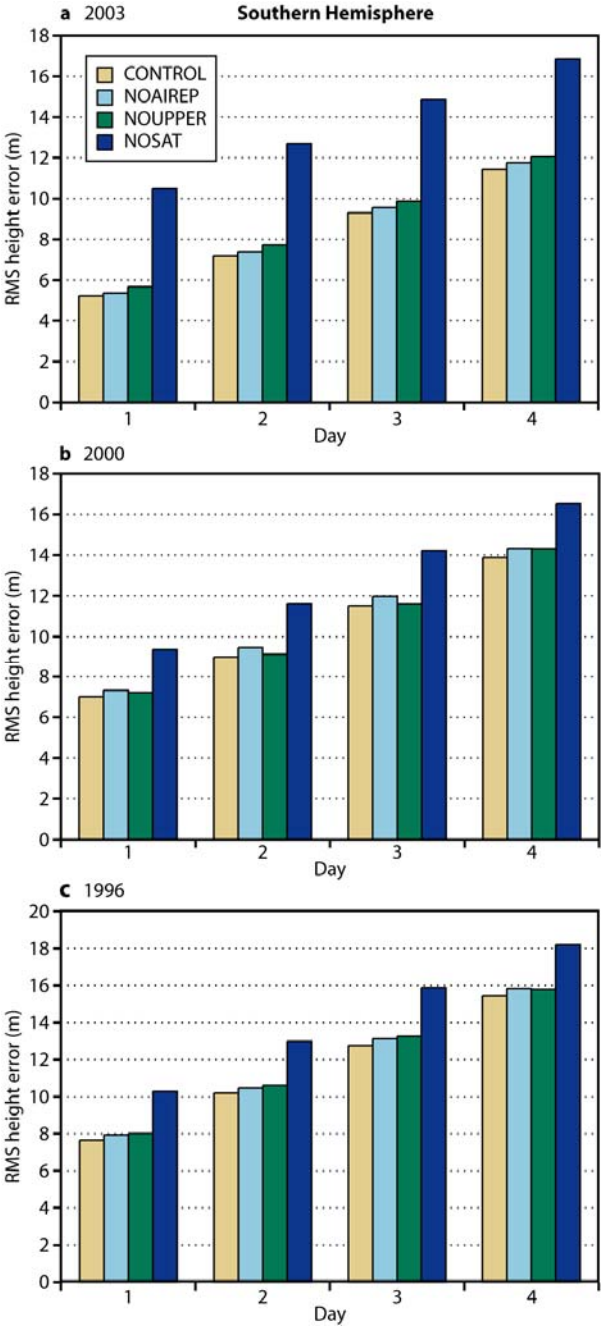

Figure 3: Comparison of three OSEs in the southern hemisphere for the rms error of 500 hPa geopotential height for (a) 2003, (b) 2000 and (c) 1996.

4. Studies of the various space observing systems

We now consider the relative contributions of the various space observing systems (infrared temperature soundings, microwave temperature soundings, imagers, scatterometers, etc.) within the context of a more recent ECMWF data assimilation system.

4.1. Reference systems

We have assumed in this study that the current conventional observing system is maintained (thereafter called the BASELINE system), and the main focus is to evaluate how specific satellite systems contribute individually to the robustness of the GOS, in addition to this degraded observing network.

The evaluation of satellite sensors is best done in the tropics and southern hemisphere, but the quality of the BASELINE system (equivalent to NOSAT referred to earlier) is so poor outside the northern hemisphere that it was not considered suitable as a reference by itself. Instead, two special reference systems have been designed to ensure a reasonable quality of the atmospheric analyses and forecasts in the tropics and southern hemisphere. These special reference systems are:

- AMV(REF): BASELINE plus the Atmospheric Motion Vectors (AMVs).
- AMSUA(REF): BASELINE plus data from one AMSU-A instrument.

4.1.1. Experimental setup

The data assimilation framework used for all the OSEs corresponds to the system that was used in operations close to the time of the periods under investigation. The main characteristics of the data assimilation system are given in Appendix 2.

The experiments were carried out for two periods, each covering a winter and summer.

- Period 1. Winter from 4 December 2004 until 25 January 2005 and summer from 17 July to 15 September 2005 using IFS Cy29r1 and Cy29r2 respectively. For this period, the OSEs were based on AMV(REF) as a reference.
- Period 2. Winter from 5 December 2006 to 14 Feb-ruary 2007 and summer from 1 June to 18 August 2006 using IFS Cy31r1. For this period, the OSEs were based on AMSUA(REF) as a reference.

All forecasts were run from 00 UTC.

4.1.2. Standard experiments

Two sets of assimilation were performed.

- AMV(REF) as reference for Period 1. The observational scenarios tested with AMVs as reference (i.e. AMV(REF)) are described in Table 2. These experiments are based on the winter and summer forming Period 1. The first ten days of each assimilation scenario are excluded from the verification to ensure a reasonable warm-up phase. No real difference in the impact was found between summer and winter so the mean scores are combined to give a sample of 89 days for each experiment. All experiments are validated using the operational analysis.
- AMSUA(REF) as reference for Period 2. The observational scenarios tested with one AMSU-A as reference (i.e. AMSUA(REF)) are described in Table 3. These experiments are based on the winter

and summer forming Period 2. These experiments were delayed as long as possible in order to make use of the AMSU-A and MHS instruments from the EUMETSAT MetOp satellite. The first two weeks are excluded from the verification to ensure a reasonable warm-up phase for each assimilation scenario. For Period 2, the Variational Bias Correction for satellite radiances was operational and therefore activated during the warm-up phase of the experiments (bias correction coefficients are then kept constant for the remaining of the assimilation period). No real difference in the impact was found between summer and winter so the mean scores are combined to give a sample of 117 days for each experiment. All experiments are validated using the operational analysis.

Experiment	Datasets
BASELINE	All conventional observations used in NWP (radiosonde + aircraft + profiler network + surface land data + buoy observations + ship data)
AMV(REF)	*BASELINE* + AMVs from GEO & MODIS
AMV(REF)+HIRS	*AMV(REF)* + HIRS radiances
AMV(REF)+AMSUA	*AMV(REF)* + AMSU-A radiances
AMV(REF)+AMSUB	*AMV(REF)* + AMSU-B radiances
AMV(REF)+SSMI	*AMV(REF)* + SSMI radiances
AMV(REF)+CSRs	*AMV(REF)* + CSRs (Clear Sky Radiances) from GEO
AMV(REF)+AIRS	*AMV(REF)* + AIRS radiances
AMV(REF)+SCAT	*AMV(REF)* + SCAT winds
CONTROL	Full operational system (all the observations)

Table 2: Observational scenarios tested with AMV(REF) (BASELINE plus AMVs from GEO and MODIS) as reference for Period 1.

Experiment	Datasets
BASELINE	All conventional observations used in NWP (radiosonde + aircraft + profiler network + surface land data + buoy observations + ship data)
AMSUA(REF)	*BASELINE* + AMSU-A radiances from NOAA-16
AMSUA(REF)+AMVs	*AMSUA(REF)* + AMVs from GEO & MODIS
AMSUA(REF)+AMSUA	*AMSUA(REF)* + AMSU-A radiances
AMSUA(REF)+AMSUB	*AMSUA(REF)* + AMSU-B radiances
AMSUA(REF)+CSRs	*AMSUA(REF)* + CSRs (Clear Sky Radiances) from GEO
AMSUA(REF)+AIRS	*AMSUA(REF)* + AIRS radiances
AMSUA(REF)+SCAT	*AMSUA(REF)* + SCAT winds
CONTROL	Full operational system (all the observations)

Table 3: Observational scenarios tested with AMSUA(REF) (BASELINE plus AMSU-A from NOAA-16) as reference for Period 2.

4.1.3. Additional experiments

During the course of the study two additional sets of experiments using AMV(REF) and AMSUA(REF) have been carried out to specifically assess the impact of MODIS and AVHRR AMVs, the impact of various AIRS channel combinations (as a scientific preparation for the assimilation of IASI), and finally the respective contribution of clear and cloud/rain effected SSMI radiances.

The experiments using AMV(REF) are as follows.

- Polar wind impact: An experiment evaluating the impact of the MODIS winds by removing those winds from AMV(REF).
- Temperature and humidity impact: An experiment adding AMSU-A and AMSU-B data to AMV(REF) to assess their impact compared to that of AIRS data.

The following additional experiments have been conducted using AMSUA(REF) as a reference.

- Impact of various AIRS channel combinations: Four experiments (summer only) adding various combinations of AIRS channels. A data denial experiment has also been run by removing AIRS data from CONTROL.
- SSMI impact: Three experiments (summer only) adding SSMI (clear sky), SSMI(rainy) and SSMI(clear sky + rainy) data to the AMSUA(REF). In addition, two data denial experiment have also been run: removing SSMI(clear sky) and SSMI(rainy) data from CONTROL.
    - SSMI(clear sky) are those SSMI radiances considered to be not affected by cloud or rain using a regression based cloud liquid check.
    - SSMI(rainy) are those radiances that fail the previous cloud liquid test and pass the convergence test in the SSMI 1D-Var (Bauer et al., 2002, 2005a and 2005b).
- Polar wind impact: An experiment (winter only) adding each wind set to AMSUA(REF) to evaluate the impact of the MODIS and AVHRR winds.

5. Assimilation assessment

In order to assess the impact of each OSE several statistical quantities have been calculated for temperature, humidity and wind at various levels. These include anomaly correlations, mean rms errors, geographical maps of rms error differences and mean rms error differences along with statistical significance. All these quantities have been computed but only a small selection is shown here; the remainder will be contained in a comprehensive report to be delivered to EUMETSAT. Most results shown are for the southern hemisphere or tropics where the impact is largest. In the northern hemisphere the impact is generally similar but reduced.

As stated above, in the southern hemisphere and tropics the BASELINE assimilation (terrestrial observations only) is poor and not suitable as a reference. The addition to the BASELINE of either AMVs (geostationary and polar) or data from one AMSU-A instrument considerably improves the quality of the assimilation with the southern hemispheric forecast skill increasing by about two days at day 4.

Figure 4 shows the mean anomaly correlation at 500 hPa for the combined summer and winter assimilation sets of Period 1. The experiments are:

- BASELINE (NOSAT), AMV(REF) and CONTROL as described in Table 2.

- EUCOS(REF) which uses all satellite data and a reduced terrestrial network, i.e. the GCOS Upper Air Network (GUAN), GCOS Surface Network (GSN), and the buoys' network.

Figure 5 is similar to Figure 4 but for Period 2 and using AMSUA(REF) in place of AMV(REF). The EUCOS experiments have not been not run for this period.

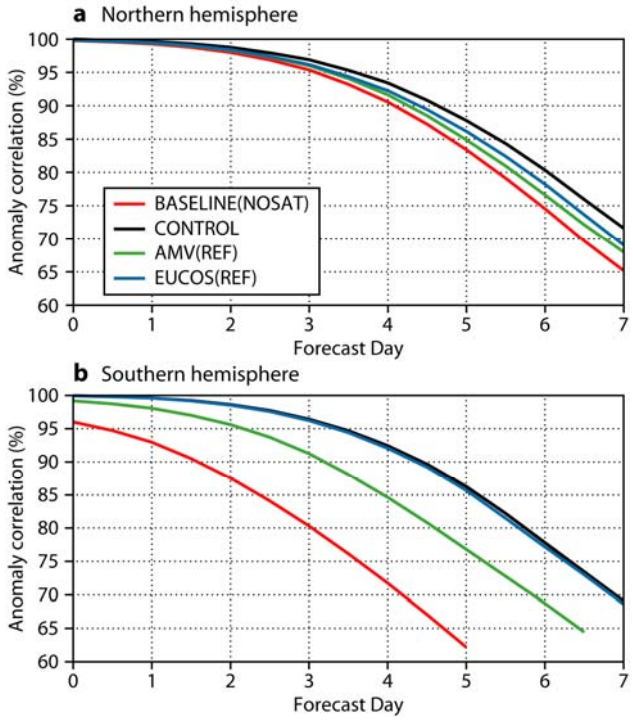

Figure 4: Comparison of EUCOS(REF) and AMV(REF) with BASELINE (NOSAT) and CONTROL for (a) northern hemisphere (20°–90°N) and (b) southern hemisphere (20°–90°S).

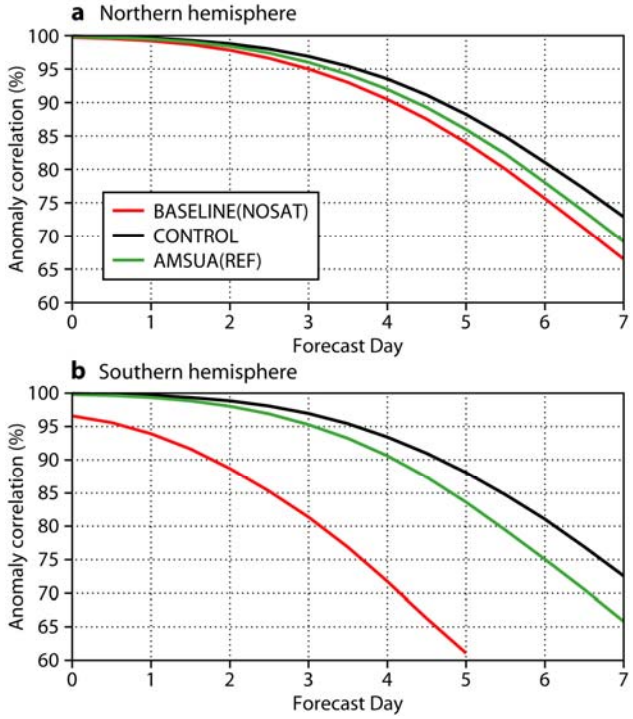

Figure 5: Comparison of AMSUA(REF) with BASELINE (NOSAT) and CONTROL for (a) northern hemisphere (20°–90°N) and (b) southern hemisphere (20°–90°S).

For the northern hemisphere all experiments reach day 6 before the anomaly correlation drops to 0.75; this indicates the forecasts are of general good quality. When the anomaly correlation drops below 0.6 the forecasts are considered poor. In the southern hemisphere the BASELINE assimilations for both Period 1 and Period 2 are poor; their anomaly correlations reach 0.6 soon after day 5.

EUCOS(REF) is also shown for comparison with the satellite references (see Appendix 2). With the addition of the remaining terrestrial observations the forecast improves by 8 hours at day 6 in the northern hemisphere. On the other hand, in the southern hemisphere, as expected, EUCOS(REF) is close to CONTROL.

Additional verification plots for 500 hPa geopotential height are displayed in appendix A.

6. Impact of sensors

To present the results of eleven sets of data assimilation experiment in a concise way is a somewhat daunting task. There are two sets of OSEs based on AMV(REF) and AMSUA(REF). There is also a variety of variables and levels used for evaluation: 500 hPa geopotential height, relative humidity at 850, 500 and 200 hPa, and wind at 1000 and 200 hPa.

The results have been condensed into a series of bar graphs containing all experiments. Generally the sensors are ranked in order of increasing rms error for the first verified forecast range. Usually this ranking is maintained throughout the forecast, though there are some exceptions.

Generally all sensors impact in a positive way on some parameters but some sensors have a neutral or slightly negative impact on other parameters. The small negative impact, mostly noticed on the 500 hPa geopotential height parameter and when using AMV(REF) as a reference, may be due to the fact that the accuracy of the AMV(REF) temperature field is still not quite good enough to assimilate radiances that are mostly sensitive to moisture. This negative impact of some sensors is not generally found when AMSUA(REF) is used as a reference instead.

6.1. 500 hPa geopotential height

The accuracy of the 500 hPa geopotential height forecast is an important and classical measure of forecast skill.

- OSEs based on AMV(REF). Figure 6 shows the performance of all the OSEs as described in Tables 2 at days 2, 5 and 7. The largest impact can be seen in the southern hemisphere and is maintained throughout the full forecast range. Clearly the most important sensors are AMSU-A and AIRS followed by HIRS. All other sensors have a relatively small impact; some sensors even show a small negative impact relative to AMV(REF) for this particular parameter. However, other scores are improved by these sensors (this is for example the case for the CSRs which improve the humidity scores). The impact in the northern hemisphere is similar to that in the southern hemisphere but smaller in magnitude.
- OSEs based on AMSUA(REF). The performance of all the OSE experiments as described in Table 3 at days 2, 5 and 7 is shown in Figure 7. First of all, it is worth noticing that the relative difference for 500 hPa geopotential height between AMSUA(REF) and CONTROL compared to the relative difference between AMV(REF) and its CONTROL is smaller, and therefore gives less margin to measure quantitatively the impact of individual sensors. However, the largest sensor impacts can still be seen in the southern hemisphere and these are maintained throughout the full forecast range. Clearly the most important sensors are AIRS and the AMSU-A/B combination. All other sensors

have a relatively small impact. In the northern hemisphere the impact of the sensors is similar but smaller in magnitude.

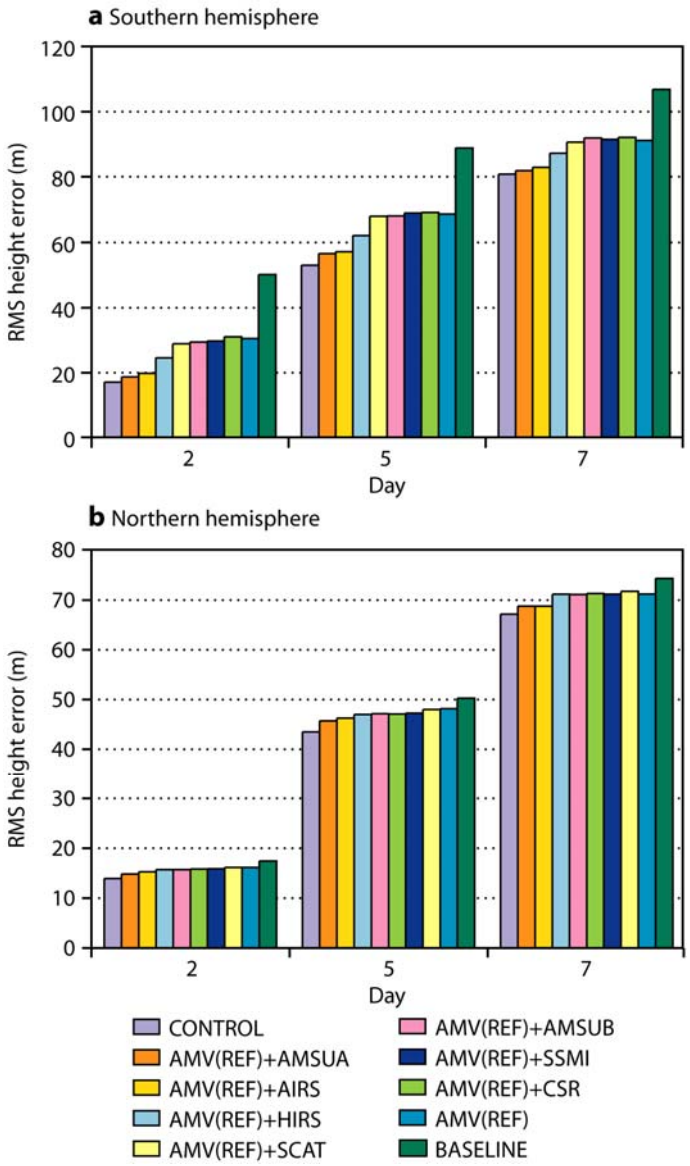

Figure 6: Impact of all sensors (based on AMV(REF) on 500 hPa geopotential height for (a) southern hemisphere (20°–90°S) and (b) northern hemisphere (20°–90°N).

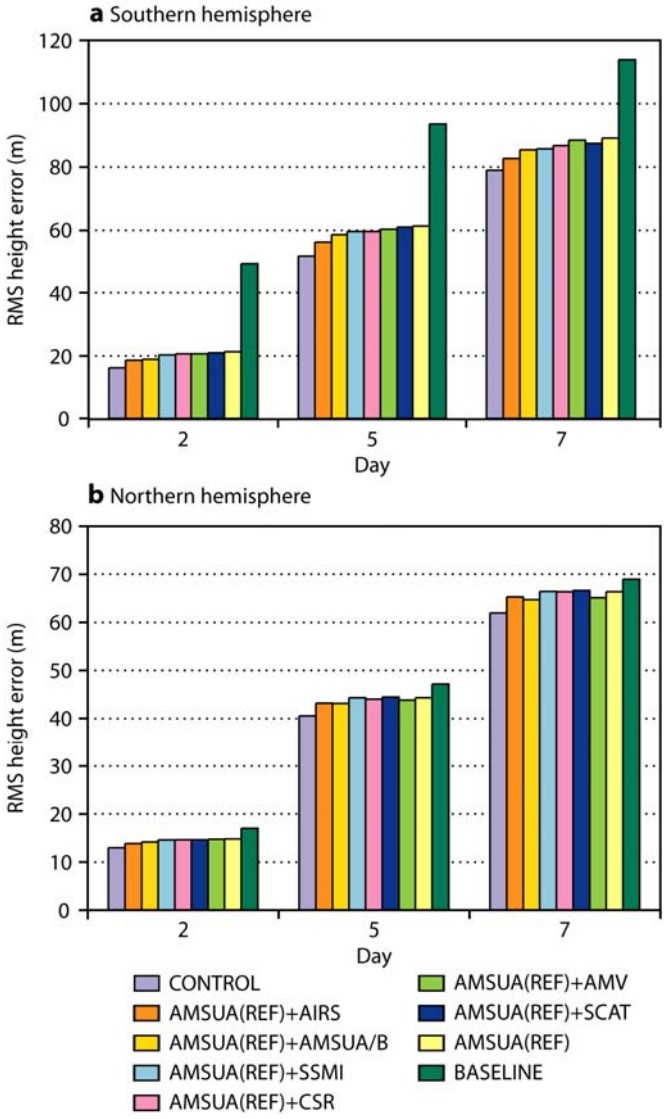

Figure 7: Impact of all sensors (based on AMSUA(REF)) on 500 hPa geopotential height for (a) southern hemisphere (20°–90°S) and (b) northern hemisphere (20°–90°N).

Additional verification plots for 500 hPa geopotential height are displayed in appendix A.

6.2. 850 hPa relative humidity

Moisture forecasts, particularly in the tropics, tend to be less accurate than forecasts of mid-latitude geopotential height. After day 4, the moisture forecast becomes less dependent on the initial moisture conditions and the model moisture processes dominate. For this reason all the moisture validations are presented for days 1 to 3.

- OSEs based on AMV(REF). Figure 8(a) shows the performance of all the OSEs as described in Table 2 for the tropics. SSMI is the most important sensor at day 1 but by day 3 the impact is reduced and overtaken by that of AIRS. However the gap between the CONTROL and the AMV(REF)+SSMI at day 1 is much larger than the difference between AMV(REF)+SSMI and AMV(REF) suggesting it is the combination of all sensors that is important rather than a single sensor. The impact in the northern hemisphere and southern hemisphere is similar to that in the tropics but smaller.

- OSEs based on AMSUA(REF). Figure 8(b) shows the performance of all the OSEs as described in Table 3 for the tropics where the impacts are the largest. In this set, AMSUA(REF)+SSMI now includes both clear-sky and rain/cloud affected radiances and SSMI is the most important sensor for low level humidity. How-ever there is still a gap between the CONTROL and AMSUA(REF)+SSMI, which again suggests that it is the combination of all sensors that is important for improving the moisture analysis and forecasts rather than a single sensor. The impact in the northern hemisphere and southern hemisphere is similar but smaller in magnitude than in the tropics.

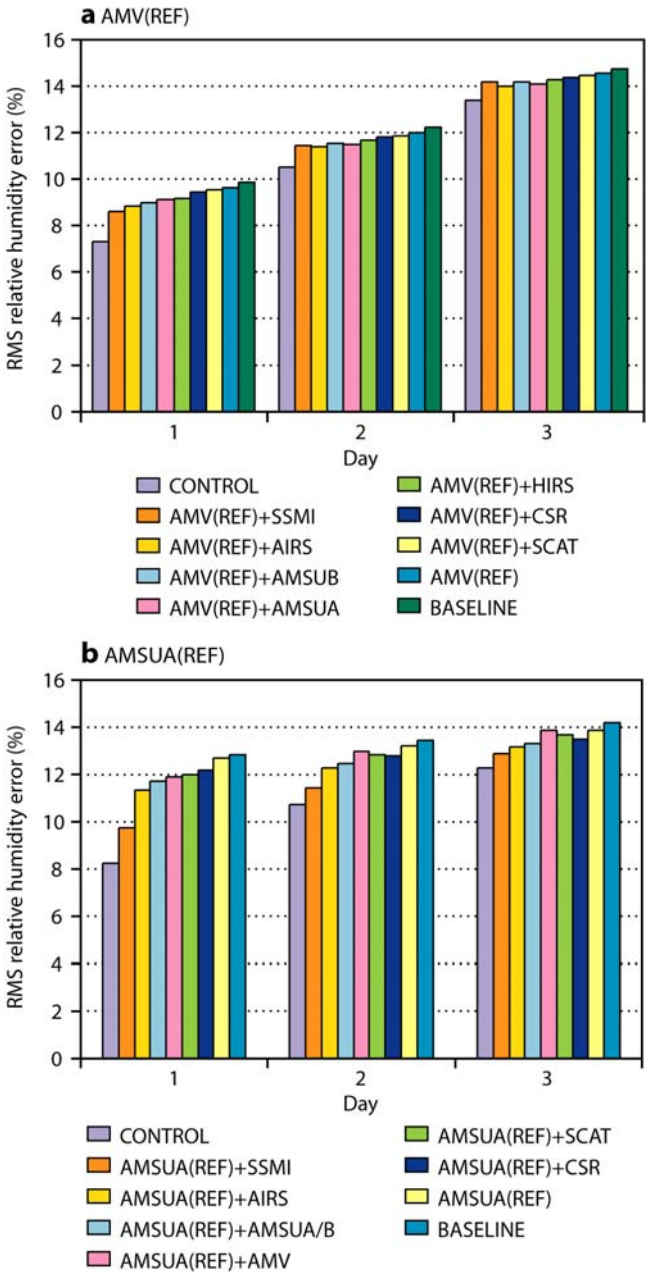

Figure 8: Impact of all sensors on 850 hPa relative humidity for the tropics based on (a) AMV(REF) and (b) AMSUA(REF).

Additional verification plots for 850,500 and 200 relative humidity are displayed in appendix (C).

6.3. 1000 hPa wind

Wind forecasts in the tropics tend to be less accurate than in mid latitudes. In the tropics after day 4 the model wind forecast becomes less dependent on the initial conditions. Therefore all the wind validations presented here are for days 1, 2 and 3.

OSEs based on AMV(REF). Figure 9(a) shows the performance of all the OSEs as described in Table 2. In the tropics SSMI is the most important sensor. However the gap between the AMV(REF)+SSMI and CONTROL at day 1 is much larger than the difference between AMV(REF)+SSMI and AMV(REF) suggesting again that it is the combination of all sensors that is important. The impact in the northern hemisphere and southern hemisphere is similar to that in the tropics but smaller in magnitude.

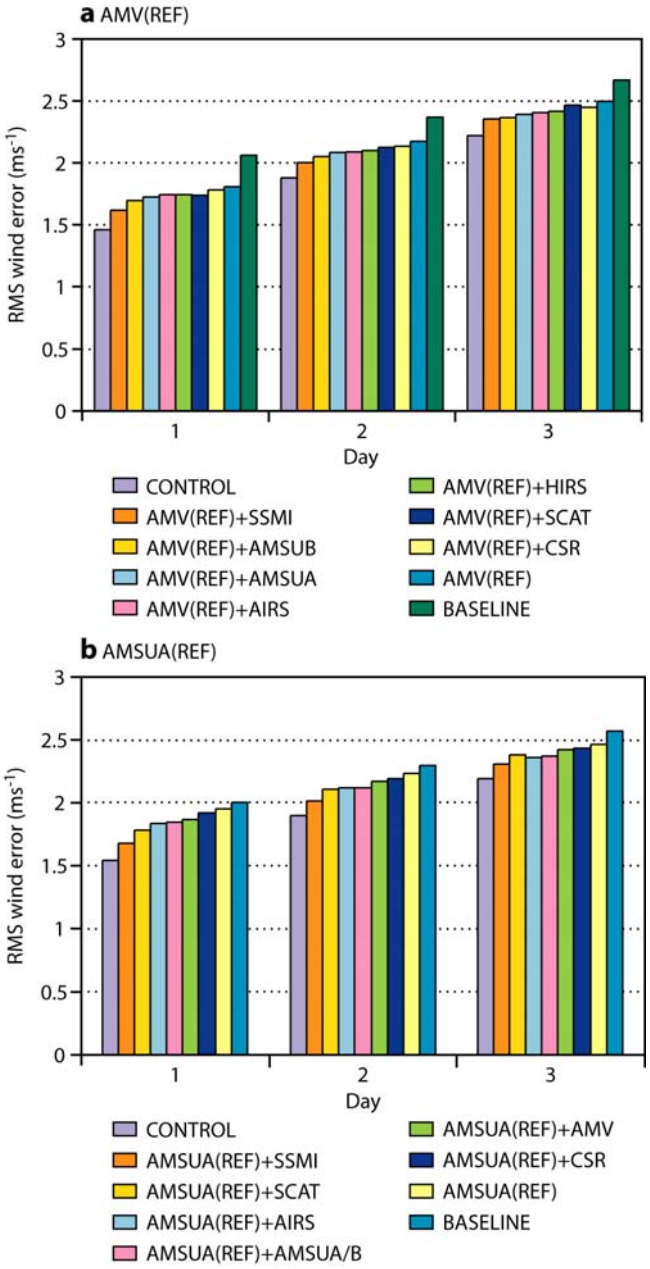

Figure 9: Impact of all sensors on 1000 hPa vector wind for the tropics based on (a) AMV(REF) and (b) AMSUA(REF).

OSEs based on AMSUA(REF). Figure 9(b) shows the performance all the OSEs as described in Table 3. In the tropics SSMI is the most important sensor, though SCAT winds are also important in the early part of the forecast. However the gap between the CONTROL and AMSUA(REF)+SSMI suggests it is the combination of all sensors that is important. The impact in the northern hemisphere and southern hemisphere is similar but smaller in magnitude to that in the tropics.

Additional verification plots for 1000 and 200 hPa wind are displayed in appendix D.

7. Impact of MODIS AMVs

An experiment was run to evaluate the impact of the MODIS AMVs. This experiment is identical to AMV(REF) but with the MODIS AMVs removed. One can see that the impact of these AMVs on the 500 hPa geopotential height is very positive in the southern hemisphere (Figure 10(a)) and northern hemisphere (Figure 10(b)). The AMVs are clearly very important for observing the polar flow.

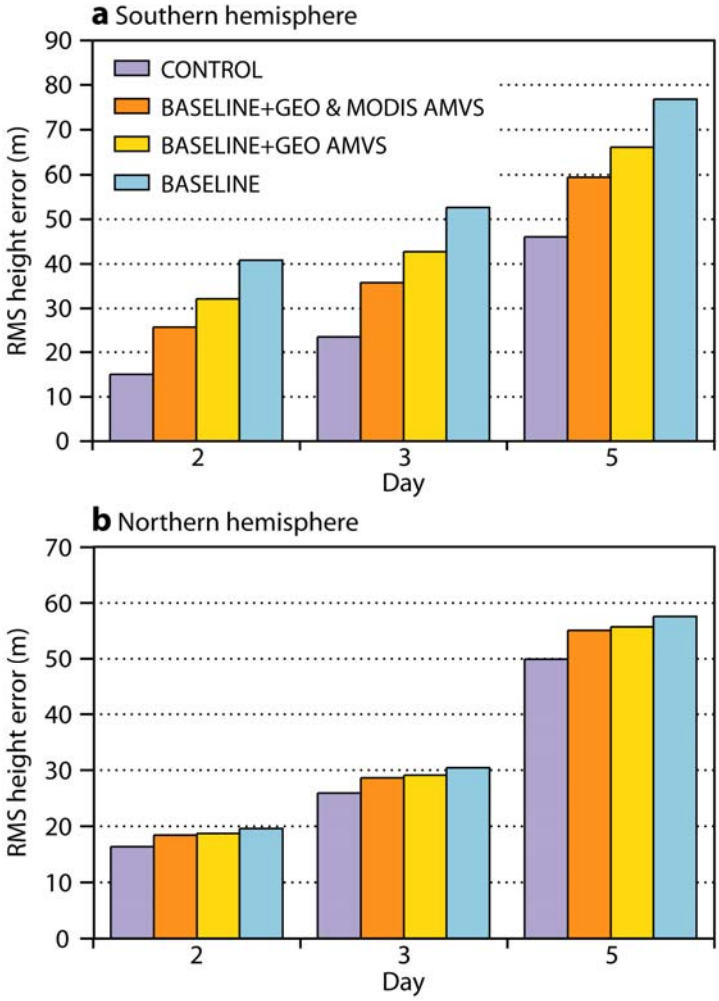

Figure 10: Impact of MODIS AMVs on 500 hPa geopotential height for (a) southern hemisphere (20°–90°S) and (b) northern hemisphere (20°–90°N).

Additional verification plots for 500 hPa geopotential are displayed in appendix E.

7.1. Comparison of AIRS with a combination of AMSU-A and AMSU-B

In the standard set of impact experiments using AMV (REF), Table 2, the AMV(REF)+AMSUA assimilation used all four AMSU-A instruments. This is a somewhat unfair comparison if one wants to directly compare the impact of AIRS data with that of AMSU-A. The AIRS channels used in the operational assimilation are mostly sensitive to temperature and moisture (McNally et al., 2004). A microwave assimilation experiment was therefore run adding one AMSU-A/B combination to the AMV(REF). This OSE was then compared with the AMV(REF)+AIRS assimilation referred to in Table 2. The results are shown in Figures 11(a) and 11(b).

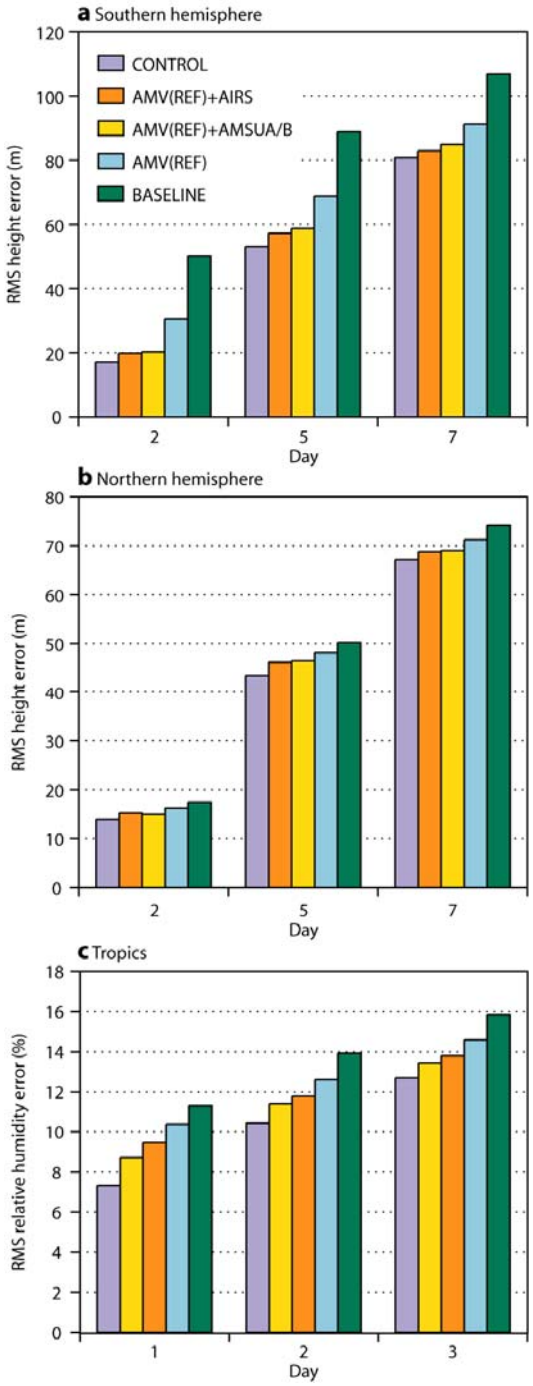

Figure 11: Comparison of AIRS with the two microwave instruments (AMSU-A and AMSU-B) on NOAA-16 for (a) 500 hPa geopotential height in the southern hemisphere, (b) 500 hPa geopotential height in the northern hemisphere and (c) 500 hPa relative humidity in the tropics.

In the southern hemisphere at day 2 the impact of AIRS and AMSU-A/B data on the geopotential height scores is similar but at days 5 and 7 the impact of the AIRS data becomes larger. However, the impact on tropical moisture, Figure 11(c), shows that AMSU-A/B data has a larger impact than AIRS in terms of the short-range forecast of tropical moisture.

Additional verification plots for 500 hPa geopotential and (500,200) relative humidity are displayed in appendix F.

7.2. Additional studies with AMSUA(REF)

7.2.1. AIRS channel combinations

For a number of reasons (including CPU time, memory size and file space constraints) the current operational system uses a reduced channel set for AIRS (and more recently IASI) radiances. The aim of this study was to explore which AIRS channels are the most important. Experiments have been run (summer only) by adding various AIRS channel combinations to the AMSUA(REF), and also denying AIRS data from CONTROL. The results are shown in Figure 12 for 500 hPa geopotential height in the southern hemisphere. The respective performance of each scenario is consistent throughout the forecast range up to day 5.

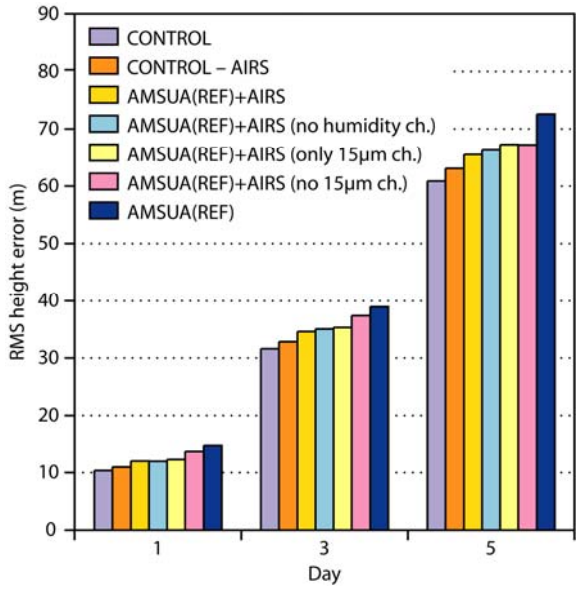

Figure 12: Comparison of the impact of various AIRS channel combinations on 500 hPa geopotential height based on AMSUA(REF).

When looking at the day 3 impact on the geopotential height at 500 hPa, one notices that:

- The positive impact of AIRS data can be seen from the differences between the data denial experiment and CONTROL. There is also a clear separation between AMSUA(REF) and AMSUA(REF)+AIRS.
- AMSUA(REF)+AIRS is close to the AIRS experiment not using humidity channels, indicating that AIRS humidity channels do not have a large effect on the geopotential height at 500 hPa.
- The fact that AMSUA(REF)+AIRS is close to the experiment using only the 15 micron channels from AIRS suggests that these channels contribute most to the impact of this instrument.

Additional verification plots for 500 hPa geopotential and relative humidity are displayed in appendix G.

7.2.2. Impact of the SSMI clear-sky and rain-affected radiances

In addition to the AMSUA(REF) plus all SSMI data (clear-sky and rain affected observations, Bauer et al., 2002, 2006a and 2006b), CONTROL (all data) and AMSUA(REF) the following experiments have been performed to separate the effects of clear-sky and rain-affected SSMI radiances:

- AMSUA(REF) plus SSMI rain affected radiances.
- AMSUA(REF) plus SSMI clear-sky radiance radiances.
- CONTROL minus all SSMI (clear-sky and rain-affected) radiances.

Figure 13 shows the impact of denying and adding SSMI radiances (in the various configurations explained above) on the 850 and 500 hPa relative humidity forecast scores. The rain-affected radiances contribute more to the moisture forecast skill at 500 hPa whereas the clear-sky radiances are more important at 850 hPa. The experiment that combines both SSMI radiance types further improves the forecast. It is therefore clear that both types for SSMI radiances are important for the global moisture analysis.

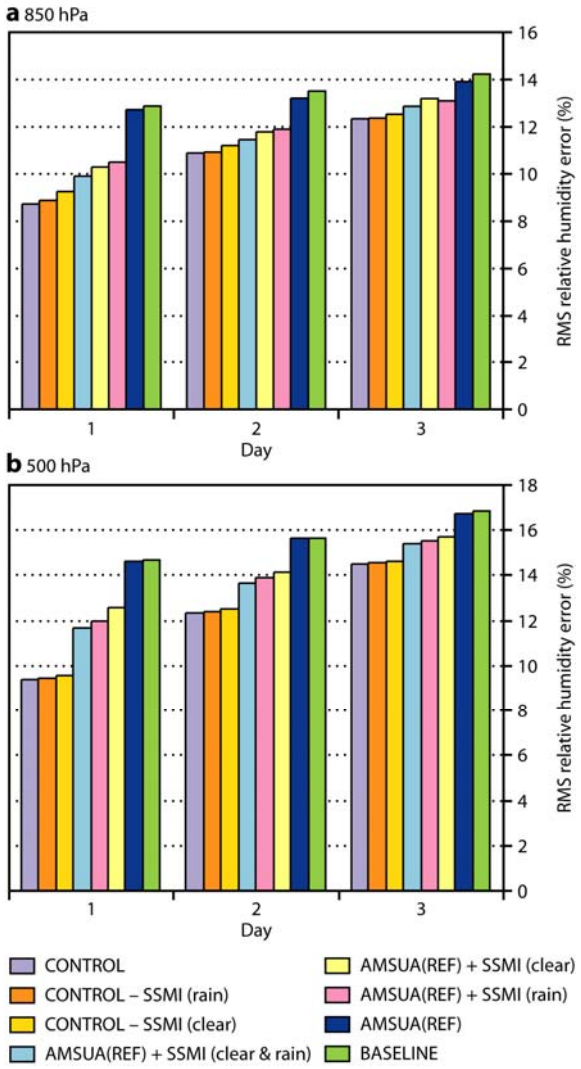

Figure 13: Comparison of the impact of various SSMI usage configurations based on AMSUA(REF) for (a) 850 hPa relative humidity and (b) 500 hPa relative humidity.

Additional verification plots for 850 and 500 hPa relative humidity are displayed in appendix H.

7.3. Impact of AVHRR AMVs

During the study, a new experimental AMV product became available from CIMSS and it was decided to evaluate them in this OSE framework. These AMVs are produced from overlapping orbits from the AVHRR imager onboard the NOAA polar satellite series. Unfortunately this instrument does not have a water vapour channel like MODIS and this greatly reduces the amount of AMVs produced, particularly over the polar ice. The impact on mean scores is small but positive and can be best seen on the mean geographical rms forecast error difference with AMSUA(REF) for the 500 hPa geopotential height (Figure 14(a)). Very little impact is found in the northern hemisphere. For comparison a similar plot is shown when MODIS AMVs are assimilated instead (Figure 14(b)). The impact from the MODIS AMVs is similar to that of AVHRR AMVs over the Southern Ocean but extends further to the south over the polar ice.

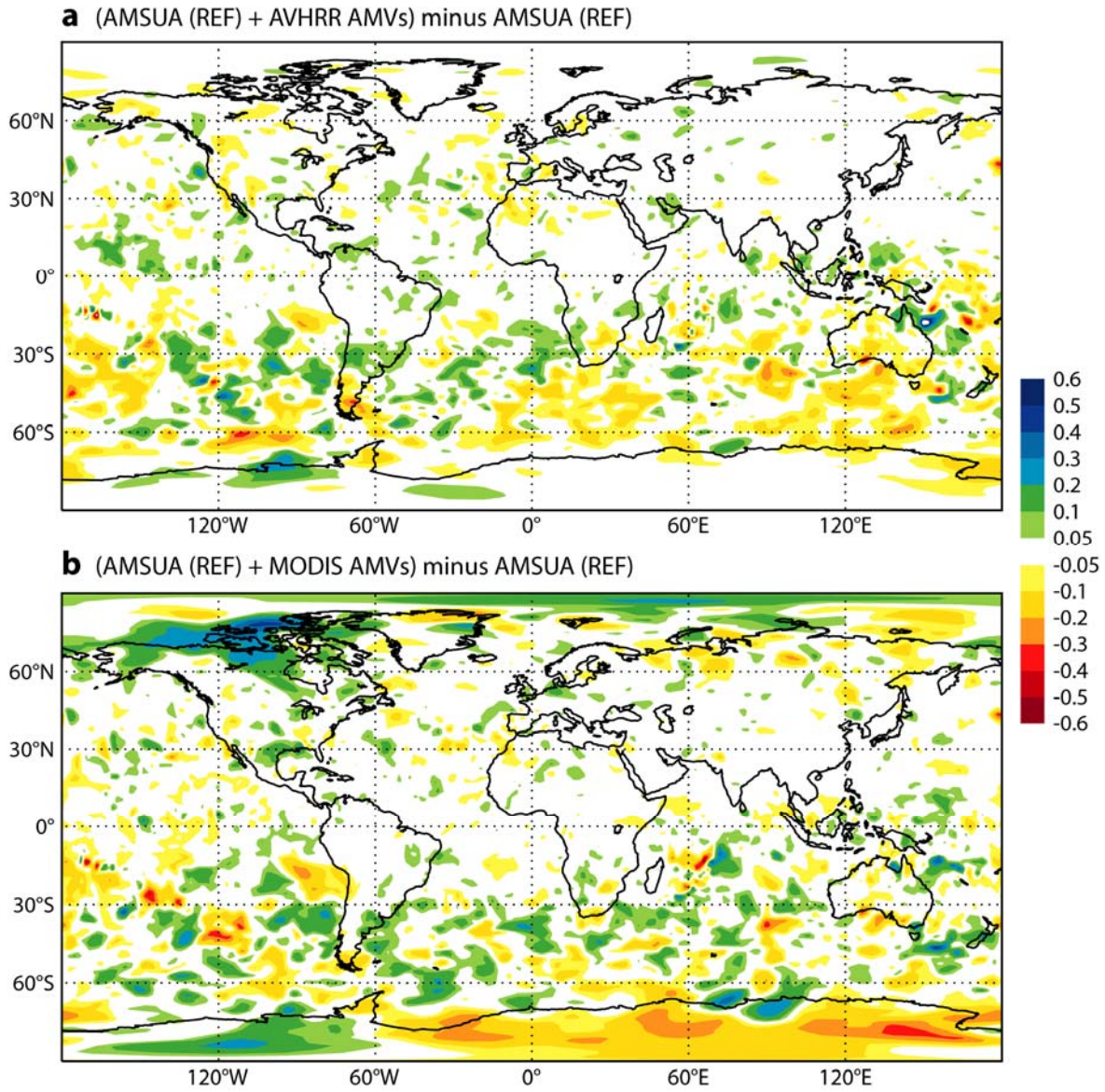

Figure 14: Mean normalized 48-hour forecast error difference between (a) AVHRR AMVs and AMSUA(REF), and (b) MODIS AMVs and AMSUA(REF) for the 500 hPa geopotential height.

Additional verification plots for 500 hPa wind are displayed in appendix I

7.4. Overall assessment and further prospects

All the space based sensors contribute in a positive way to the overall improvement of the ECMWF forecast system. Sensors like AMSU-A, AIRS and HIRS are clearly the most important for mass and wind forecasts. However the accuracy of the humidity forecast relies on AMSU-B/MHS, GEO CSRs and SSMI. The positive impact of AMVs (GEO and MODIS) and SCAT on the forecast is also clearly demonstrated.

At present, there are no plans to fly an instrument with MODIS-like water vapour channels on future polar satellites. This is a concern as the positive impact of MODIS AMVs in polar regions and mid-latitudes has clearly been demonstrated. The experiment using AVHRR derived AMVs show that their quality is similar to MODIS AMVs but the coverage is and will remain much poorer over the frozen regions due to a lack of water vapour channel on the instrument.

The studies also show that AIRS is the sensor that has the most impact on the mass field and experiments indicate that most of the impact comes from its 15 micron spectral band. Otherwise SSMI is vital for humidity analysis and the newly introduced cloud/rain effected SSMI radiances further improve the humidity analysis.

These experiments confirm the crucial impact of satellite data on the performance of the ECMWF NWP system. Since the completion of the OSEs, the importance of satellite data has further increased with, for example, the implementation of GPS radio-occultation observations or more recently the introduction of IASI. On the scientific side, further changes are expected in the near future that include the use of more infrared and microwave radiances in cloudy and rainy conditions, and an improved use of all types of satellite radiances over land and sea-ice.

8. References

Andersson, E., R. Dumelow, H. Huang, J.-N. Thépaut & A. Simmons, 2004: *Space/Terrestrial Link – Outline study proposal for consideration by EUCOS Management* (available from EUCOS Secretariat).

Andersson, E., J. Pailleux, J.-N. Thépaut, J.R. Eyre, A.P. McNally, G.A. Kelly & P. Courtier, 1994. Use of cloud-cleared radiances in three/four-dimensional variational data assimilation. *Q.J.R. Meteorol. Soc.*, **120**, 627–654.

Bauer, P., G. Kelly & E. Andersson, 2002: SSM/I radiance assimilation at ECMWF. In *Proc. ECMWF/GEWEX Workshop on Humidity Analysis*, Reading, United Kingdom, ECMWF, 167-175. Available from http://www.ecmwf.int/publications/

Bauer, P., P. Lopez, A. Benedetti, D. Salmond & E. Moreau, 2006a: Implementation of 1D+4D-Var assimilation of precipitation affected microwave radiances at ECMWF, Part I: 1D-Var. *Q.J.R. Meteorol. Soc.*, **132**, 2277–2306.

Bauer, P., P. Lopez, A. Benedetti, D. Salmond, S. Saarinen & M. Bonazzola, 2006b: Implementation of 1D+4D-Var assimilation of precipitation affected microwave radiances at ECMWF, Part II: 4D-Var. *Q.J.R. Meteorol. Soc.*, **132**, 2307-2332.

Bouttier, F. & G. Kelly, 2001: Observing-system experiments in the ECMWF 4D-Var data assimilation system. *Q.J.R. Meteorol. Soc.*, **127**, 1469–1488.

Kelly, G. 1997:Influence of observations on the operational ECMWF system. *Bulletin of WMO*, **46**, 336–341.

Kelly, G., A. McNally, J.-N. Thépaut & M. Szyndel, 2004. Observ-ing System Experiments of all main data types in the ECMWF operational system. In *Proc. of the Third WMO Workshop on the Impact of Various Observing Systems on NWP*, Alpbach, Austria, 9–12 March 2004.

McNally, A.P., P.D. Watts, J.A. Smith, R. Engelen, G. Kelly, J-N. Thépaut & M. Matricardi, 2004: The assimilation of AIRS radiance data at ECMW. In *Workshop on Assimilation of High Spectral Resolution Sounders in NWP*, 28 June-1 July 2004, Shinfield Park, Reading 73–88. Available from http://www.ecmwf.int/publications/

Thépaut, J.-N. & G.A. Kelly, 2007. Relative contributions from various terrestrial observing systems in the ECMWF NWP system. *Final Report EUCOS*, 23 June 2007 (available from EUCOS Secretariat).

Appendix 1: Terrestrial observing system studies (EUCOS)

The set of terrestrial observing system studies coordinated by EUCOS has been completed following the guidelines indicated in Andersson et al. (2004). These impact studies aimed to examine the various components of the terrestrial observing system, in the presence of the current satellite-based observing system. The experiments have been run using the same first winter and summer period used for the space observing system studies with the identical assimilation setup to enable a direct comparison with the space studies. The total number of cases remains probably too short to provide statistical robustness to the findings (especially over small areas such as Europe), but it is reassuring that the impact of the various components of the terrestrial observing system remains similar to the first order between the two assessed periods.

The main findings of the winter impact studies indicate a large impact of the radiosondes (wind and temperature) and aircrafts (wind and temperature), a marginal impact of radiosonde humidity information, and a neutral impact from the wind profilers. Sole wind or temperature information from radiosondes is not sufficient to impact noticeably on the forecast skill. In contrast, coupled temperature/wind information from radiosondes seems to provide a large and significant improvement in the forecasts well into the medium-range. The experiments demonstrate that observations from aircraft and radiosondes are complementary: each observing system improves the forecast skill even in the presence of the other.

The summer impact studies confirm most of the findings from the winter experiments, although the impact of the various assessed components of the GOS is smaller, both in absolute and relative terms (Thépaut & Kelly, 2007).

Appendix 2: Main characteristics of the data assimilation system

- T511L60 forecast model resolution
- 4D-Var assimilation with a 12-hour window and the analysis inner and out loop resolutions being T95/T159L60 and T511L60 respectively
- Conventional observations currently assimilated in the system include:
    - TEMP, PILOT and PROFILER reports
    - SYNOP, SHIP, METAR and BUOY (moored and drifters) reports
    - Aircrafts (AMDAR, AIREP, ACARS) including ascent/descent reports
- Satellite observations assimilated in the system for the atmospheric analysis were at that time for the winter run:
- Atmospheric Motion Vectors from GEO (Meteosat-5/7, GOES-9/10/12) and LEO (MODIS Terra and Aqua) platforms
- Clear-sky water vapour radiances from GEO (Meteosat-5/8, GOES-9/10/12)
- Level 1c infrared radiances from NOAA-14/17 (HIRS) and Aqua (AIRS)
- Level 1c microwave radiances from NOAA-15 (AMSU-A), NOAA-16 (AMSU-A and AMSU-B), NOAA-17 (AMSU-B), Aqua (AMSU-A) and DMSP 13/14/15 (SSM/I)
- Sea surface winds from scatterometers QuikScat and ERS-2
- Ozone products from NOAA-16 (SBUV) and ENVISAT (SCIAMACHY).

As this study has been spread over two years, different model cycles have been used for the two scenarios.

- Period 1. IFS model cycles Cy29r1 (winter) and Cy29r2 (summer) have been used, differing mainly by the inclusion of NOAA-18 level-1c radiances from AMSU-A and MHS and the blacklisting of NOAA-14 HIRS radiances that had become too noisy. AMV(REF) was used as a reference for Period 1.
- Period 2. IFS model cycle Cy31r1 has been used for both winter and summer. AMSUA(REF) was used as a reference for Period 2.

Appendix A

Reference assimilations. (REF(AMV) and REF(AMSUA)

Additional verification plots of rms error are provided to show the performance of the two reference assimilations.

(i) CONTROL minus BASELINE (NOSAT) for the *AMV(REF)*.

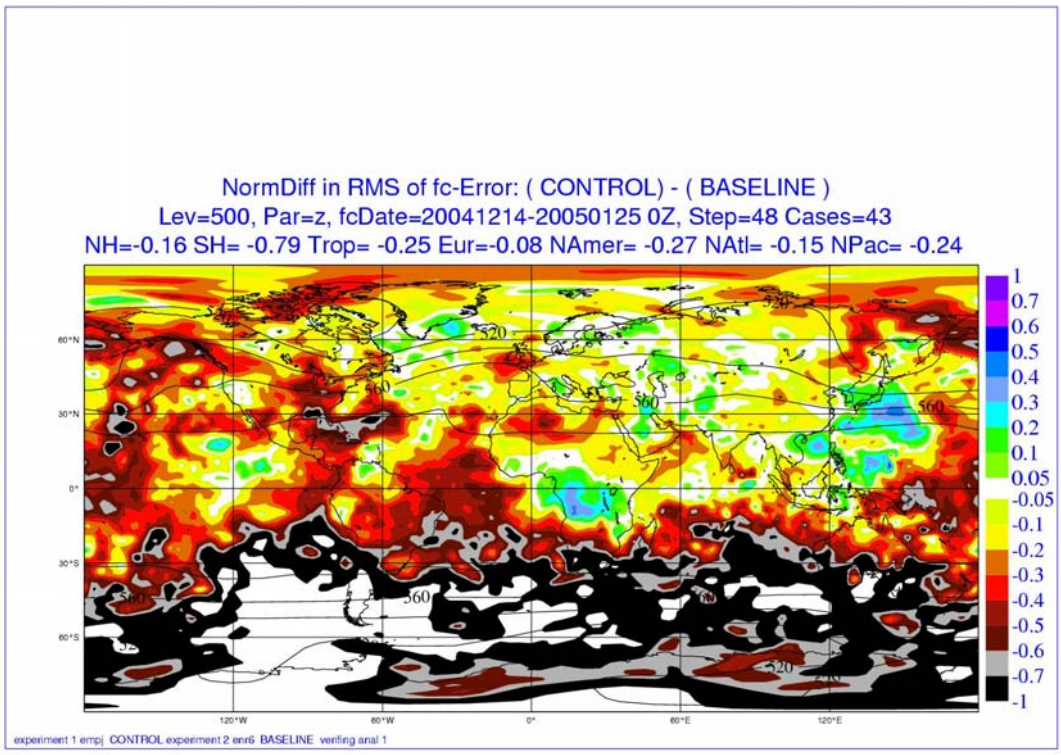

Figure A-1: Mean normalized 48-hour forecast error difference between CONTROL and BASELINE(NOSAT) for the 500 hPa geopotential height.

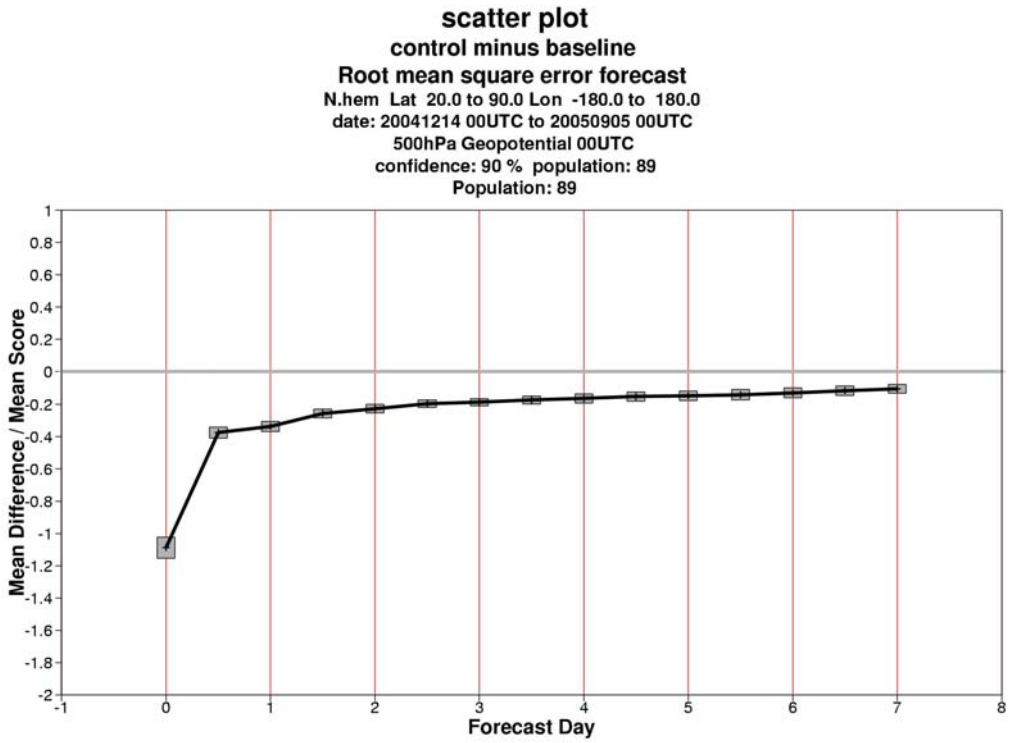

Figure A-2: Time series of normalized 500 hPa height rmse differences between CONTROL and BASELINE(NOSAT) for forecast errors up to day 7 in the Northern Hemisphere. Negative values indicate positive impact for the CONTROL.

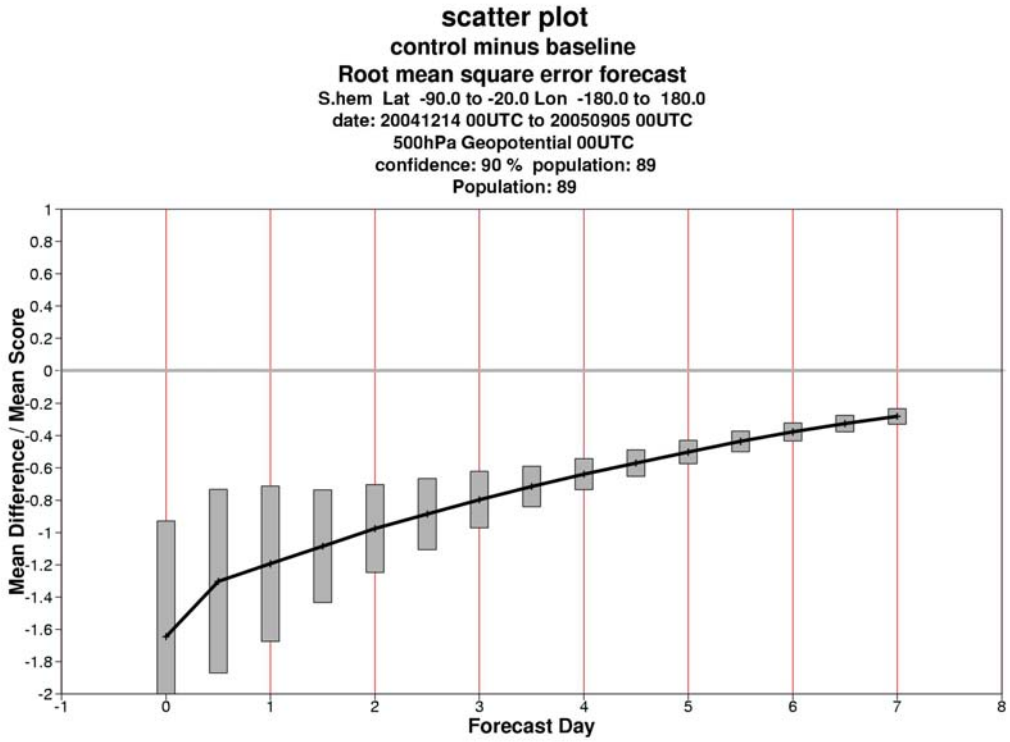

Figure A-3: AMV(REF) time series of normalized 500 hPa height rmse differences between CONTROL and BASELINE(NOSAT) for forecast errors up to day 7 in the Southern Hemisphere. Negative values show positive impact for the CONTROL.

(ii) CONTROL minus BASELINE (NOSAT) for the AMSUA(REF)

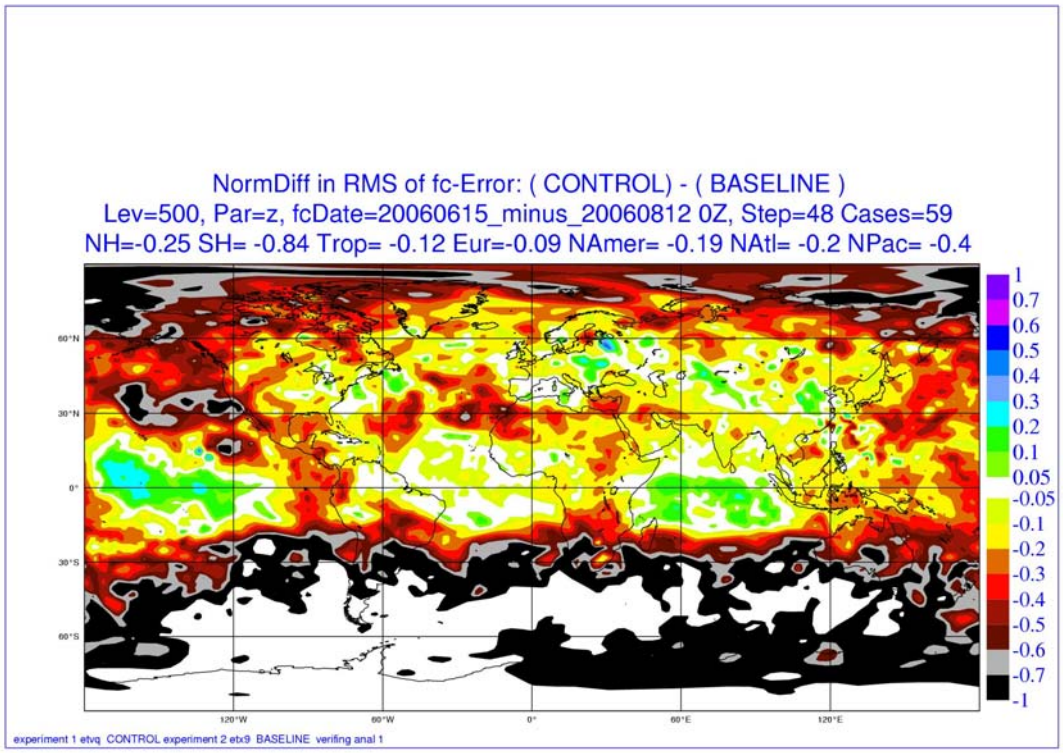

Figure A-4: Mean normalized 48-hour forecast error difference between CONTROL and BASELINE(NOSAT) for the 500 hPa geopotential height.

(iii) CONTROL minus *AMV(REF)*

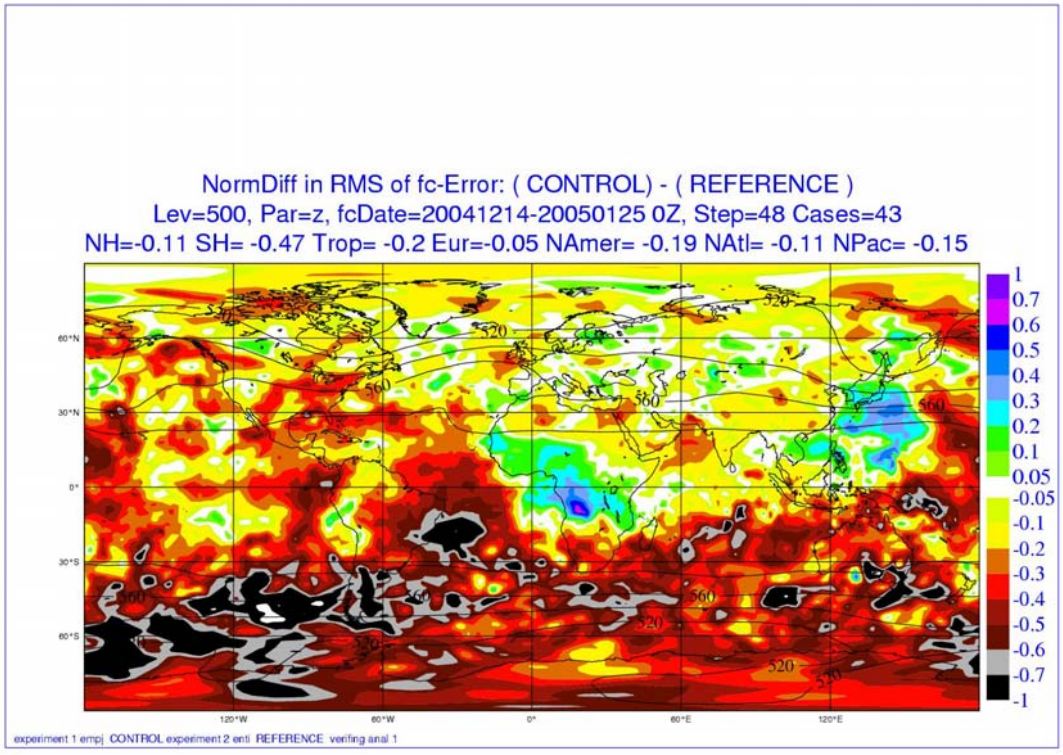

Figure A-5: Mean normalized 48-hour forecast error difference between CONTROL and AMV(REF) for the 500 hPa geopotential height..

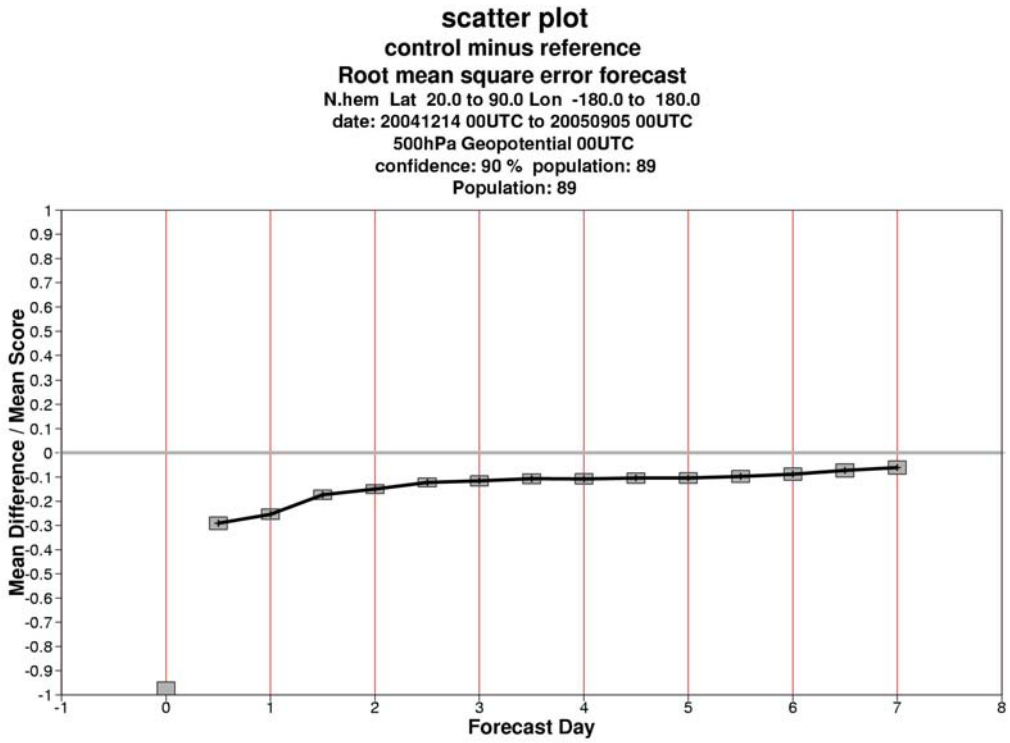

Figure A-6: AMV(REF) time series of normalized 500 hPa height rmse differences between CONTROL and AMV(REF) for forecast errors up to day 7 in the Southern Hemisphere. Negative values indicate positive impact for the CONTROL.

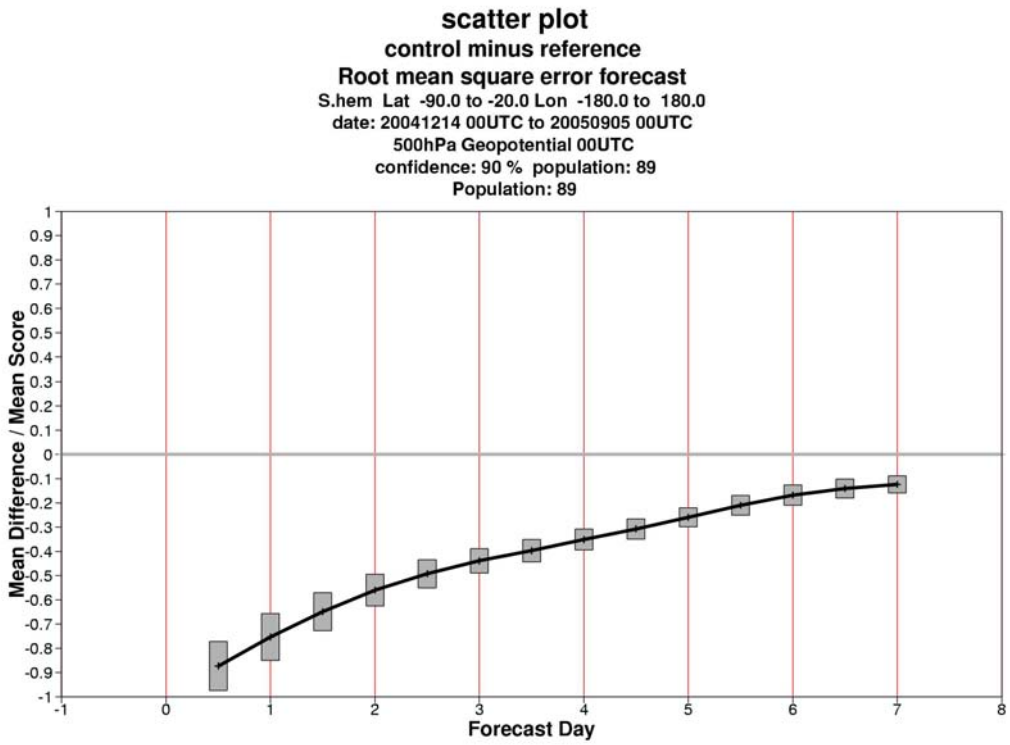

Figure A-7: AMV(REF) time series of normalized 500 hPa height rmse differences between CONTROL and AMV(REF) for forecast errors up to day 7 in the Southern Hemisphere. Negative values indicate positive impact for the CONTROL.

(iv) CONTROL minus AMSUA(REF)

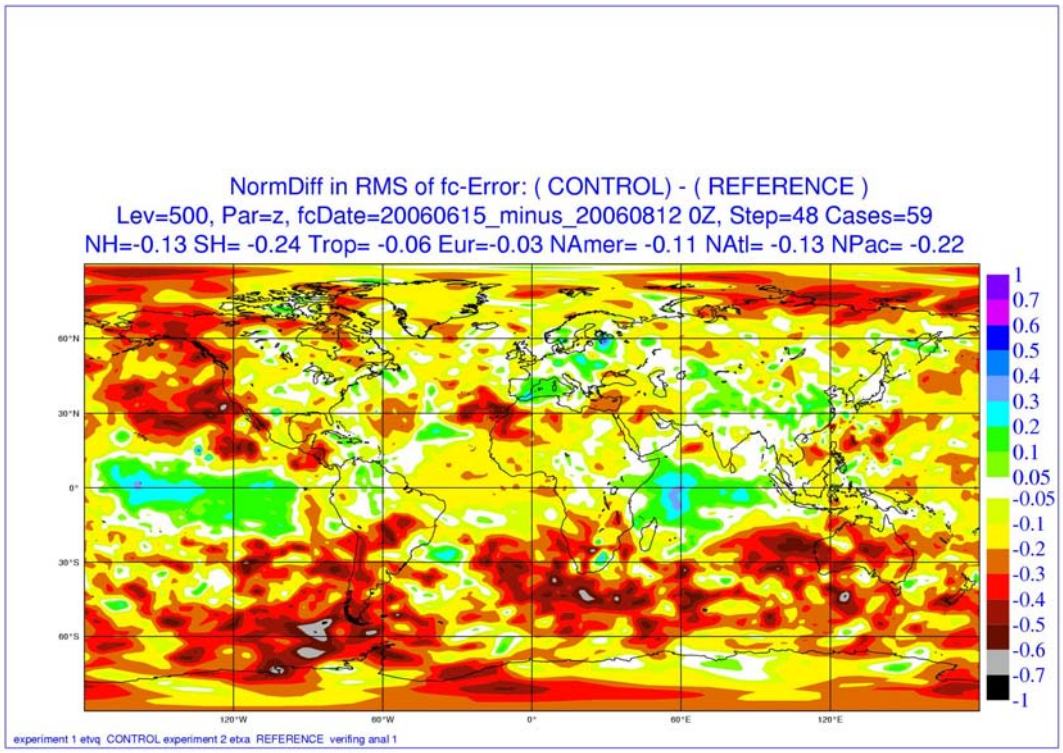

Figure A-8: Mean normalized 48-hour forecast error difference between CONTROL and AMSUA(REF) for the 500 hPa geopotential height.

(v) *AMV(REF)* minus BASELINE

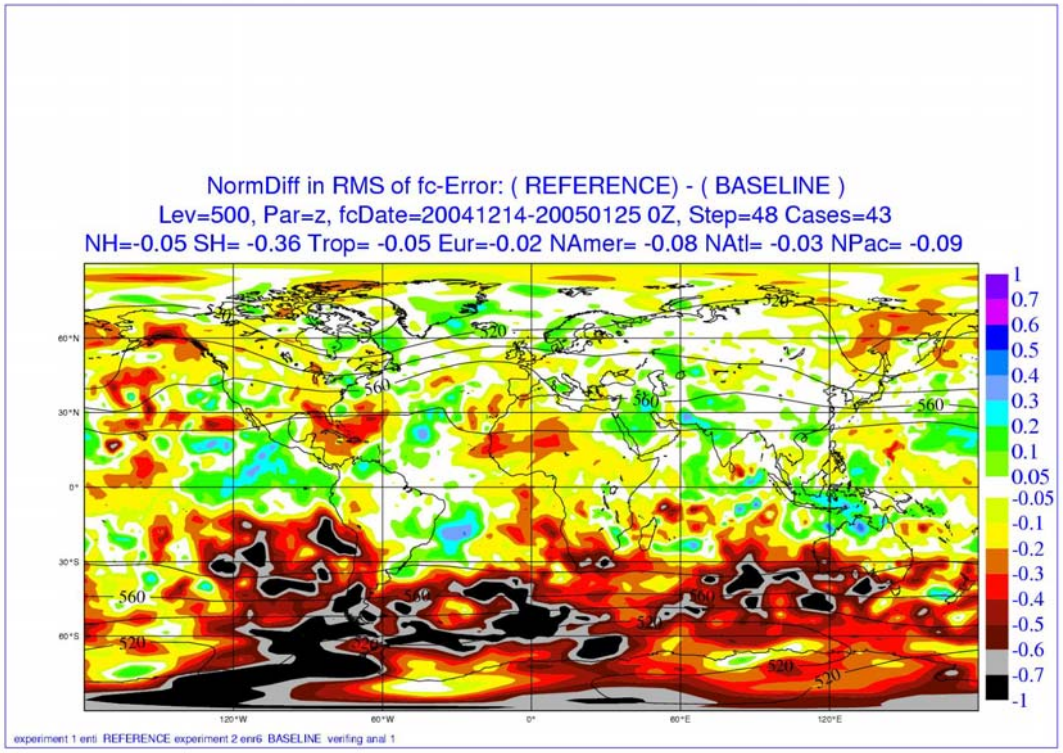

Figure A-9: Mean normalized 48-hour forecast error difference between AMV(REF) and BASELINE(NOSAT) for the 500 hPa geopotential height.

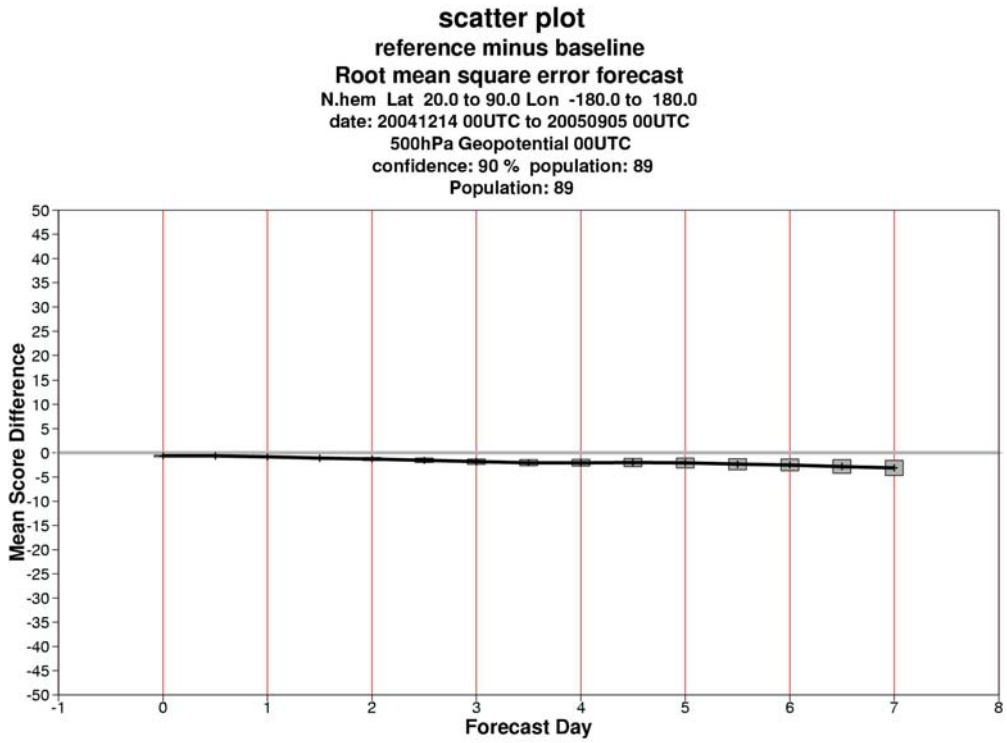

Figure A-10: Time series of normalized 500 hPa height rmse differences between AMV(REF) and BASELINE for forecast errors up to day 7 in the Northern Hemisphere. Negative values indicate positive impact for the AMV(REF).

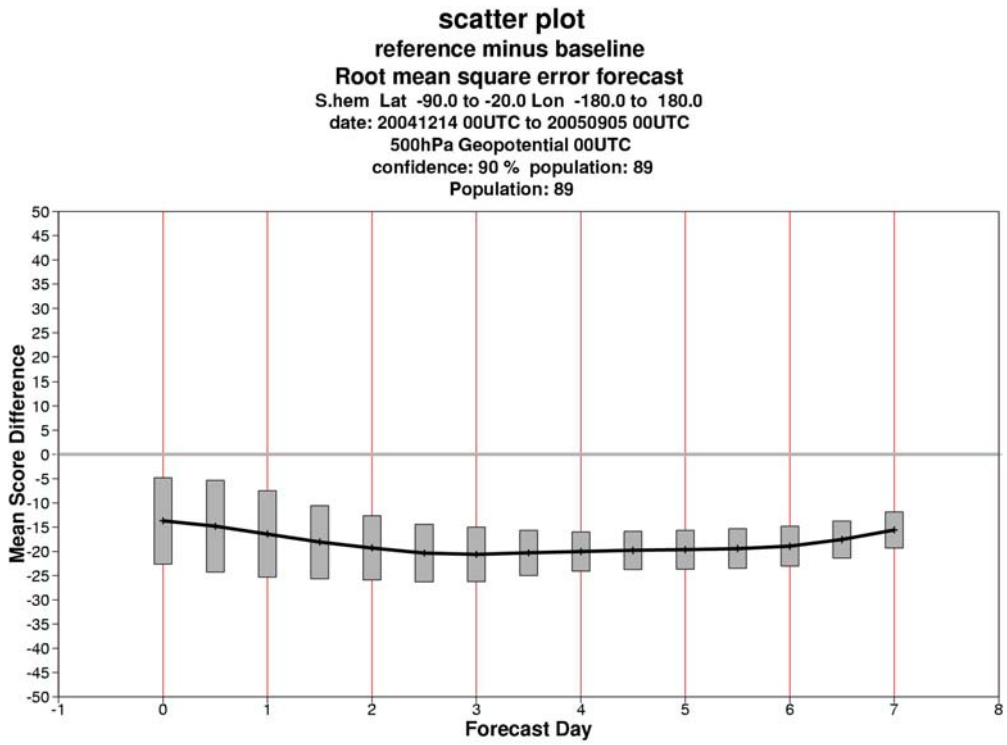

Figure A-11: Time series of normalized 500 hPa height rmse differences between AMV(REF) and BASELINE for forecast errors up to day 7 in the Southern Hemisphere. Negative values indicate positive impact for the AMV(REF).

(vi) AMSUA(REF) minus BASELINE

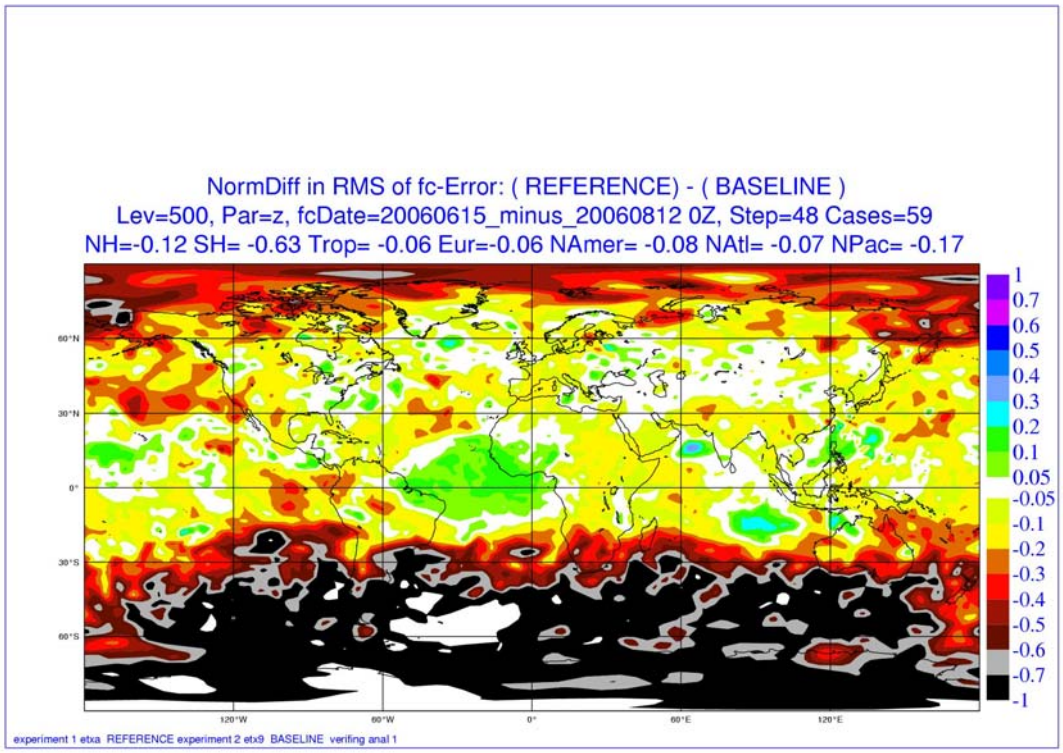

Figure A-12: Mean normalized 48-hour forecast error difference between AMSUA(REF) and BASELINE(NOSAT) for the 500 hPa geopotential height.

Appendix B

A series of seven different data assimilation (corresponding to different observation scenarios) have been run for a summer and winter period.

Geopotential 500 hPa Height (anomaly correlation for mean scores and Normalised RMS error for geographical and scatter plots)

(a) 500 hPa Geopotional Height (*AMV(REF)*

The overall impact on geopotential height in the troposphere is similar at all levels, hence, plots are shown at 500 hPa. It is evident from the three sets of plots below that AMSUA, AIRS and HIRS are clearly the sensors with the strongest impact. In addition significant impact comes from the removal of the MODIS winds from the *AMV(REF)*.

Impact of adding AMSUA to the *AMV(REF)*

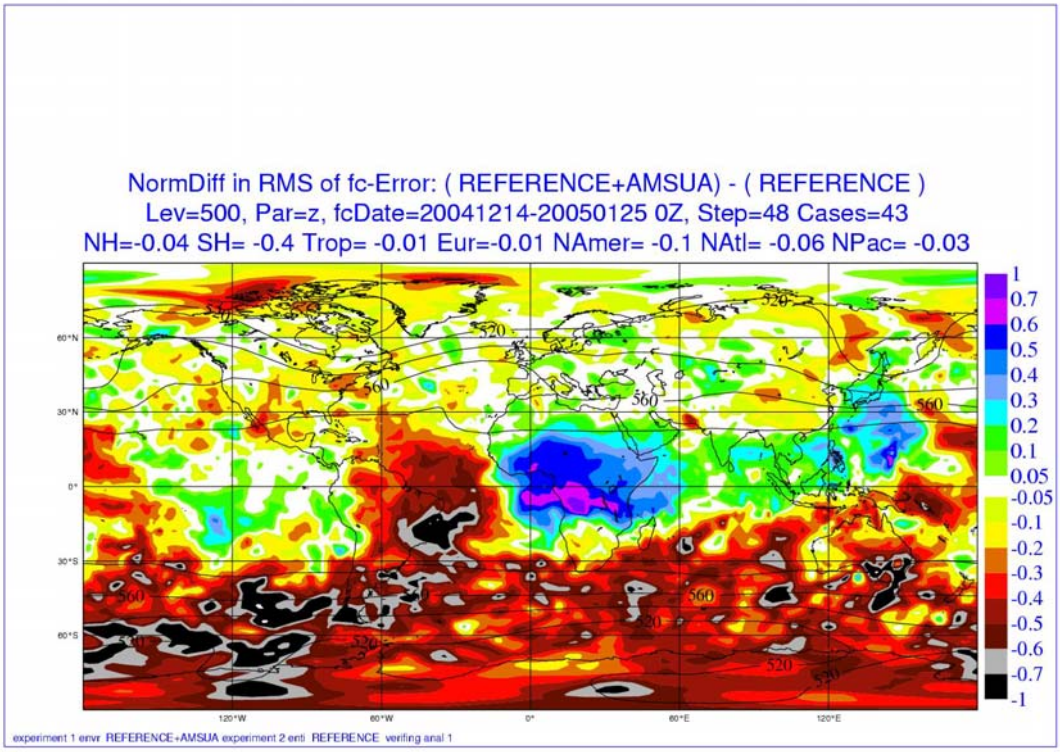

Figure B-1: Mean normalized 48-hour forecast error difference between AMV(REF)+AMSUA and AMV(REF) for the 500 hPa geopotential height.

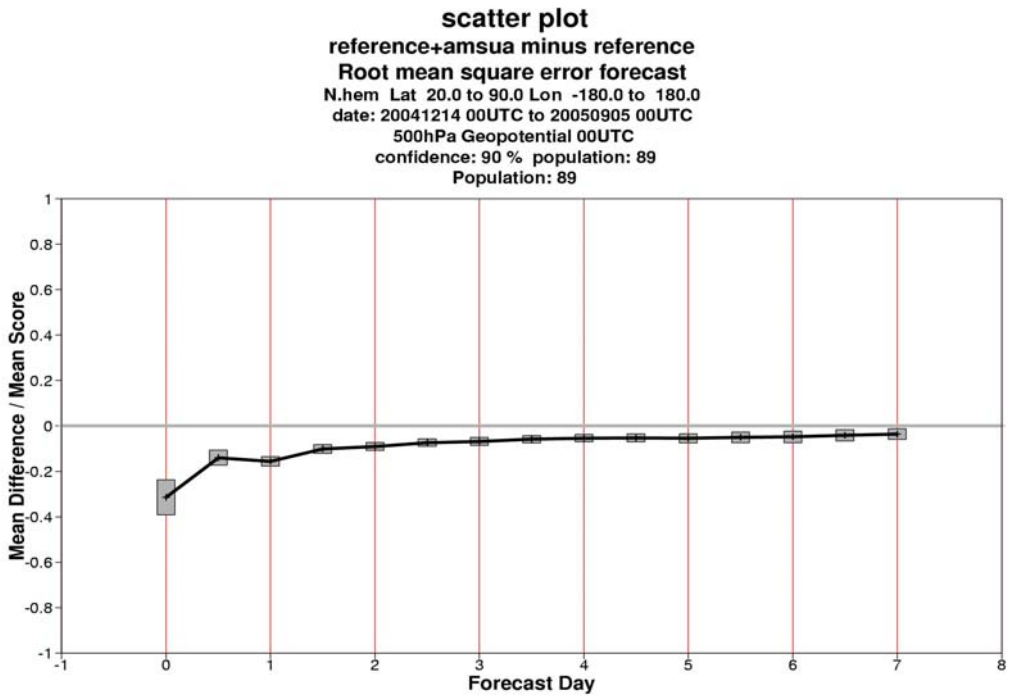

Figure B-2: Time series of normalized 500 hPa height rmse differences between AMV(REF)+AMSUA and AMV(REF) for forecast errors up to day 7 in the Northern Hemisphere. Negative values indicate positive impact for the AMV(REF).

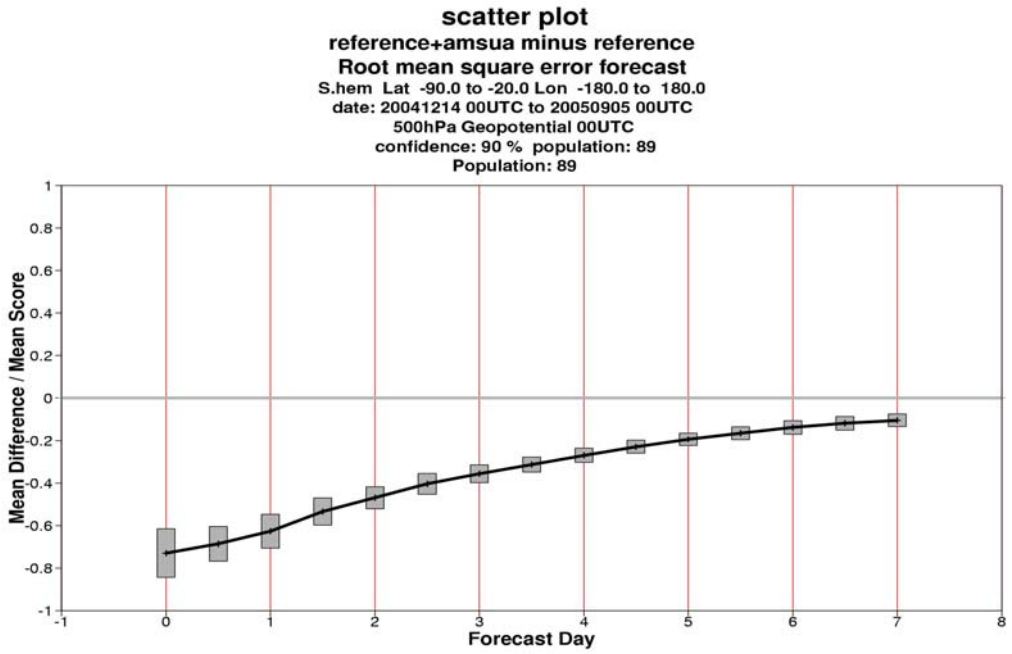

Figure B-3: Time series of normalized 500 hPa height rmse differences between AMV(REF)+AMSUA and AMV(REF) for forecast errors up to day 7 in the Southern Hemisphere. Negative values indicate positive impact for the AMV(REF).

Impact of adding AIRS to the *AMV(REF)*

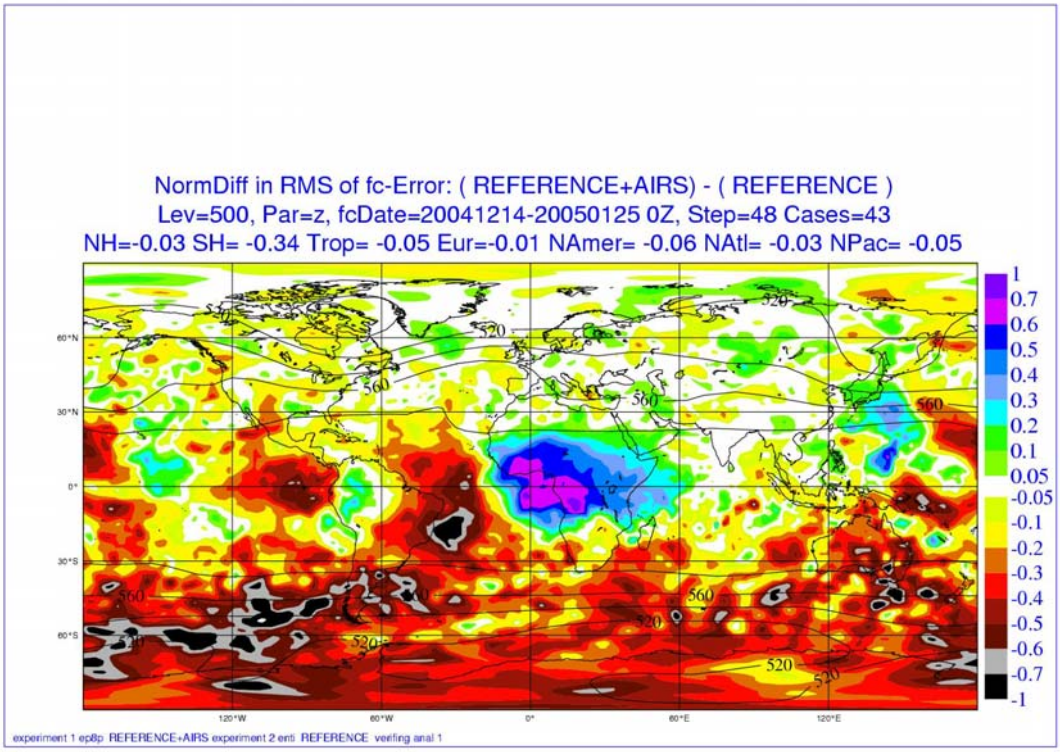

Figure B-4: Mean normalized 48-hour forecast error difference between AMV(REF)+AIRS and AMV(REF) for the 500 hPa geopotential height.

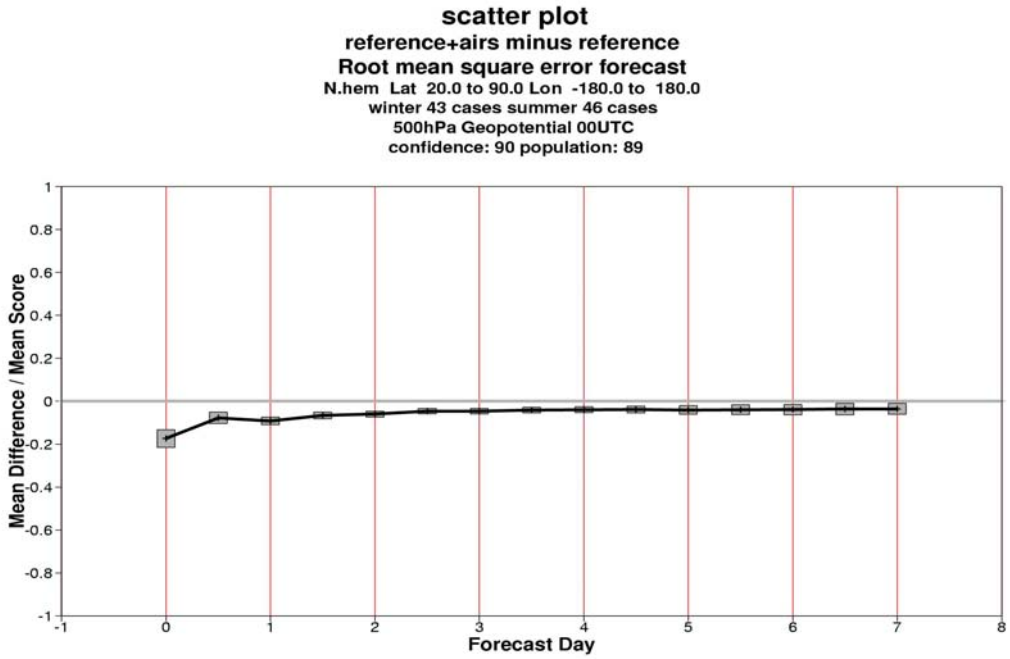

Figure B-5: Time series of normalized 500 hPa height rmse differences between AMV(REF)+AIRS and AMV(REF) for forecast errors up to day 7 in the Northern Hemisphere. Negative values indicate positive impact for the AMV(REF).

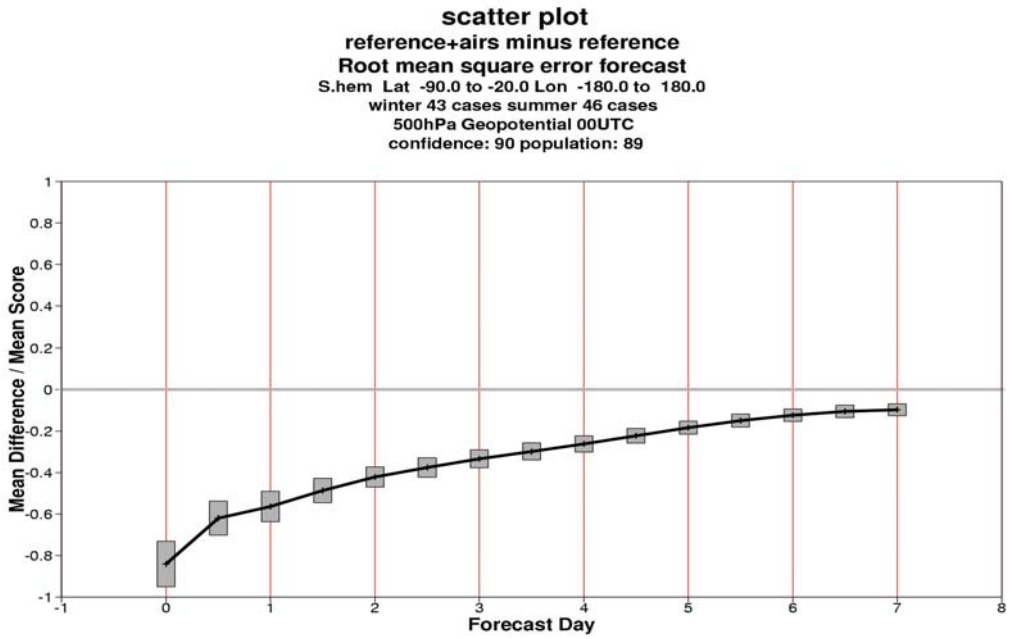

Figure B-6: Time series of normalized 500 hPa height rmse differences between AMV(REF)+AIRS and AMV(REF) for forecast errors up to day 7 in the Southern Hemisphere. Negative values indicate positive impact for the AMV(REF).

Impact of adding HIRS to the *AMV(REF)*

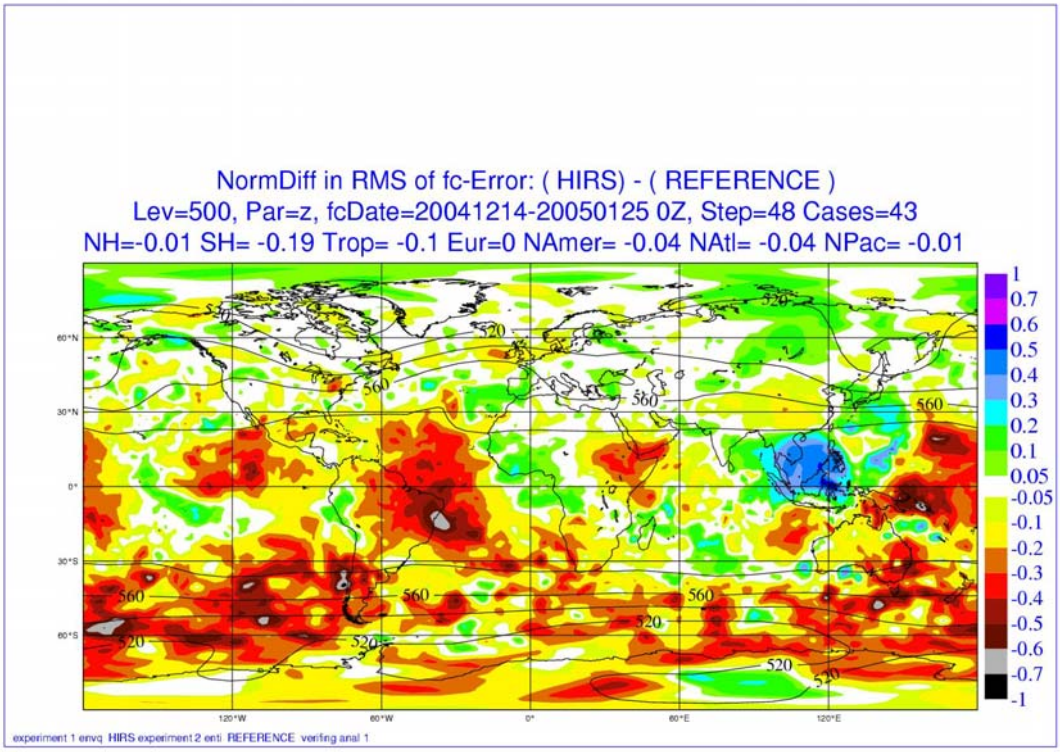

Figure B-7: Mean normalized 48-hour forecast error difference between AMV(REF)+HIRS and AMV(REF) for the 500 hPa geopotential height.

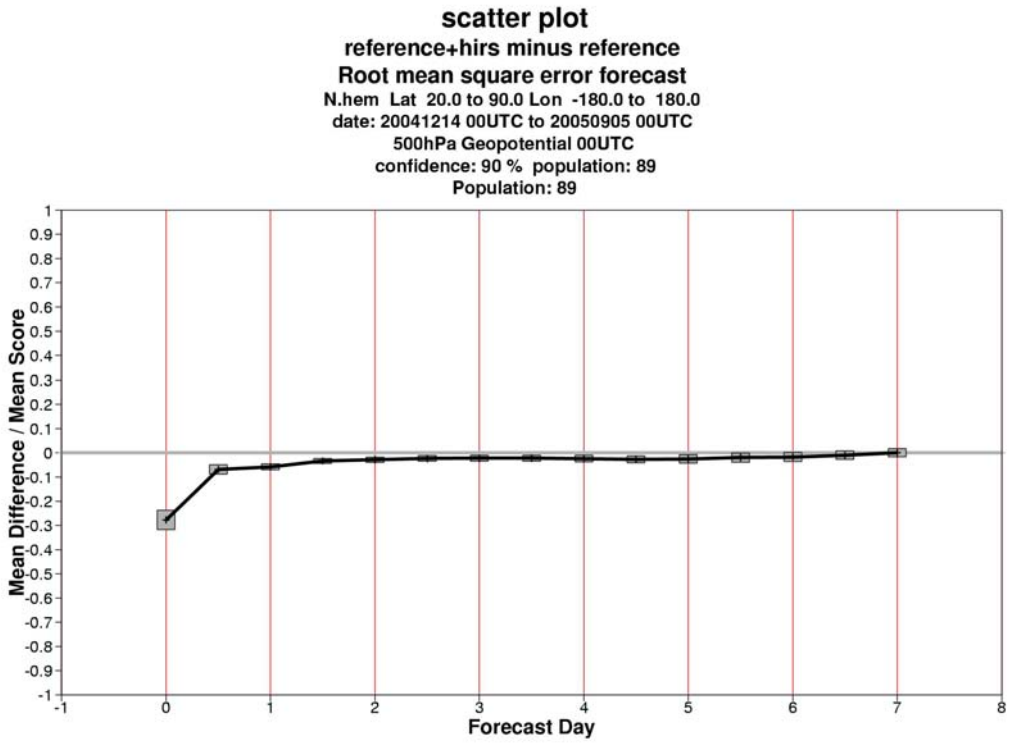

Figure B-8: Time series of normalized 500 hPa height rmse differences between AMV(REF)+HIRS and AMV(REF) for forecast errors up to day 7 in the Northern Hemisphere. Negative values indicate positive impact for the AMV(REF).

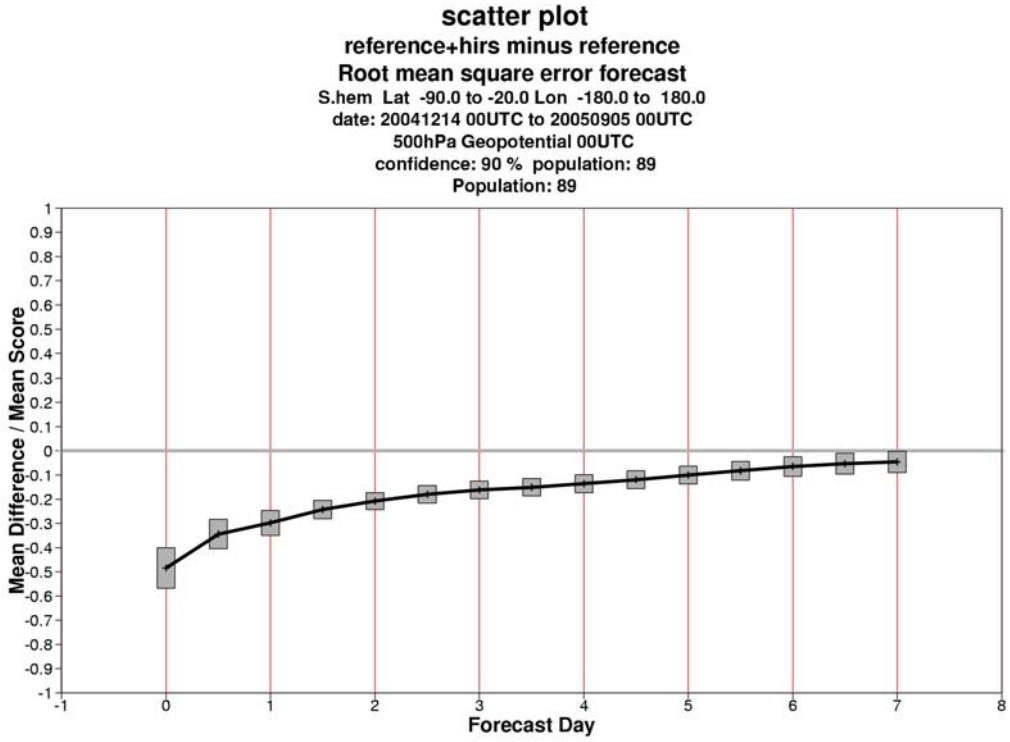

Figure B- 9: Time series of normalized 500 hPa height rmse differences between AMV(REF)+HIRS and AMV(REF) for forecast errors up to day 7 in the Southern Hemisphere. Negative values indicate positive impact for the AMV(REF).

(a) 500 hPa Geopotional Height AMSUA(REF)

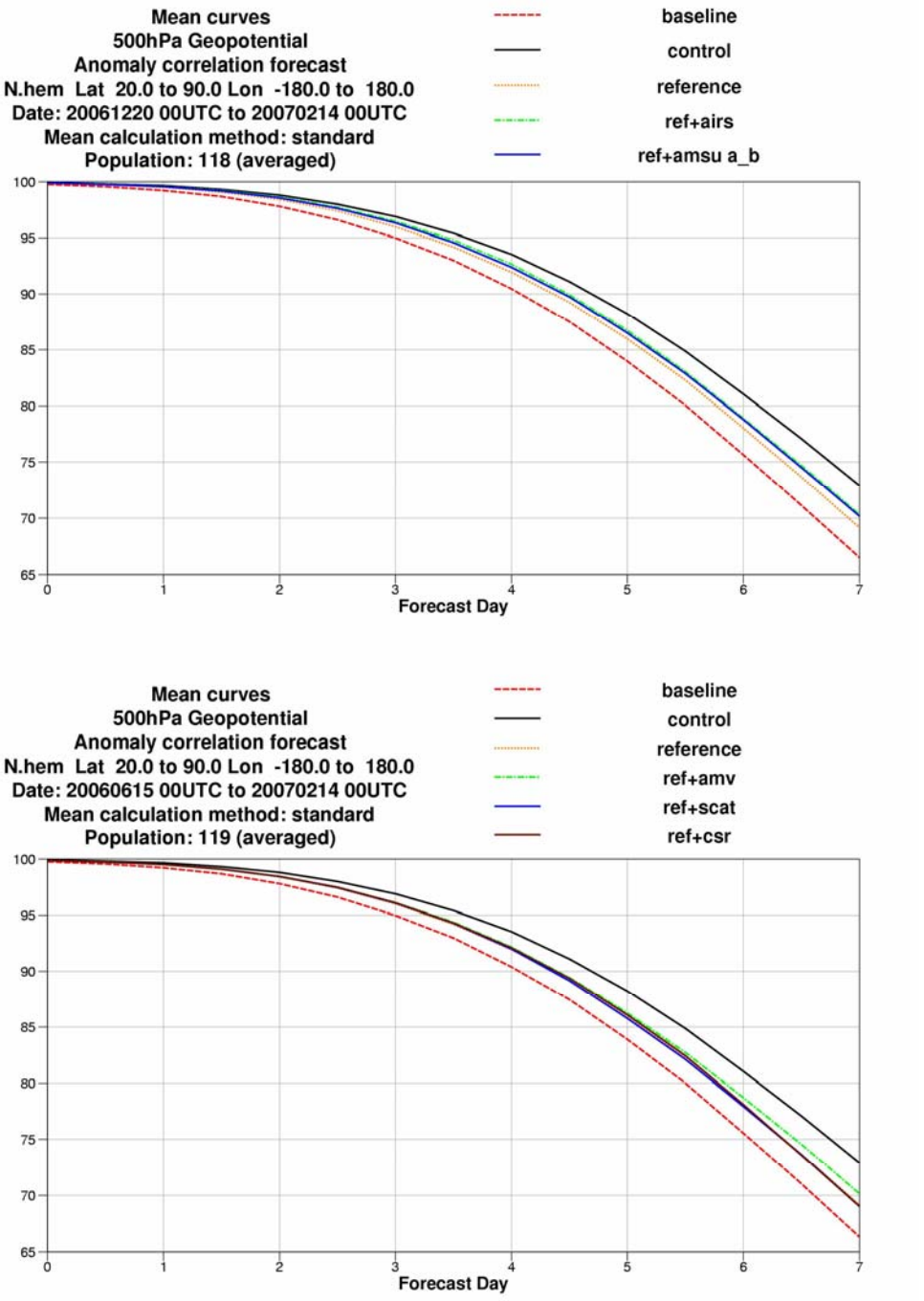

Figure B-10: Impact of all sensors (based on AMSUA(REF)) on 500 hPa geopotential height for the northern hemisphere (20°–90°N).

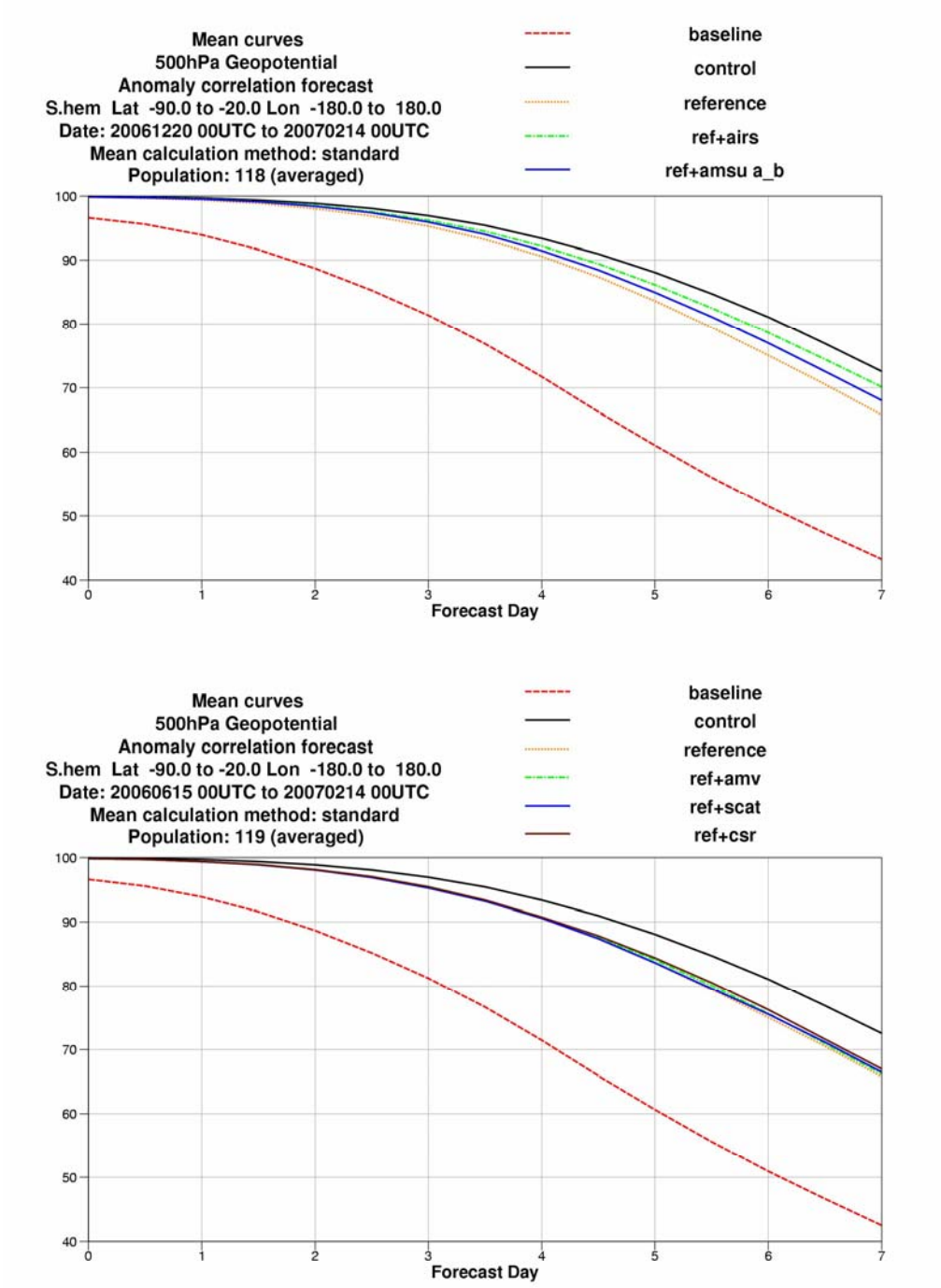

Figure B-11: Impact of all sensors (based on AMSUA(REF)) on 500 hPa geopotential height for the southern hemisphere (20°–90°N).

Appendix C

Humidity

A series of seven different data assimilation (corresponding to different observation scenarios) have been run for a summer and winter period.

Relative Humidity at 850,500 and 200 hPa (mean scores in percent and Normalised RMS error for geographical and scatter plots)

The influence of the humidity observations on the forecast are mostly in the tropics and their influence on the forecast decays more quickly in time than geopotential. As a consequence humidity verification has been focused on the short range forecast (to day four).

The results are also evaluated at three atmospheric levels as different satellite sensors sense different regions of the troposphere.

Relative humidity at 850 hPa

With reference to the mean plots below, SSMI is the most important sensor affecting this level. Even after adding SSMI to the ***AMV(REF)*** there is still relative large gap to the **CONTROL** suggesting the there is a small but additive contribution of many other sensors contributing to the moisture analysis.

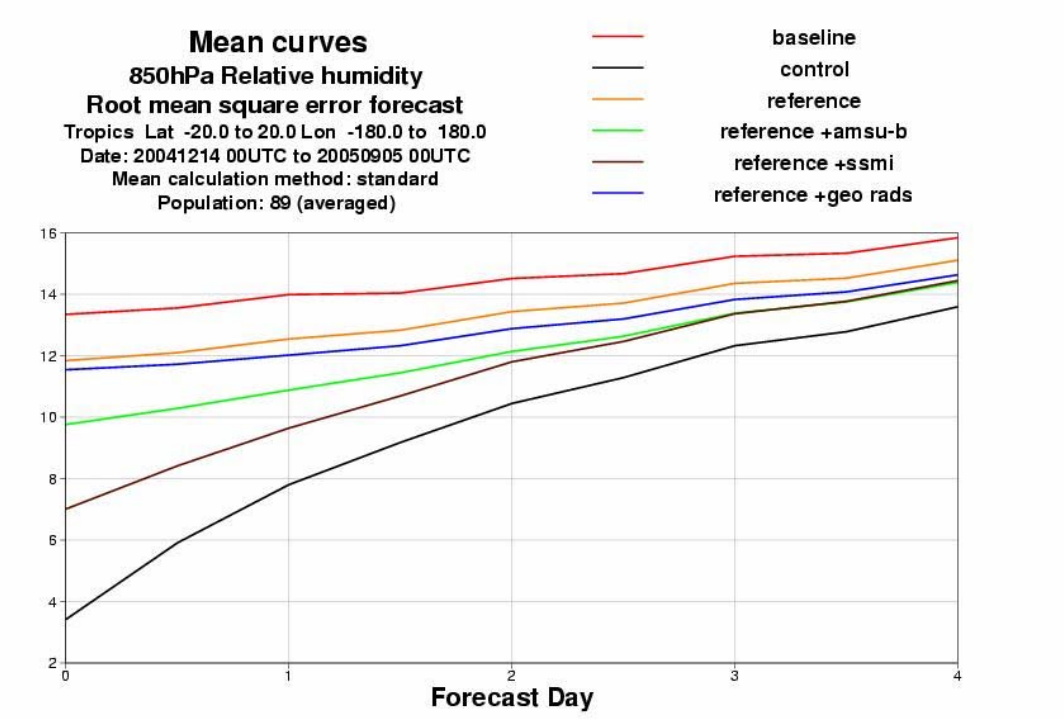

Figure C-1: Impact of three sensors (based on AMSUA(REF)) on 850 hPa relative humidity for (AMSU(REF)+ AMSUB), (AMSU(REF)+SSMI) and (AMSU(REF)+CSR) for the tropics (20°N–20°S).

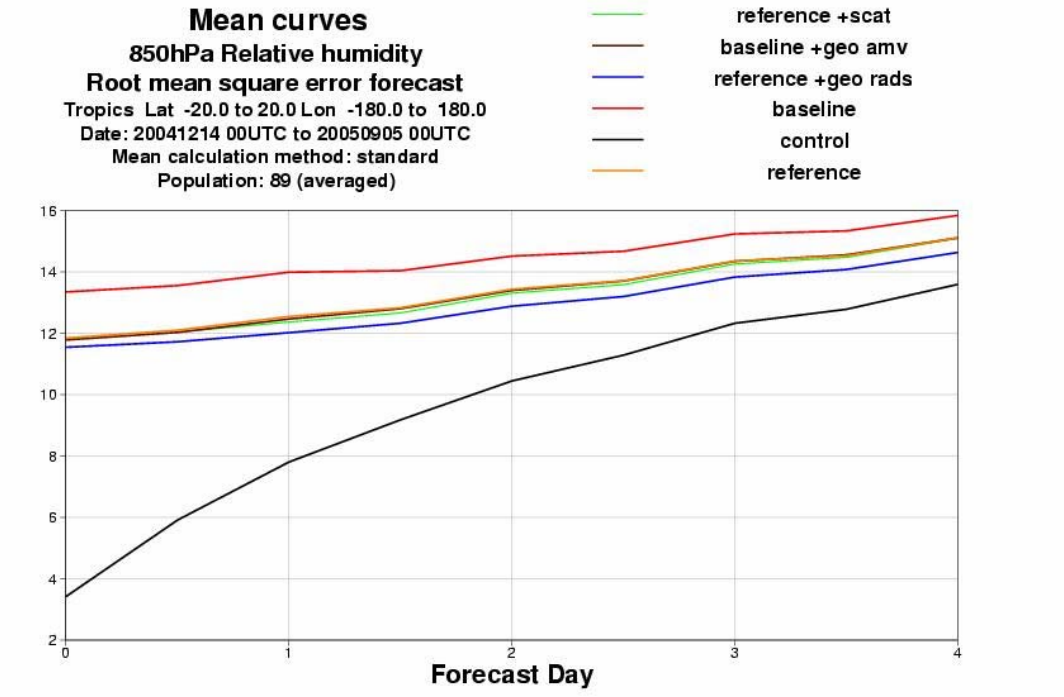

Figure C-2: Impact of three sensors (based on AMSUA(REF)) on 850 hPa relative humidity for (AMSU(REF)+SCAT), (AMSU(REF)+AMV) and (AMSU(REF)+CSR) for the tropics (20°N–20°S).

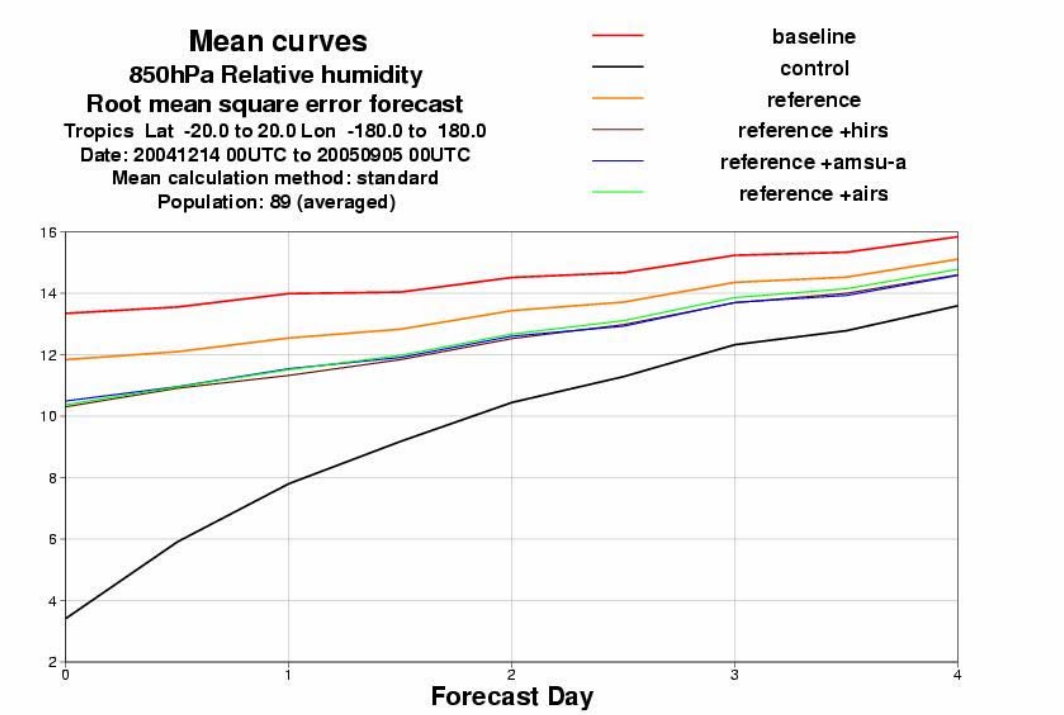

Figure C-3: Impact of three sensors (based on AMSUA(REF)) on 850 hPa relative humidity for (AMSU(REF)+HIRS), (AMSU(REF)+AMSUA) and (AMSU(REF)+AIRS) for the tropics (20°N–20°S).

Impact of adding SSMI to the AMV(REF)

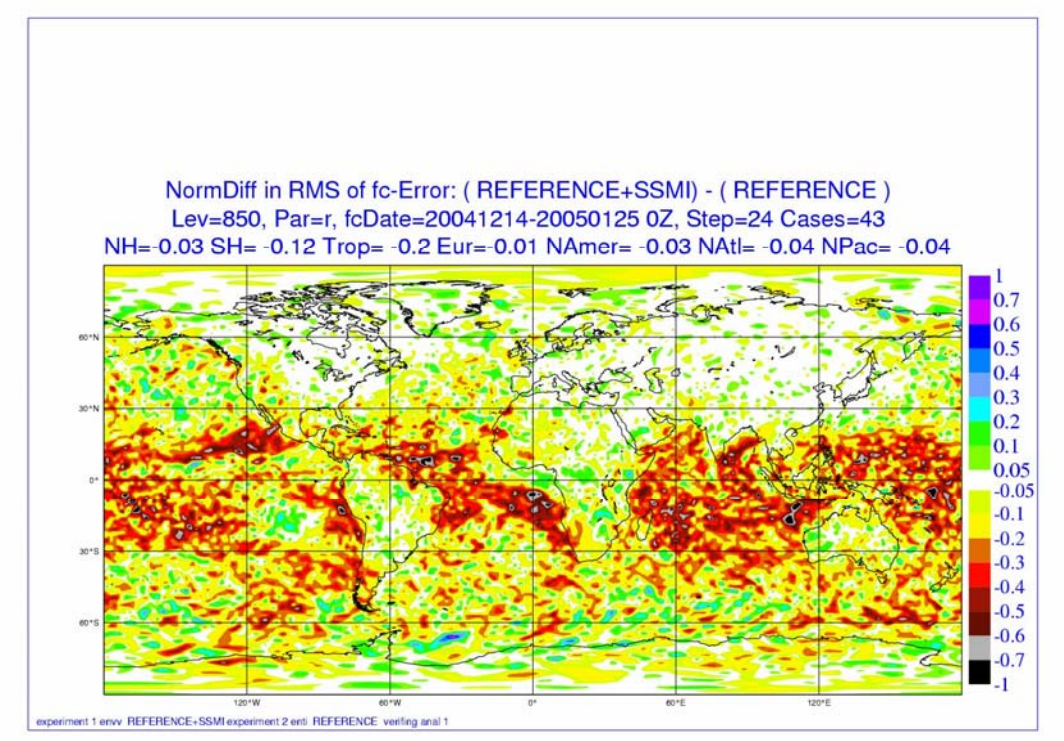

Figure C-4: Mean normalized 48-hour forecast error difference between AMV(REF)+SSMI and AMV(REF) for the 850 hPa relative humidity.

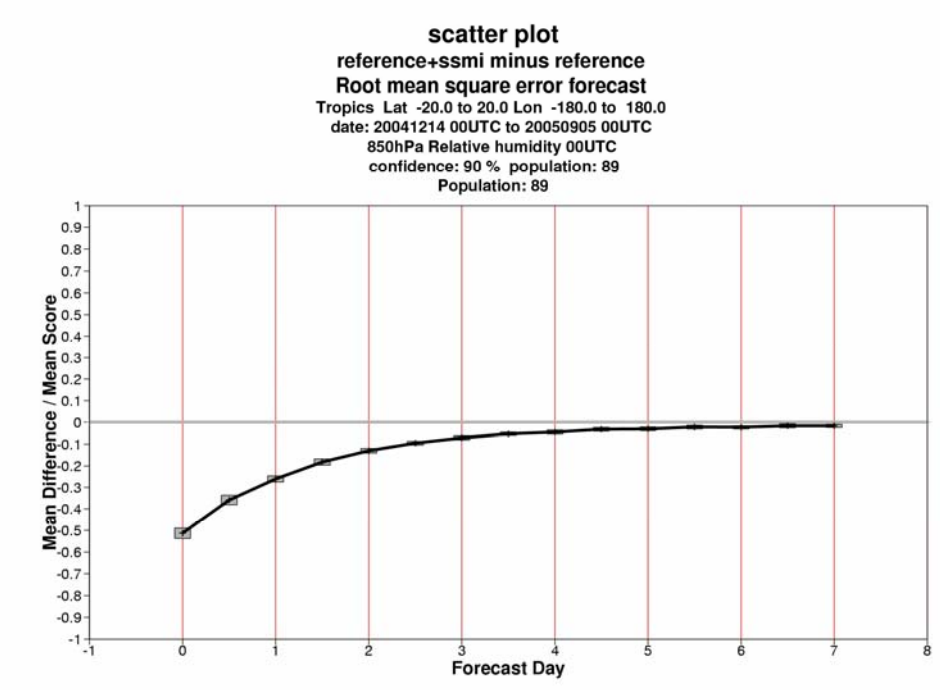

Figure C-5: Time series of normalized 850 hPa relative humidity rmse differences between AMV(REF)+SSMI and AMV(REF) for forecast errors up to day 7 in the Northern Hemisphere. Negative values indicate positive impact for the AMV(REF)+SSMI.

Relative humidity at 500 hPa *AMV(REF)*

With reference to the mean plots below AMSUB and CSRs (particularly in the SEVIRI region) are the most important sensors affecting this level.

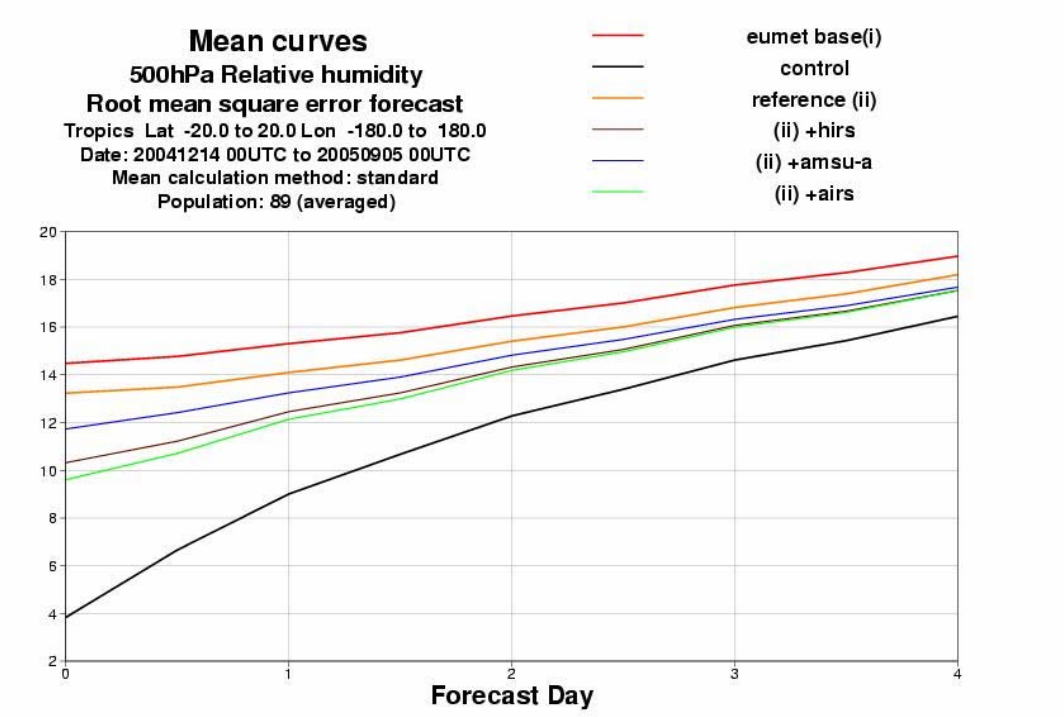

Figure C-6: Impact of three sensors (based on AMV(REF)) on 500 hPa relative humidity for (AMV(REF)+HIRS), (AMV(REF)+AMSUA) and (AMV(REF)+AIRS) for the tropics (20°N–20°S).

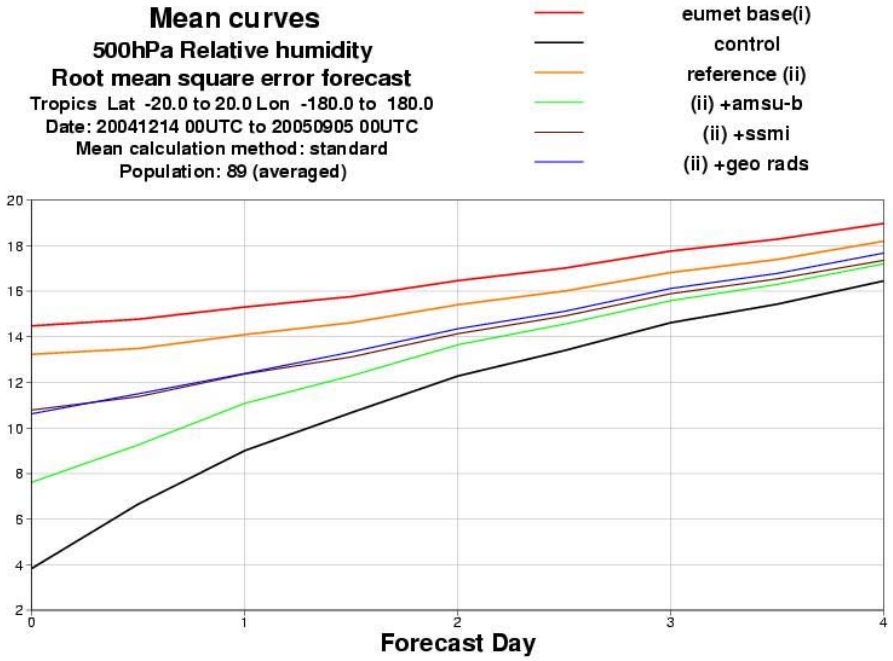

Figure C-7: Impact of three sensors (based on AMV(REF)) on 500 hPa relative humidity for (AMV(REF)+AMSUB), (AMV(REF)+SSMI) and (AMV(REF)+CSRs) for the tropics (20°N–20°S).

Impact of adding AMSUB to the AMV(REF)

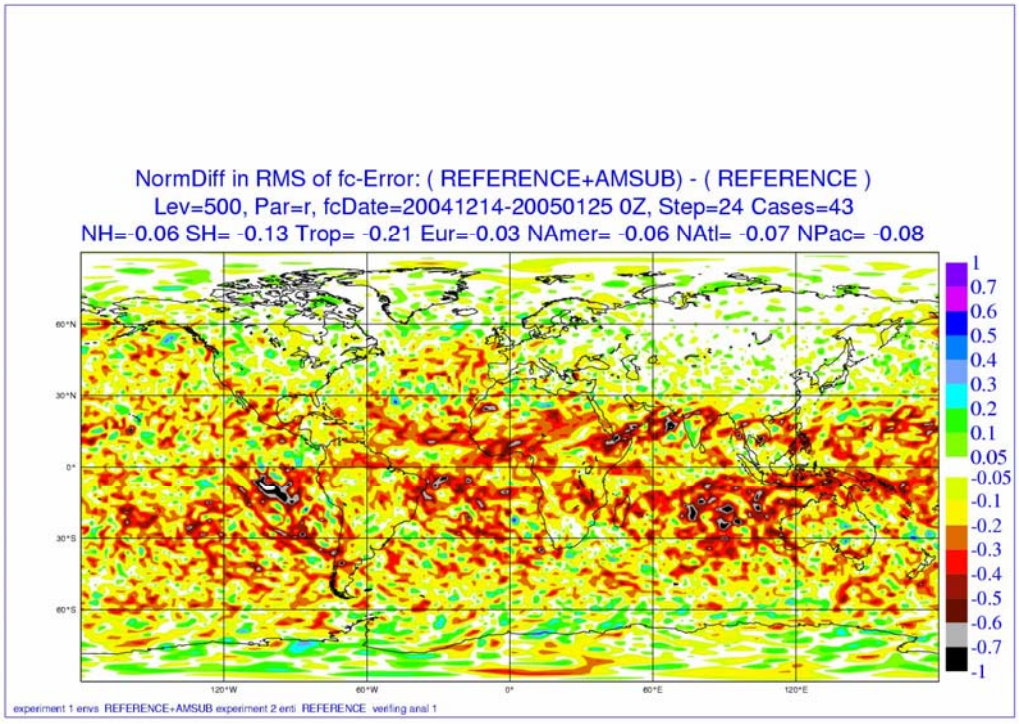

Figure C-8: Mean normalized 48-hour forecast error difference between AMV(REF)+AMSUB and AMV(REF) for the 500 hPa relative humidity.

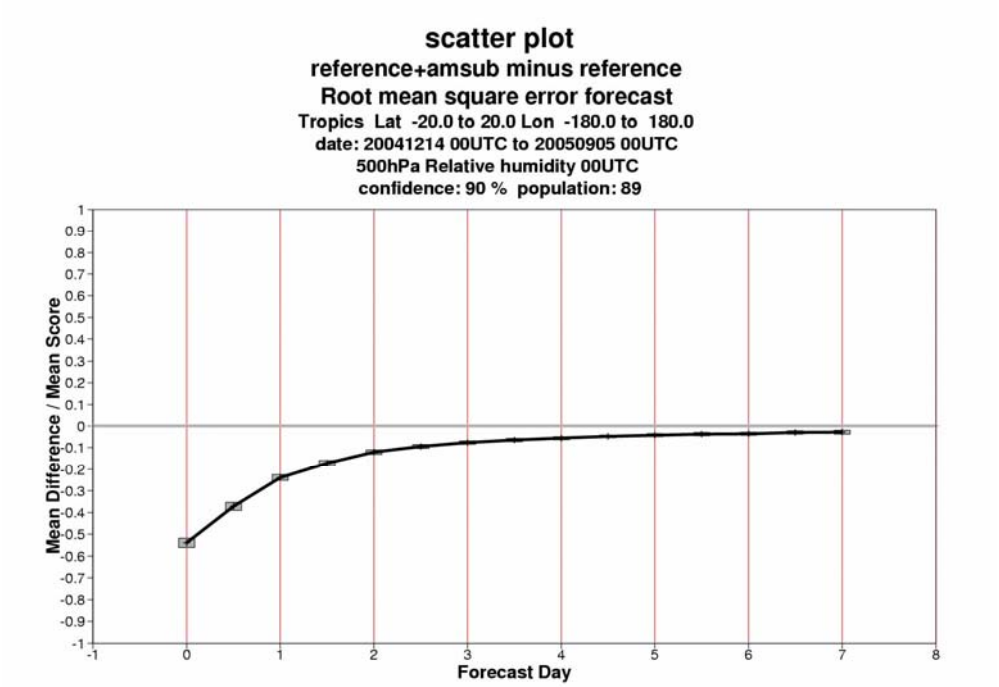

Figure C-9: Time series of normalized 500 hPa relative humidity rmse differences between AMV(REF)+AMSUB and AMV(REF) for forecast errors up to day 7 in the tropics. Negative values indicate positive impact for the AMV(REF)+AMSUB.

Impact of adding CSRs to the *AMV(REF)*

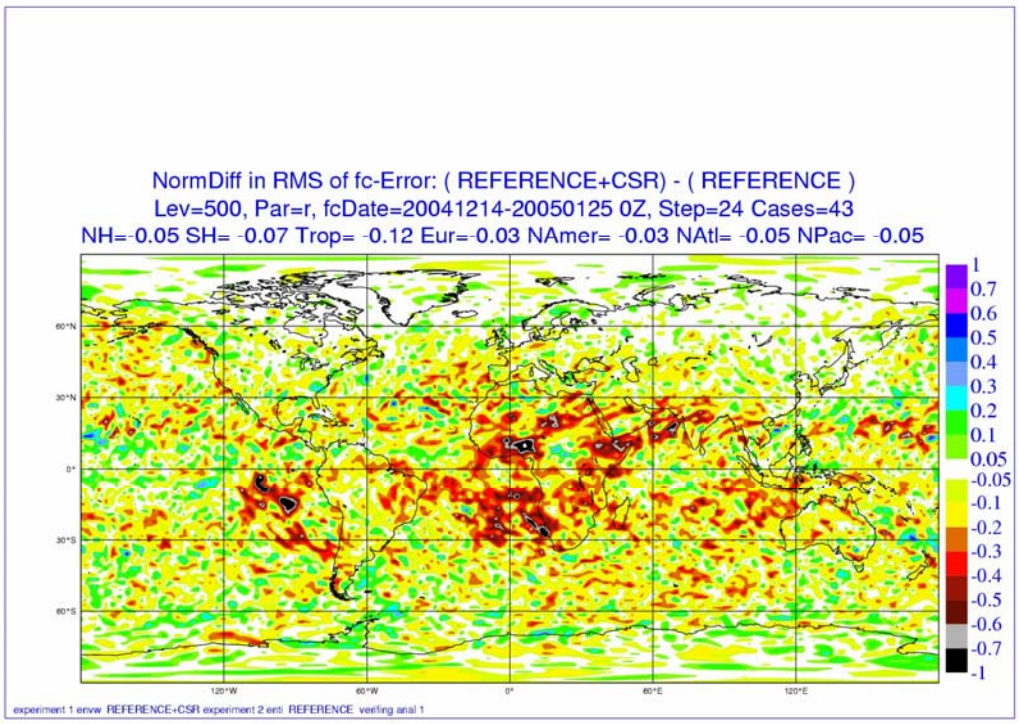

Figure C-10: Mean normalized 48-hour forecast error difference between AMV(REF)+CSRs and AMV(REF) for the 500 hPa relative humidity.

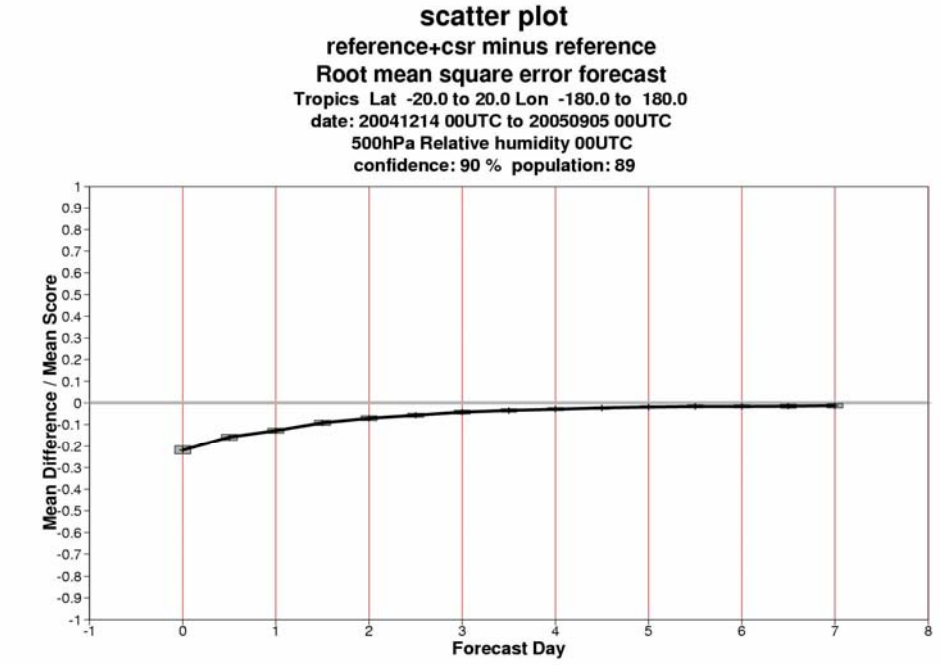

Figure C-11: Time series of normalized 500 hPa relative humidity rmse differences between AMV(REF)+ CSRs and AMV(REF) for forecast errors up to day 7 in the tropics. Negative values indicate positive impact for the AMV(REF)+CSRs.

Relative humidity at 500 hPa AMSUA(REF)

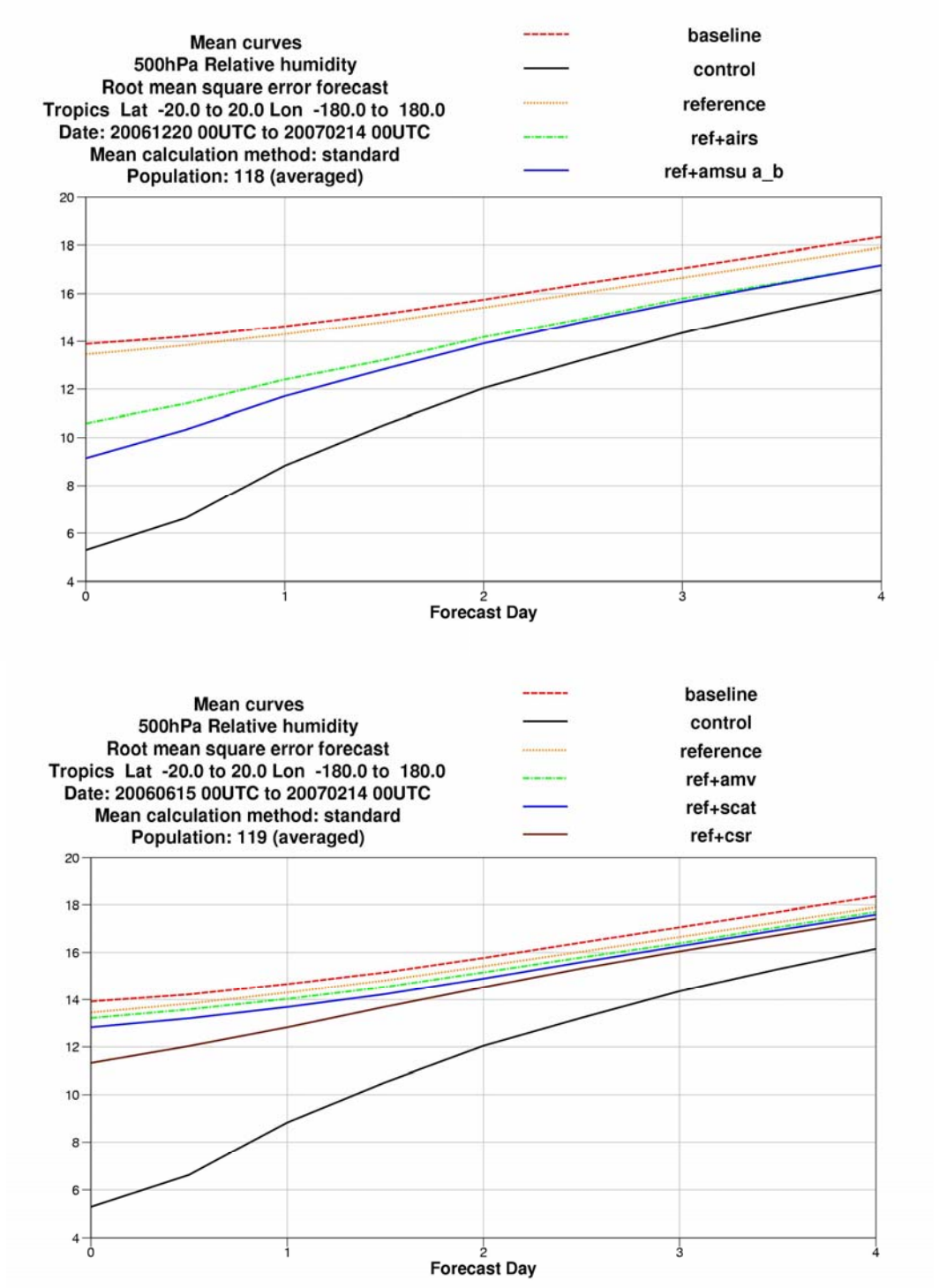

Figure C- 12: Impact of five sensors (based on AMV(REF)) on 500 hPa relative humidity for the tropics (20°N–20°S).

Relative humidity at 200 hPa *AMV(REF)*

With reference to the mean plots below AMSUB, CSRs and HIRS are the most important sensors affecting this level.

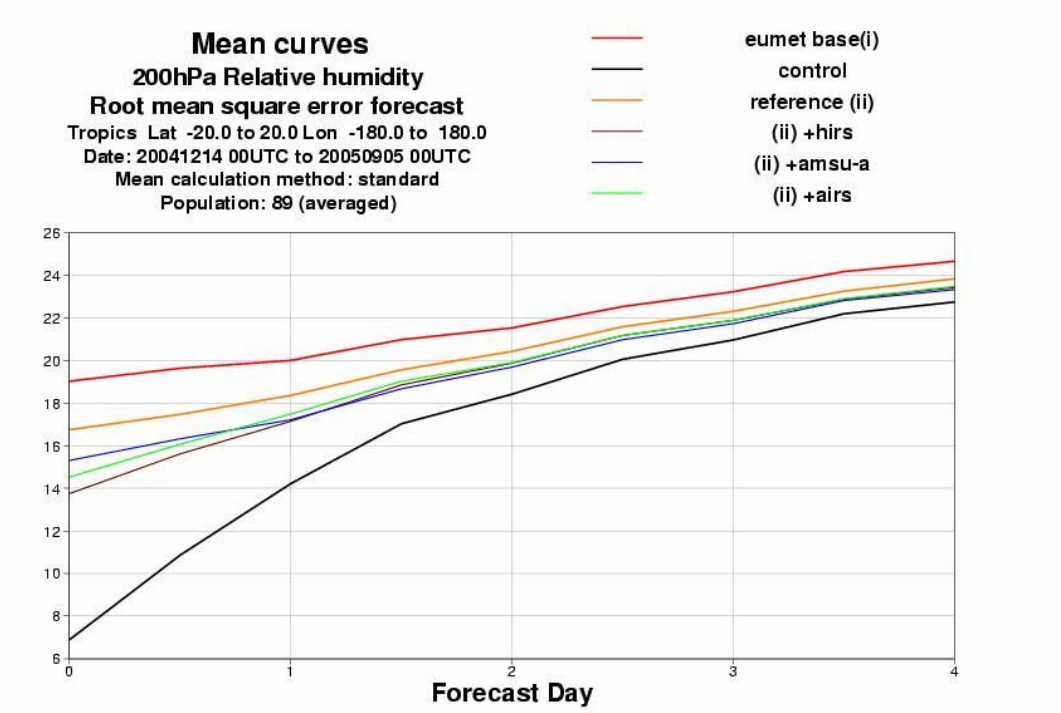

Figure C-13: Impact of three sensors (based on AMV(REF)) on 200 hPa relative humidity for (AMUSA(REF)+HIRS), (AMSUA(REF)+AMSUA+AMSUB) and (AMSUA(REF)+AIRS) for the tropics (20°N–20°S).

Impact of adding AMSUB to the AMV(REF)

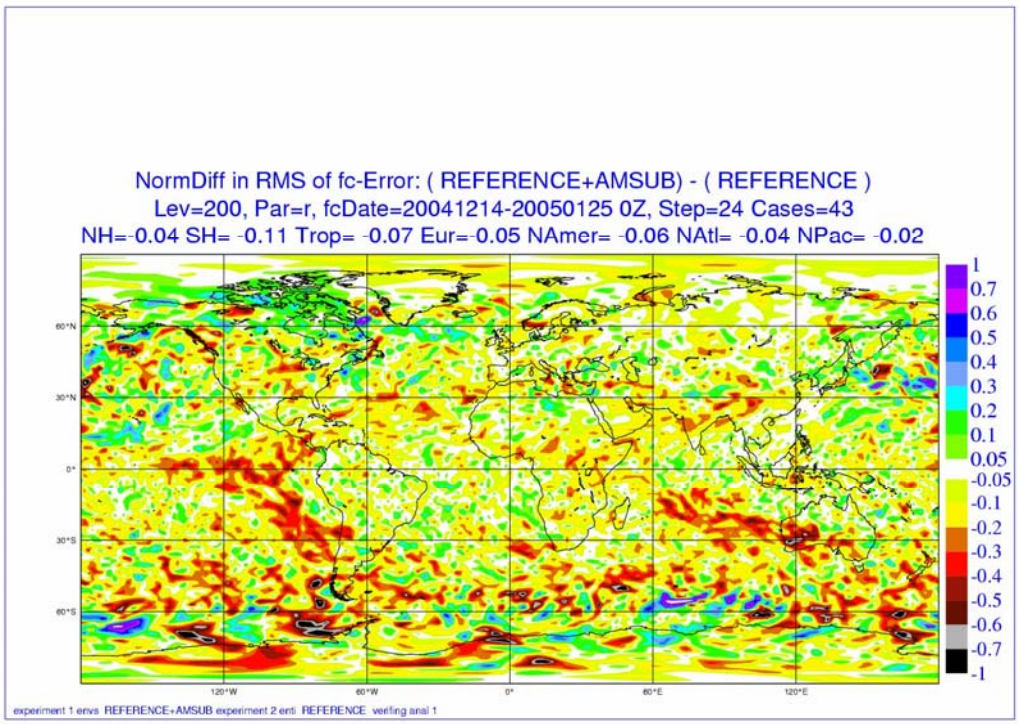

Figure C- 14: Mean normalized 48-hour forecast error difference between AMV(REF)+AMSUB and AMV(REF) for the 200 hPa relative humidity.

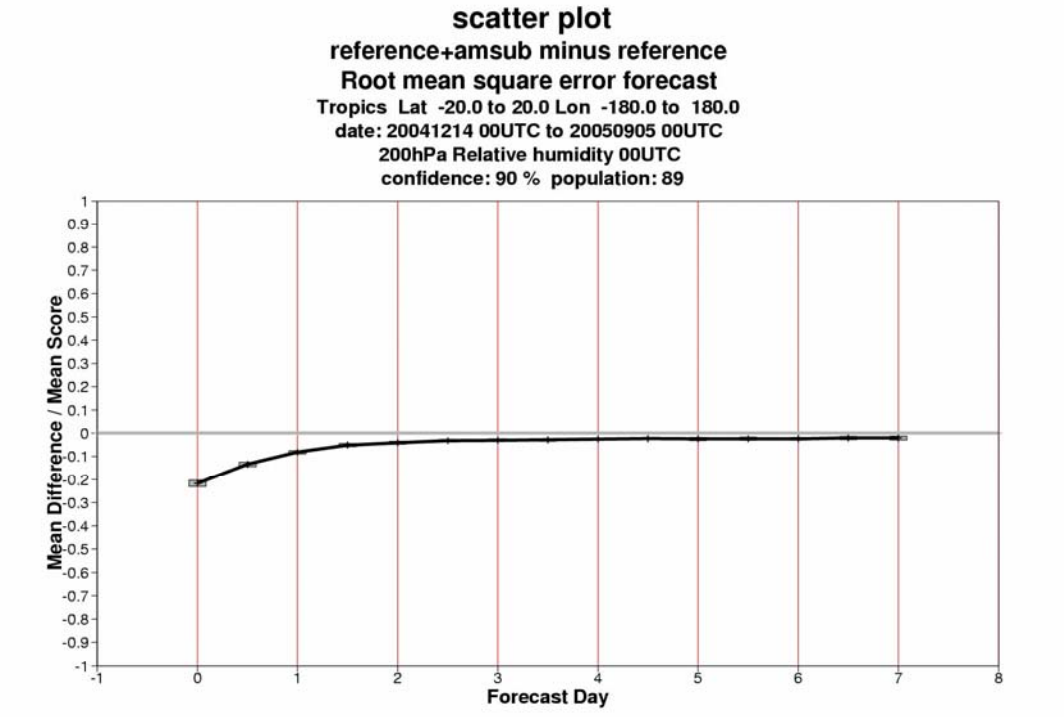

Figure C-15: Time series of normalized 200 hPa relative humidity rmse differences between AMV(REF)+ AMSUB and AMV(REF) for forecast errors up to day 7 in the Northern Hemisphere. Negative values indicate positive impact for the AMV(REF)+AMSUB.

Impact of adding CSRs to the *AMV(REF)*

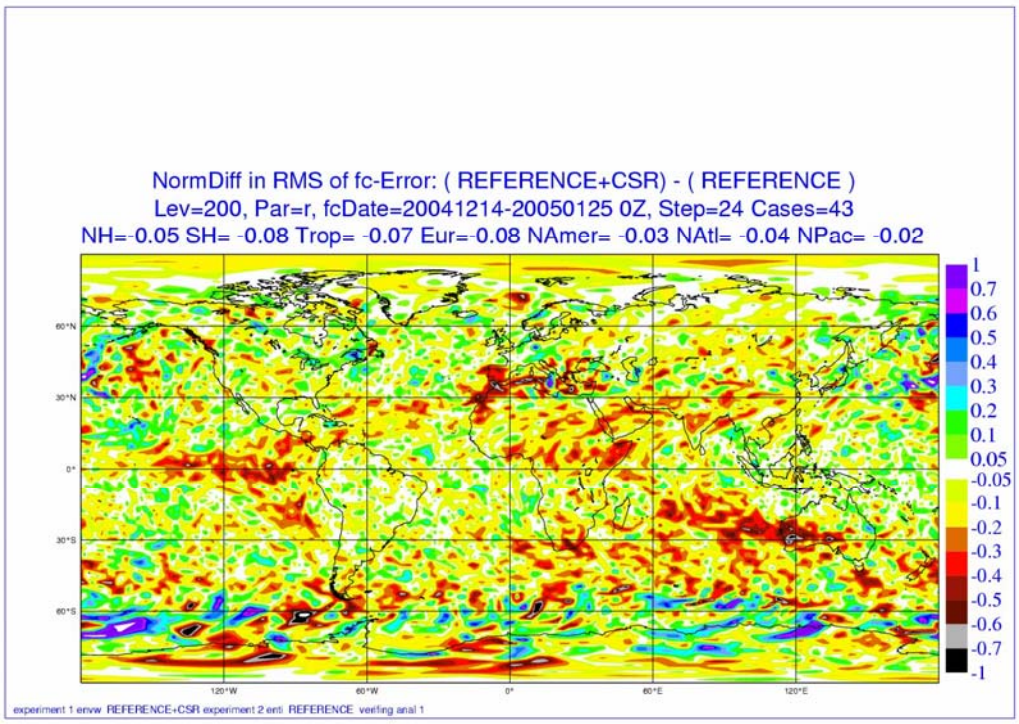

Figure C-16: Mean normalized 48-hour forecast error difference between AMV(REF)+CSR and AMV(REF) for the 200 hPa relative humidity.

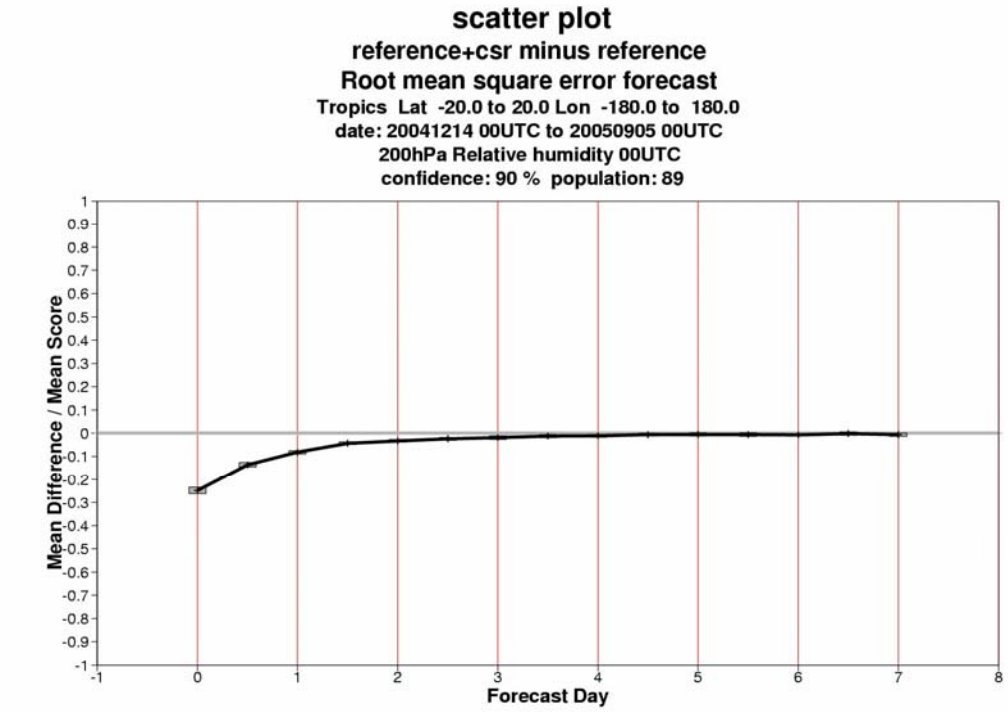

Figure C-17: Time series of normalized 200 hPa relative humidity rmse differences between AMV(REF)+ CSR and AMV(REF) for forecast errors up to day 7 in the tropics. Negative values indicate positive impact for the AMV(REF)+CSR.

Impact of adding HIRS to the *AMV(REF)*

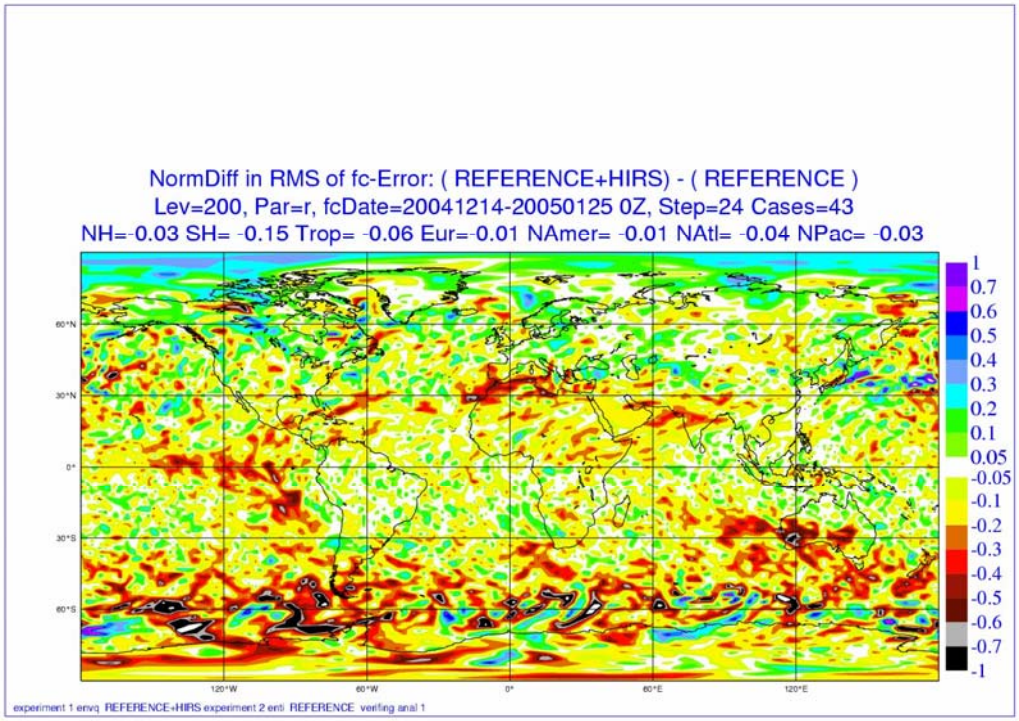

Figure C-18: Mean normalized 48-hour forecast error difference between AMV(REF)+HIRS and AMV(REF) for the 200 hPa relative humidity.

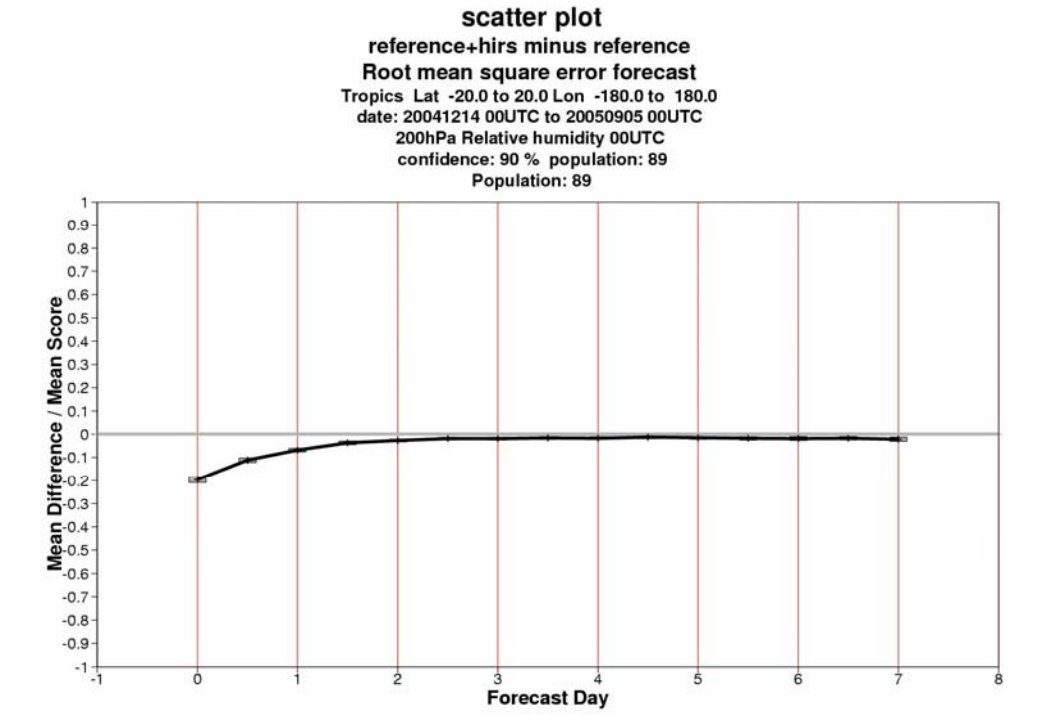

Figure C-19: Time series of normalized 200 hPa relative humidity rmse differences between AMV(REF)+HIRS and AMV(REF) for forecast errors up to day 7 in the tropics. Negative values indicate positive impact for the AMV(REF)+HIRS.

Relative humidity at 200 hPa AMSUA(REF)

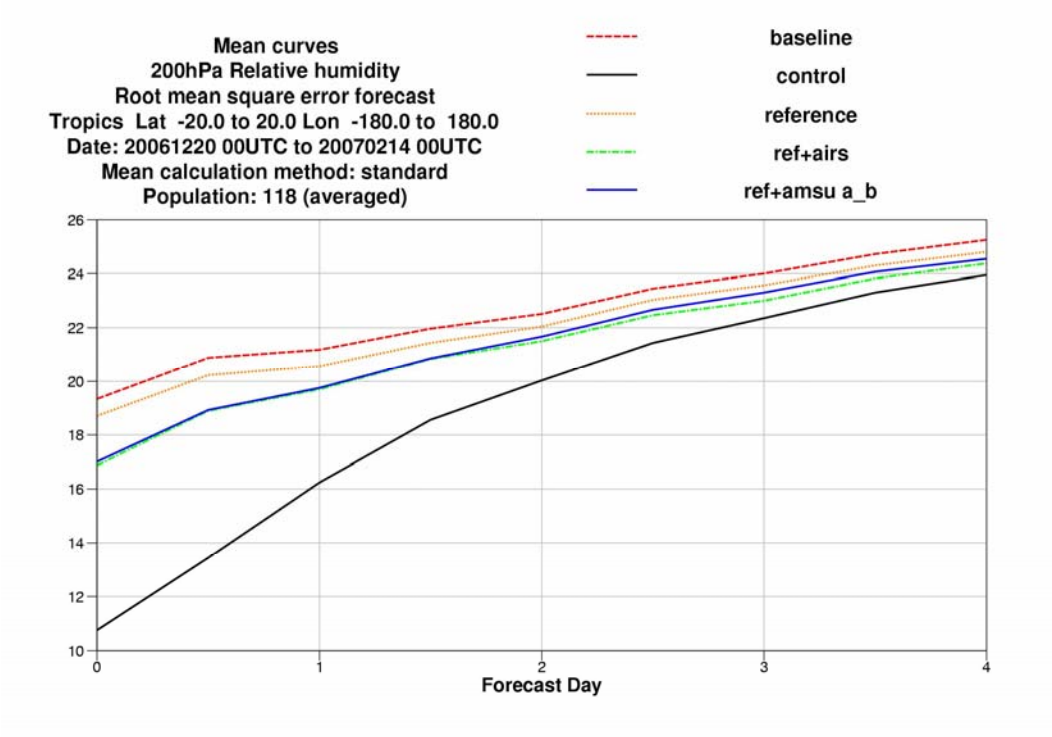

Figure C-20: Impact of two sensors (based on AMV(REF)) on 200 hPa relative humidity for (AMUSA(REF)+AIRS) and (AMSUA(REF)+AMSUA+AMSUB) for the tropics (20°N–20°S).

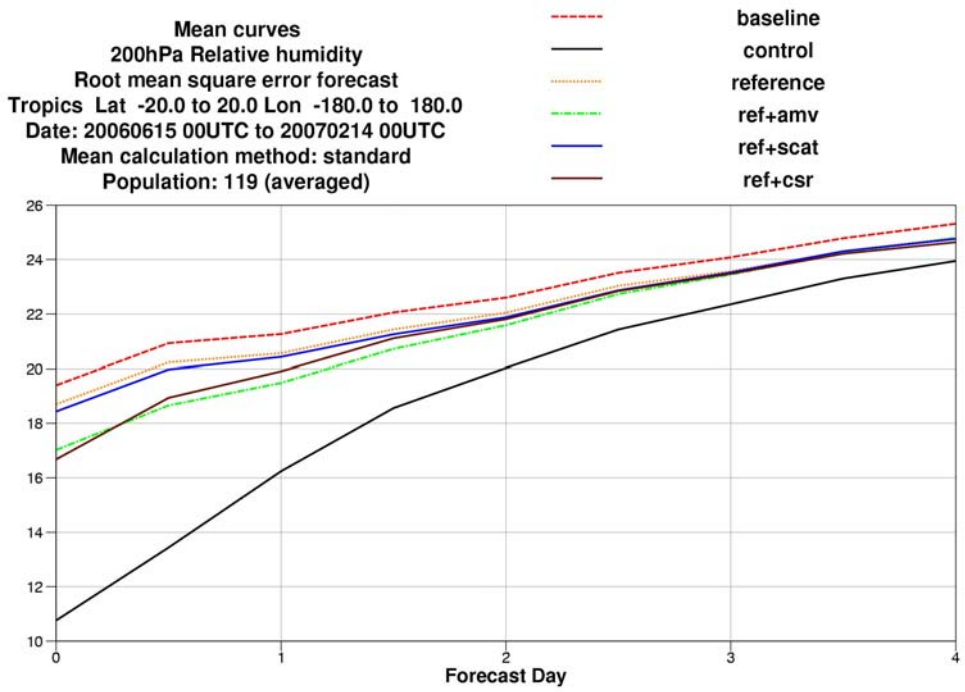

Figure C-21: Impact of three sensors (based on AMV(REF)) on 200 hPa relative humidity for (AMUSA(REF)+AMV), (AMSUA(REF)+SCAT) and (AMSUA(REF)+CSR) for the tropics (20°N–20°S).

Appendix D

Vector Wind

A series of seven different data assimilation (corresponding to different observation scenarios) have been run for a summer and winter period.

Vector wind at 1000 and 200 hPa (mean scores in percent and Normalised rmse error for geographical and scatter plots)

At a particular level and variable the mean curves show the impact from the eight experiments, however only the sensors that show impact are further validated with geographical and significance scatter plots.

The mean plots are grouped into three selections of sensors in order to avoid too much congestion on a single plot:

AMSUA, HIRS and AIRS

SSMI, AMSUB and GEO CSRs

SCATT, GEO AMV and GEO CSRs (repeated)

The influence of the satellite sensors on the vector wind is strongest in Tropics and Southern Hemisphere.

Analysis of the impact is done for lower and upper levels as different satellite sensors sense different regions of the troposphere.

Surface wind (1000 hPa *AMV(REF)*

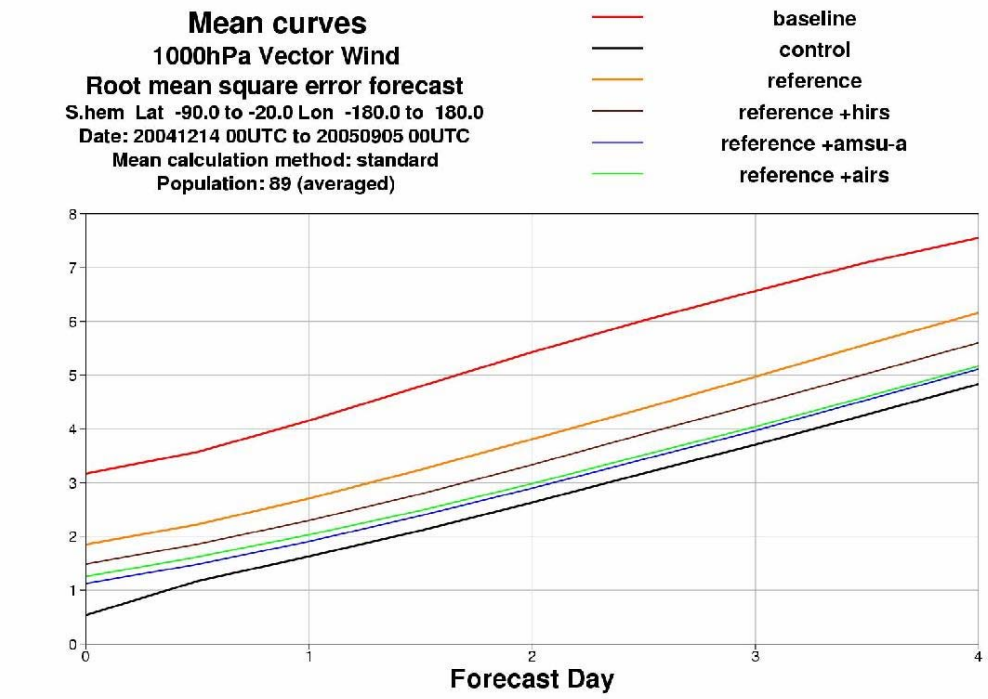

Figure D-1: Impact of three sensors (based on AMV(REF)) on 1000 hPa wind for (AMV(REF)+HIRS), (AMV(REF)+AMSUA) and (AMV(REF)+AIRS) for the southern hemisphere (20°S–90°S).

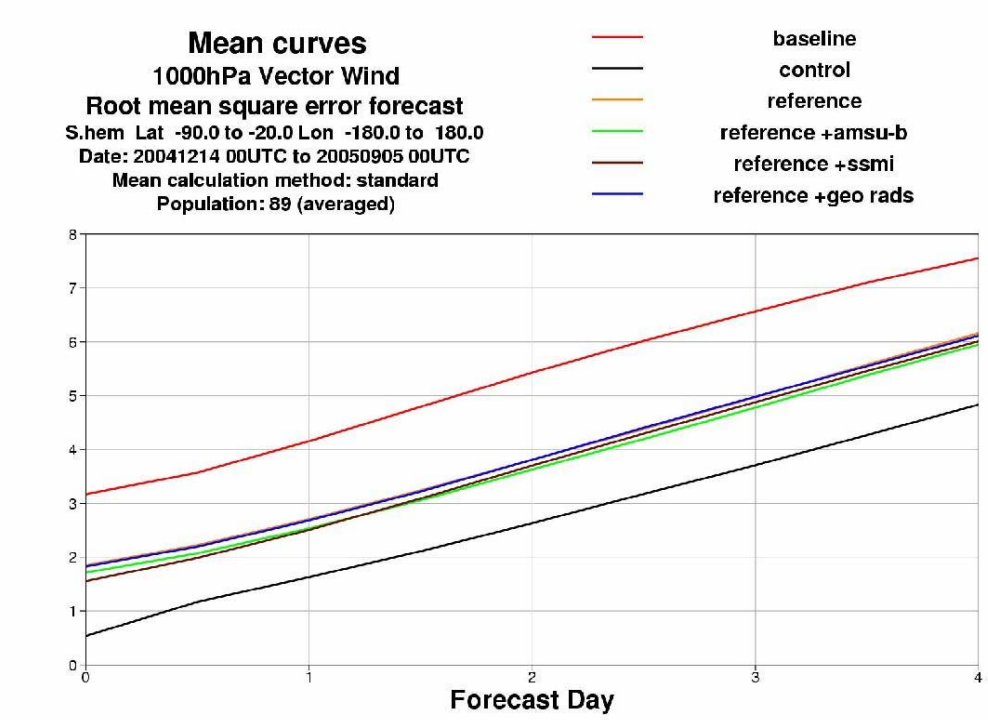

Figure D-2: Impact of three sensors (based on AMV(REF)) on 1000 hPa wind for (AMV(REF)+AMUA+AMSUB), (AMV(REF)+SSMI) and (AMV(REF)+CSRs) for the southern hemisphere (20°S–90°S).

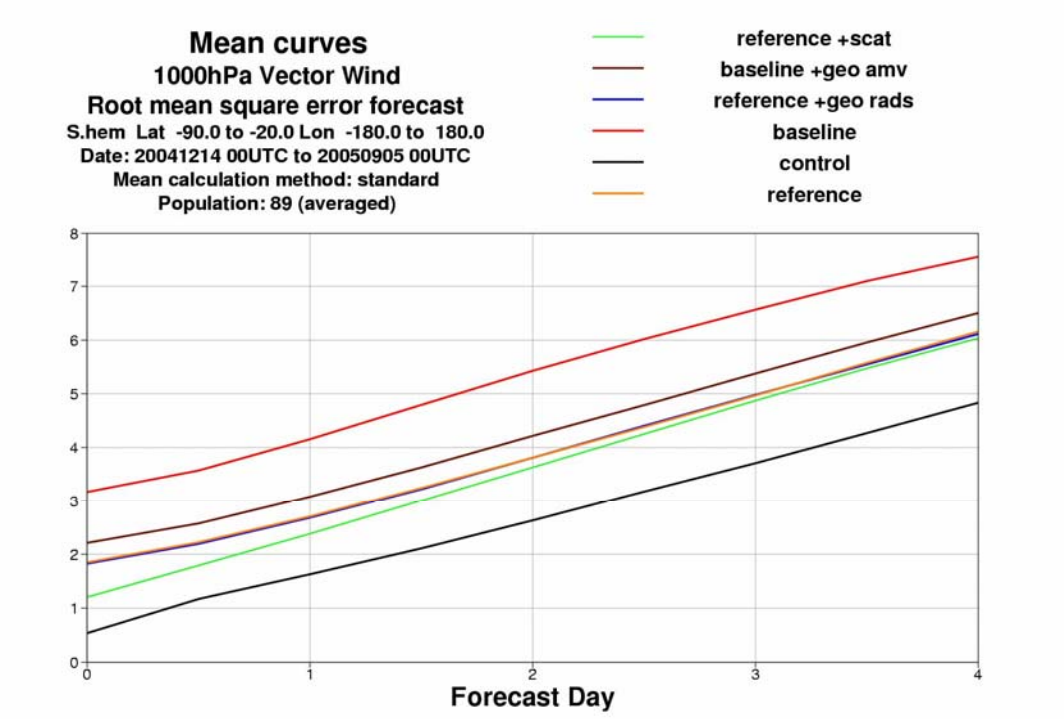

Figure D-3: Impact of three sensors (based on AMV(REF)) on 1000 hPa wind for (AMV(REF)+AMUA+SCAT), (Baseline) and (AMV(REF)+CSRs) for the southern hemisphere (20°S–90°S).

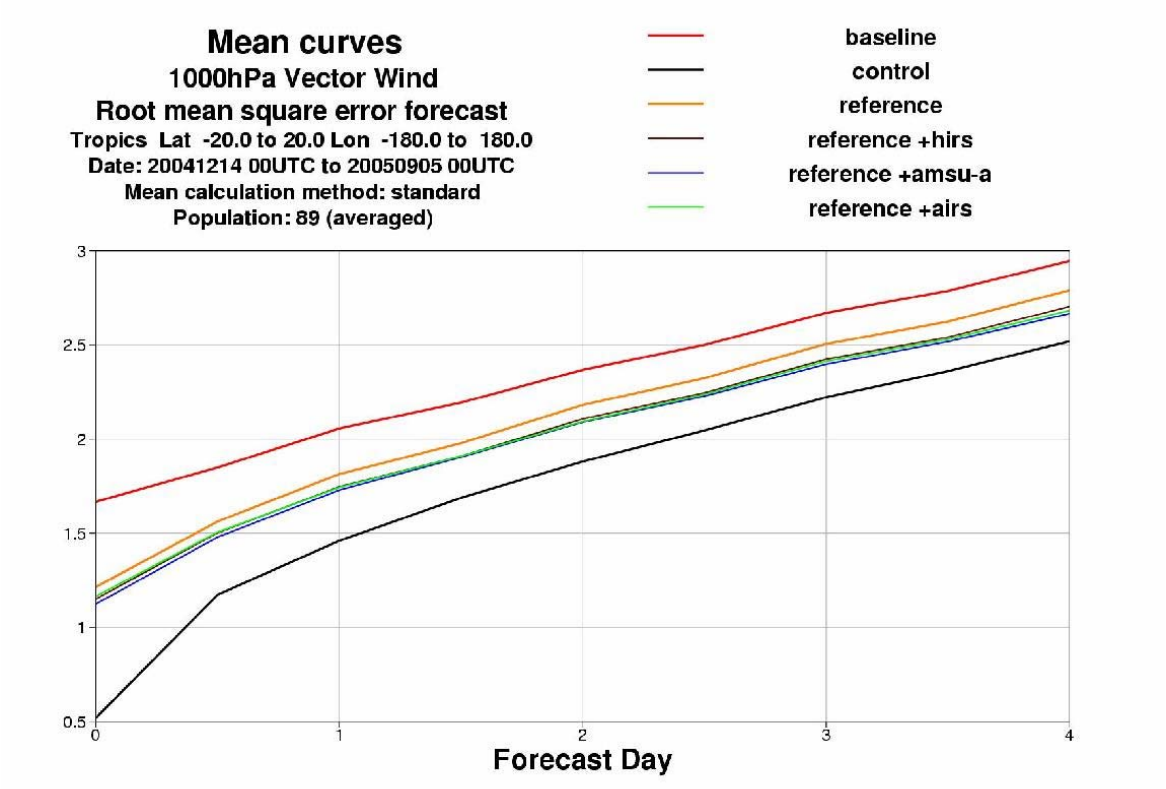

Figure D-4: Impact of three sensors (based on AMV(REF)) on 1000 hPa wind for (AMV(REF)+HIRS), (AMV(REF)+AMSUA) and (AMV(REF)+AIRS) for the tropics (20°N–20°S).

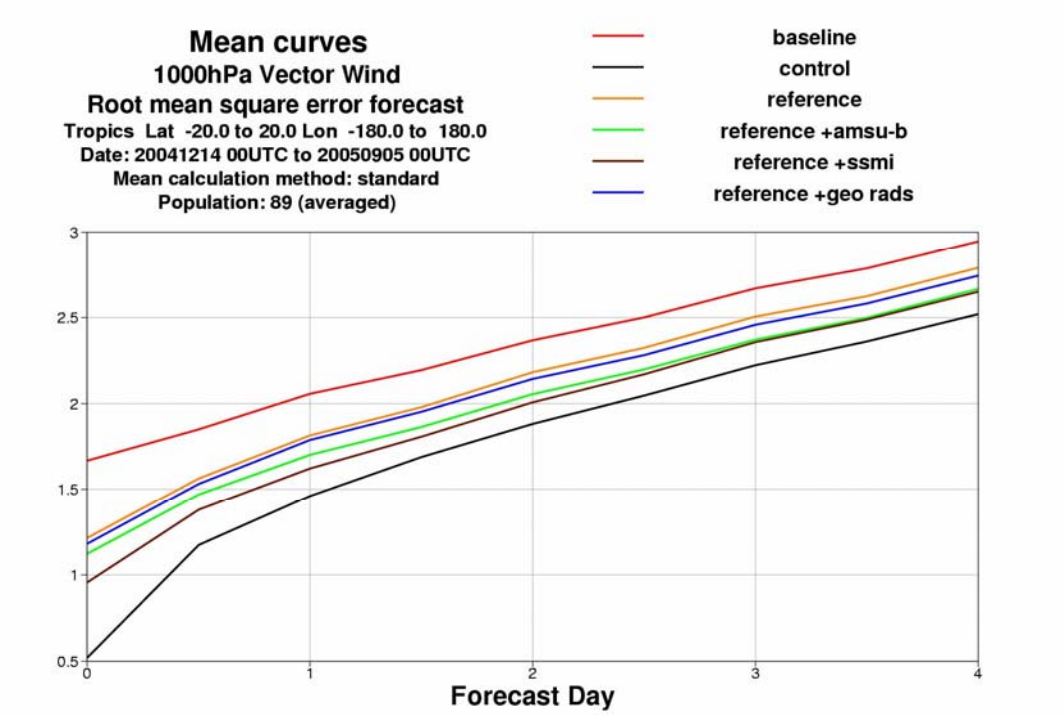

Figure D-5: Impact of three sensors (based on AMV(REF)) on 1000 hPa wind for (AMV(REF)+AMSUB), (AMV(REF)+SSMI) and (AMV(REF)+CSR) for the tropics (20°S–20°S).

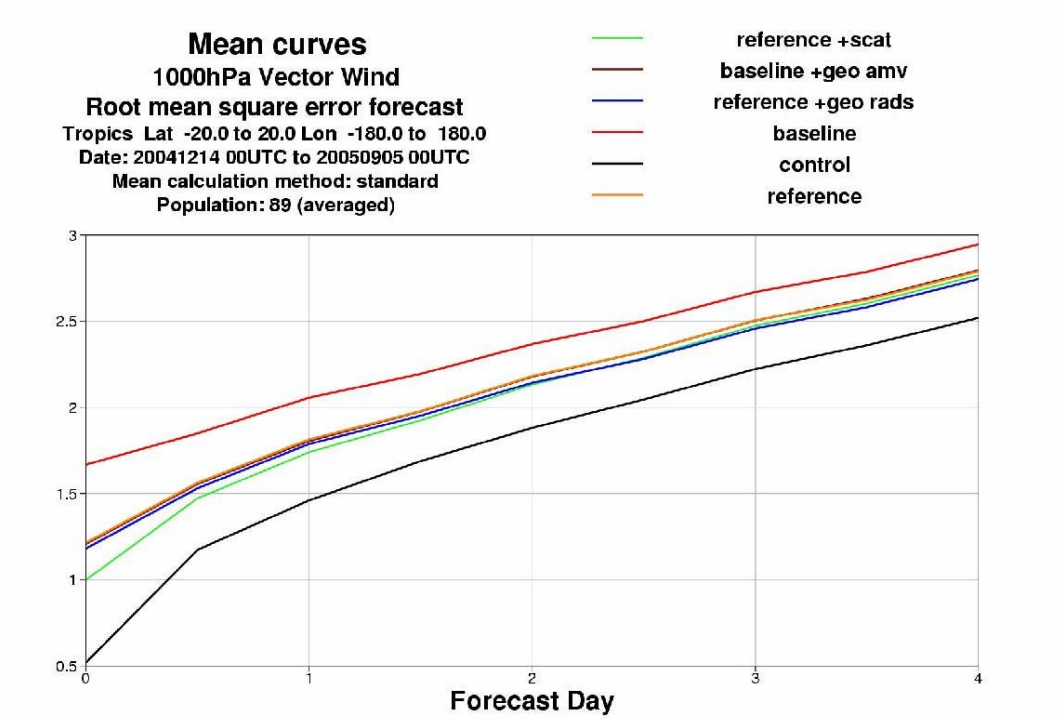

Figure D-6: Impact of three sensors (based on AMV(REF)) on 1000 hPa wind for (AMV(REF)+SCAT), (BASELINE+AMV(GEO) and (AMV(REF)+CSRs) for the tropics (20°S–20°S).

Impact of adding HIRS to the *AMV(REF)*

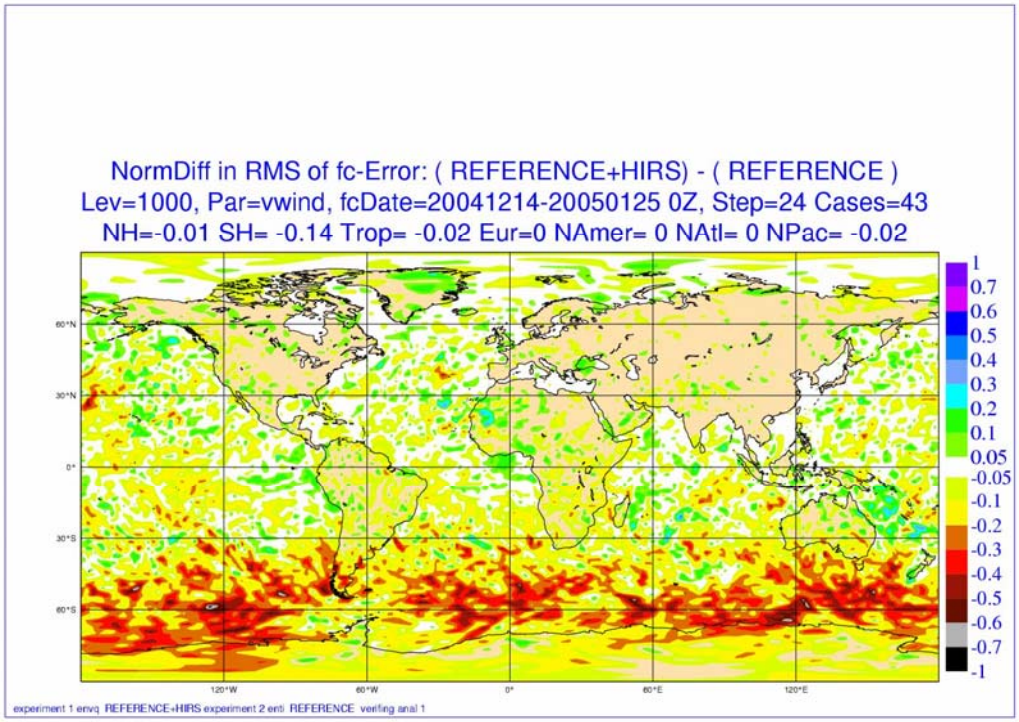

Figure D-7: Mean normalized 48-hour forecast error difference between AMV(REF)+HIRS and AMV(REF) for the 1000 hPa wind.

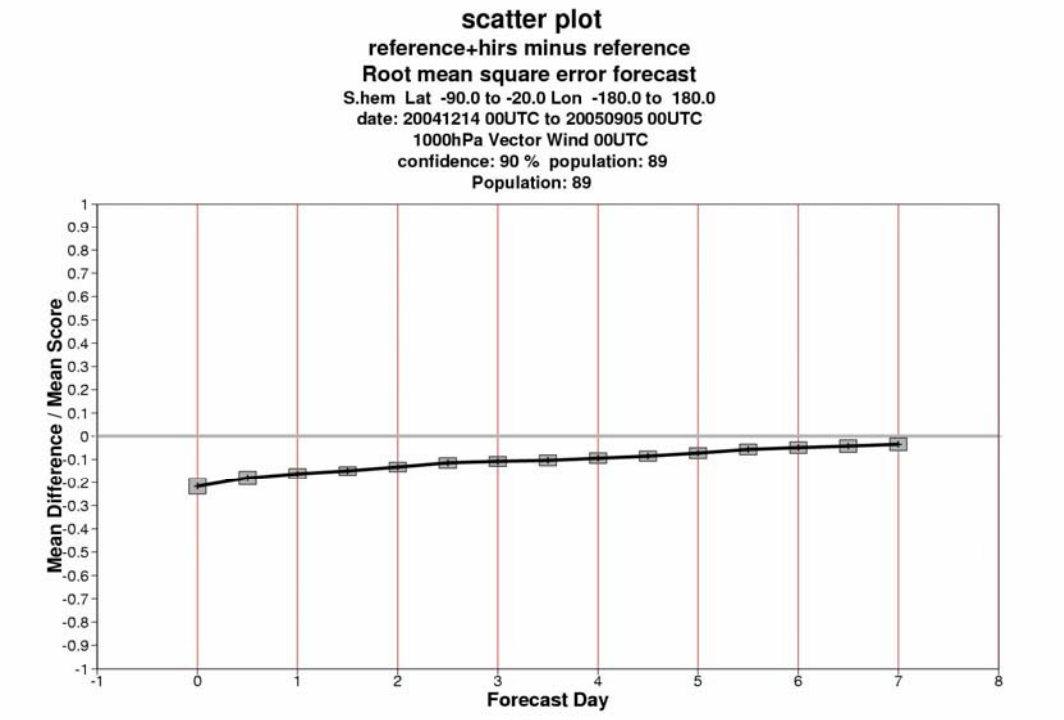

Figure D-8: Time series of normalized 1000 hPa wind rmse differences between AMV(REF)+ HIRS and AMV(REF) for forecast errors up to day 7 in the Southern Hemisphere. Negative values indicate positive impact for the AMV(REF)+HIRS.

Impact of adding AMSUA to the AMV(REF)

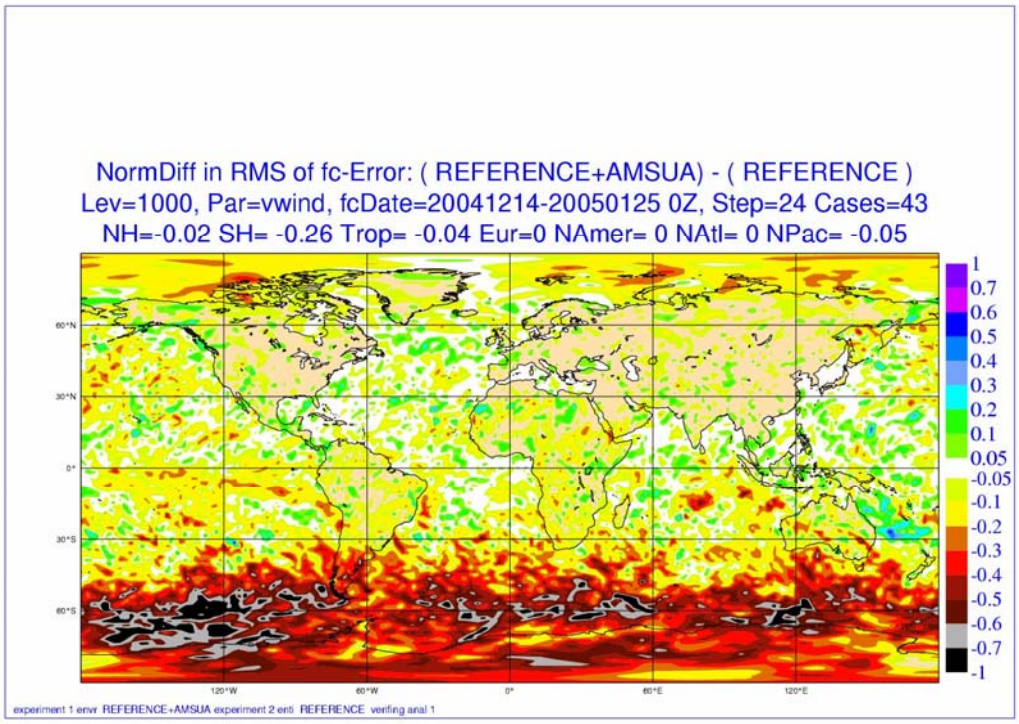

Figure D-9: Mean normalized 48-hour forecast error difference between AMV(REF)+AMSUA and AMV(REF) for the 1000 hPa wind.

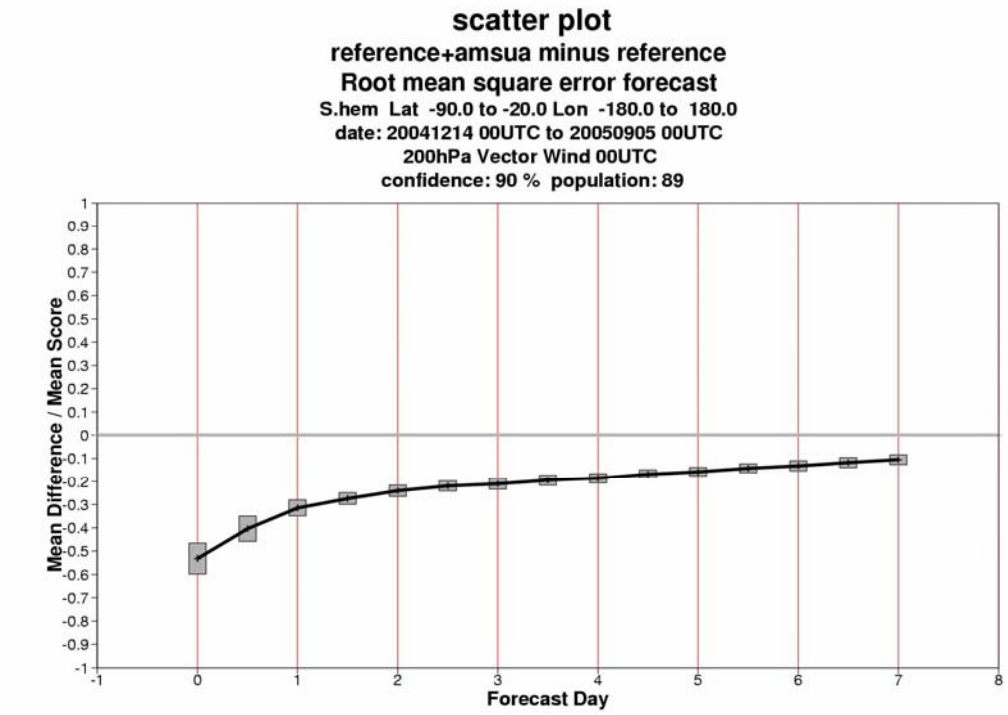

Figure D- 10: Time series of normalized 1000 hPa wind rmse differences between AMV(REF)+ AMSUA and AMV(REF) for forecast errors up to day 7 in the Southern Hemisphere. Negative values indicate positive impact for the AMV(REF)+AMSUA

Impact of adding SSMI to the *AMV(REF)*

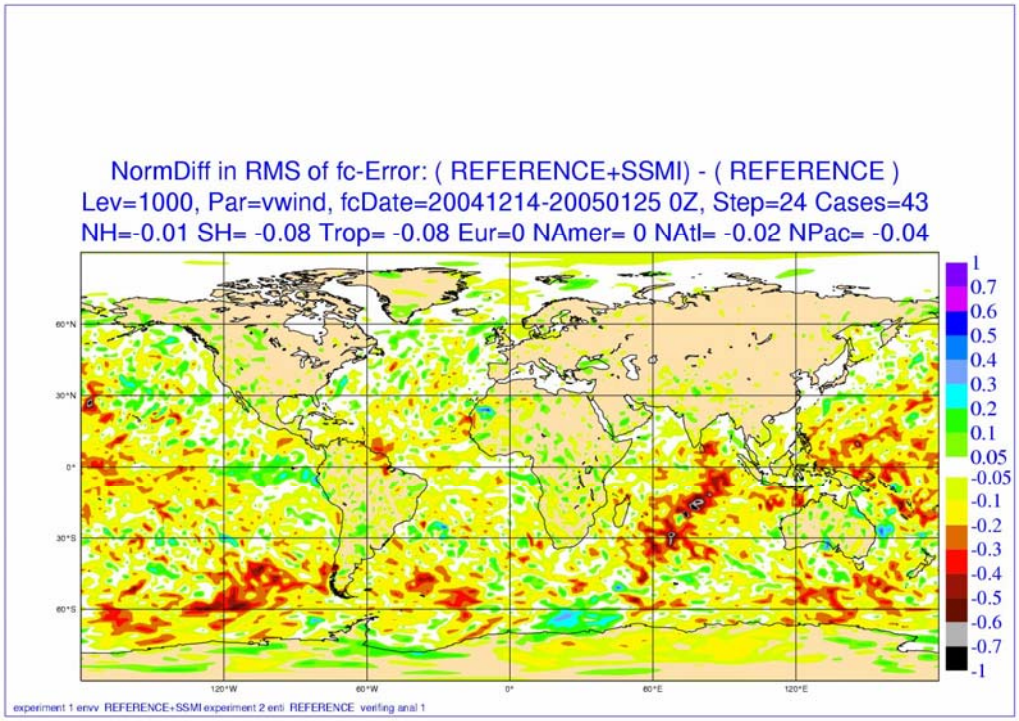

Figure D-11: Mean normalized 48-hour forecast error difference between AMV(REF)+SSMI and AMV(REF) for the 1000 hPa wind.

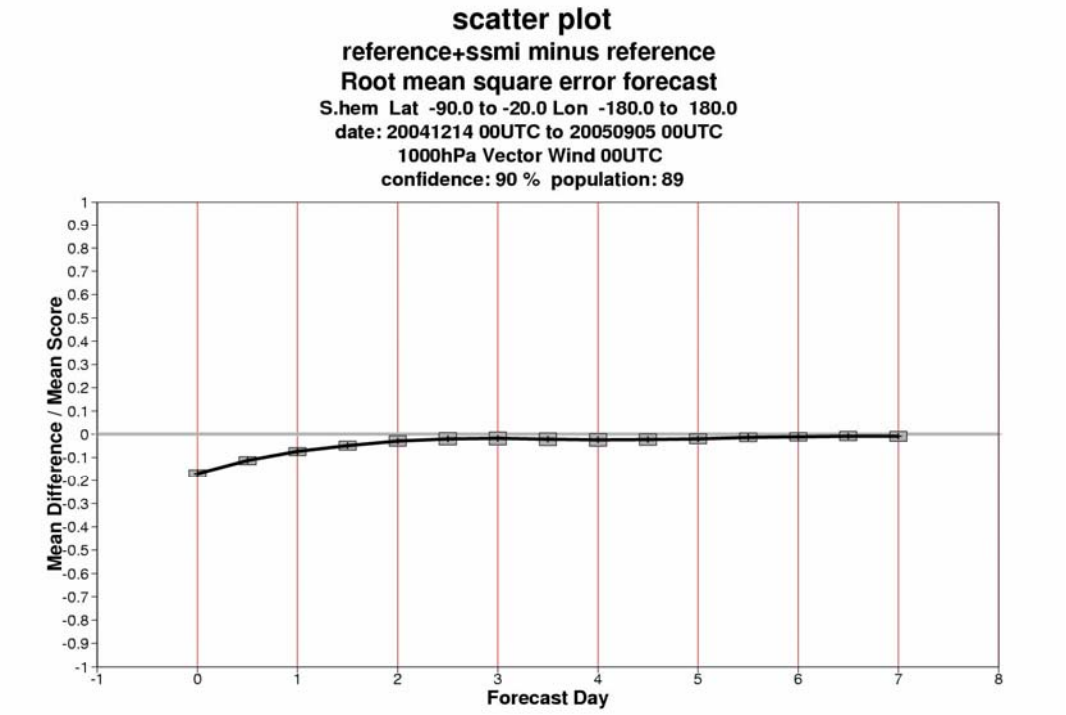

Figure D-12: Time series of normalized 1000 hPa wind rmse differences between AMV(REF)+ SSMI and AMV(REF) for forecast errors up to day 7 in the Southern Hemisphere. Negative values indicate positive impact for the AMV(REF)+SSMI.

Impact of adding AIRS to the *AMV(REF)*

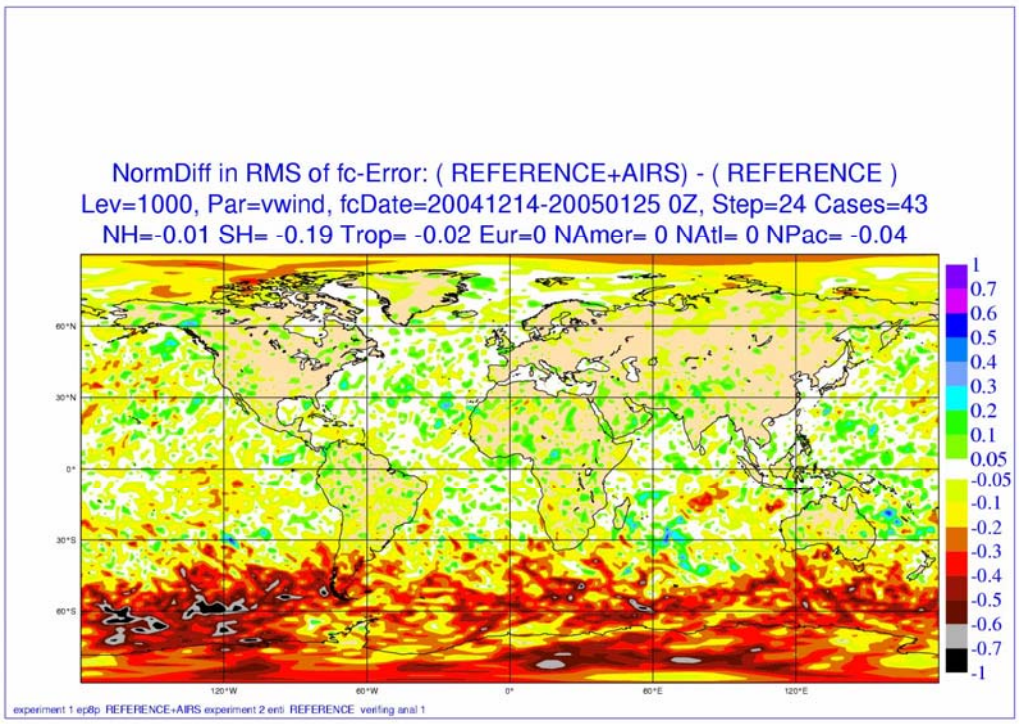

Figure D-13: Mean normalized 48-hour forecast error difference between AMV(REF)+AIRS and AMV(REF) for the 1000 hPa wind.

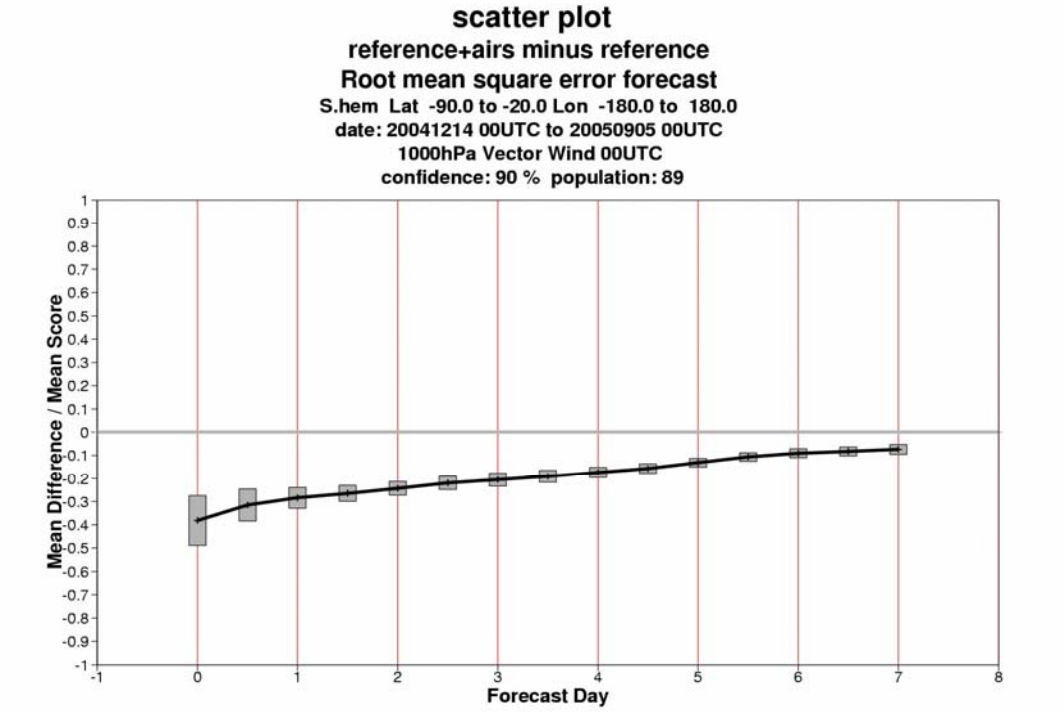

Figure D-14: Time series of normalized 1000 hPa wind rmse differences between AMV(REF)+ AIRS and AMV(REF) for forecast errors up to day 7 in the Southern Hemisphere. Negative values indicate positive impact for the AMV(REF)+AIRS.

Impact of adding SCAT to the *AMV(REF)*

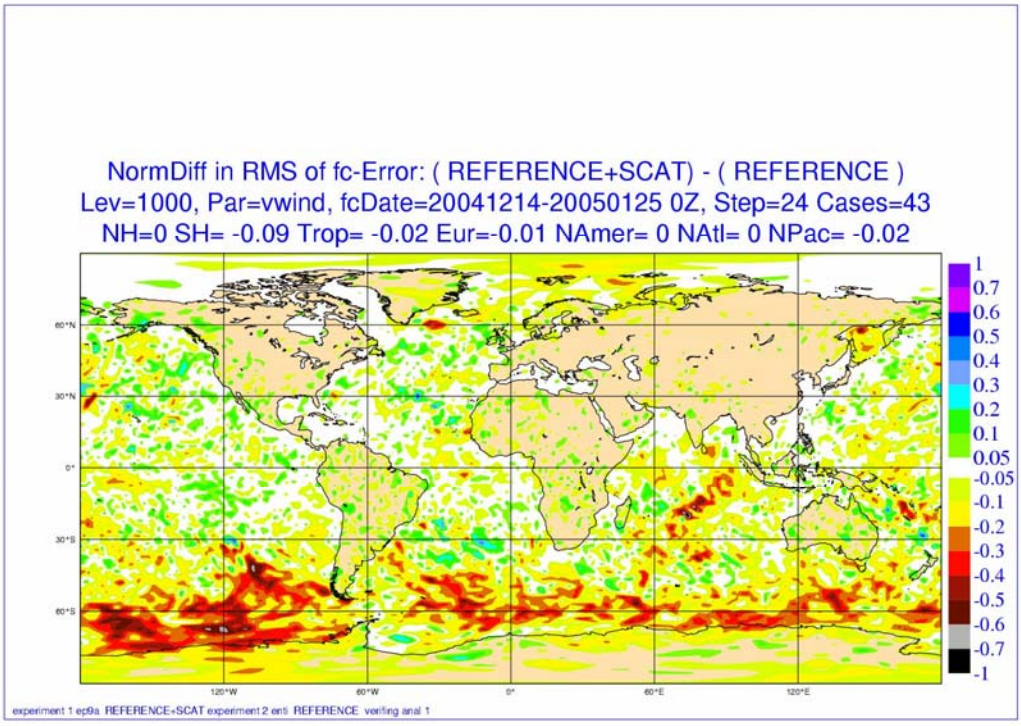

Figure D-15: Mean normalized 48-hour forecast error difference between AMV(REF)+SCAT and AMV(REF) for the 1000 hPa wind.

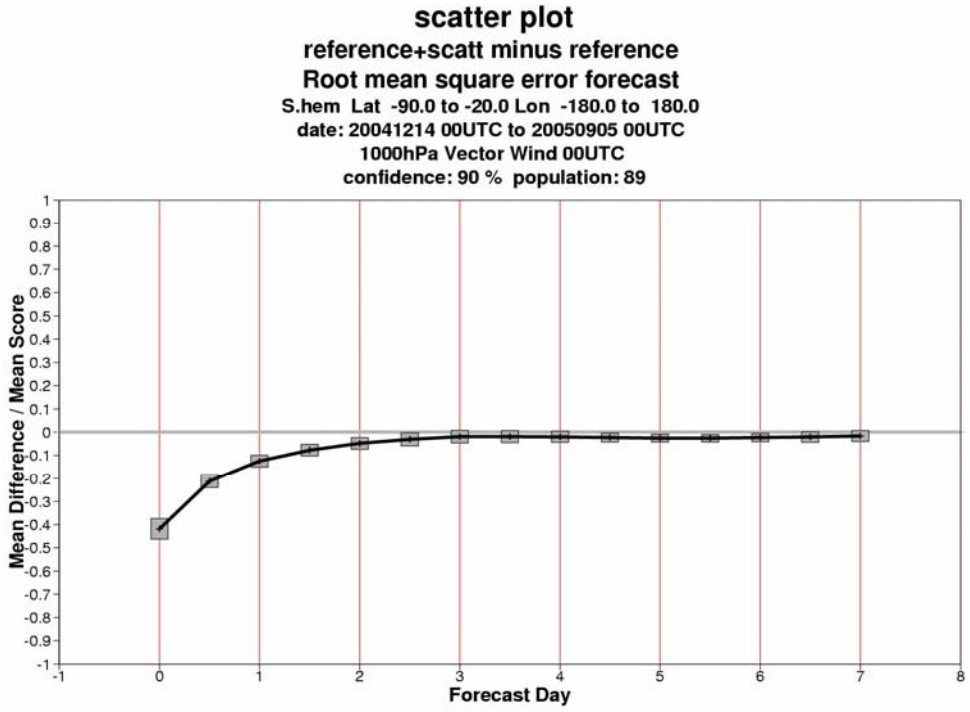

Figure D-16: Time series of normalized 1000 hPa wind rmse differences between AMV(REF)+ SCAT and AMV(REF) for forecast errors up to day 7 in the Southern Hemisphere. Negative values indicate positive impact for the AMV(REF)+SCAT.

Surface wind (1000 hPa AMSUA(REF)

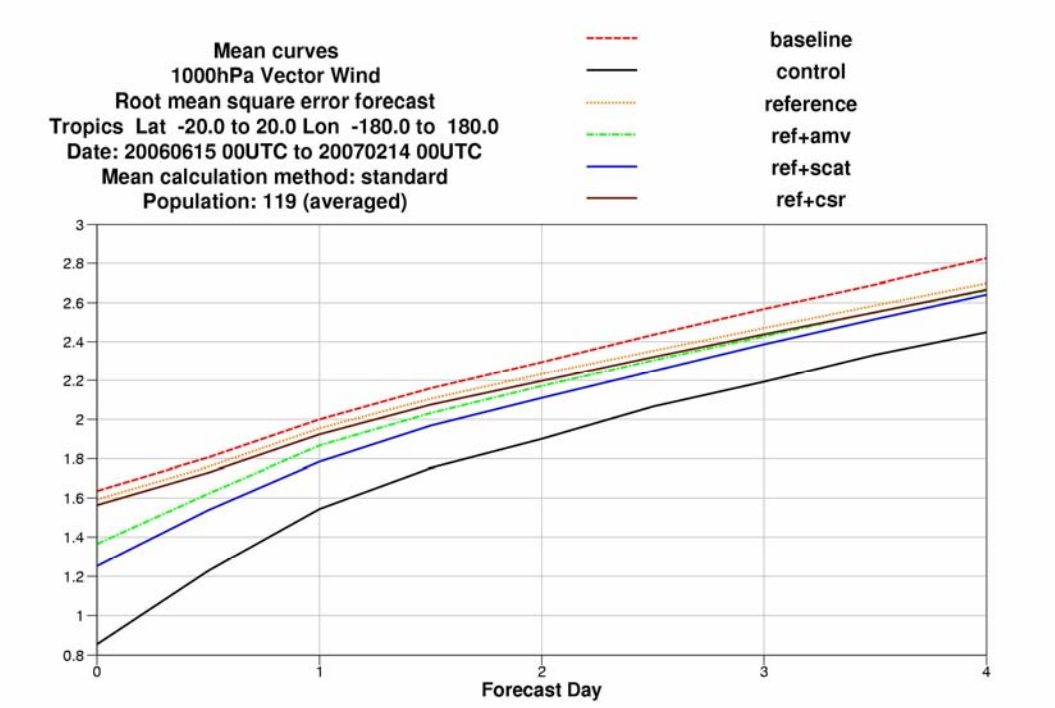

Figure D-17: Impact of three sensors (based on AMSUA(REF)) on 1000 hPa wind for (AMSUA(REF)+AMVs), (AMSUA(REF)+SCAT) and (AMSUA(REF)+CSRs) for the tropics.

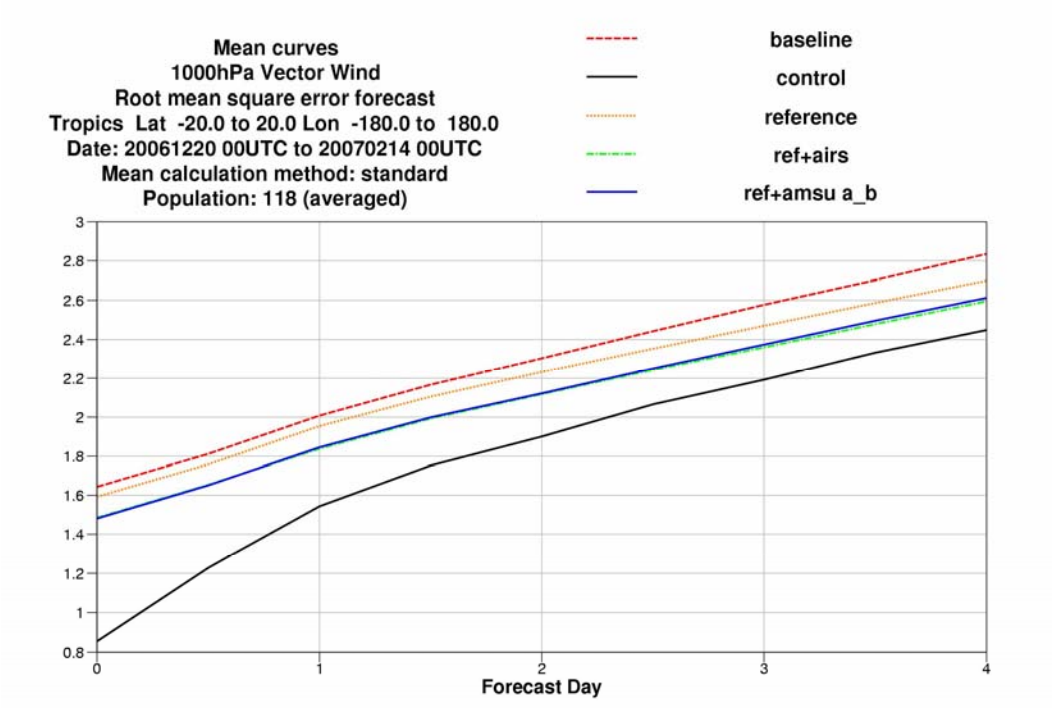

Figure D-18: Impact of two sensors (based on AMV(REF)) on 1000 hPa wind for (AMV(REF)+AMUA+AMSUB) and (AMV(REF)+AIRS) for the tropics.

Upper level wind (200hPa *AMV(REF)*

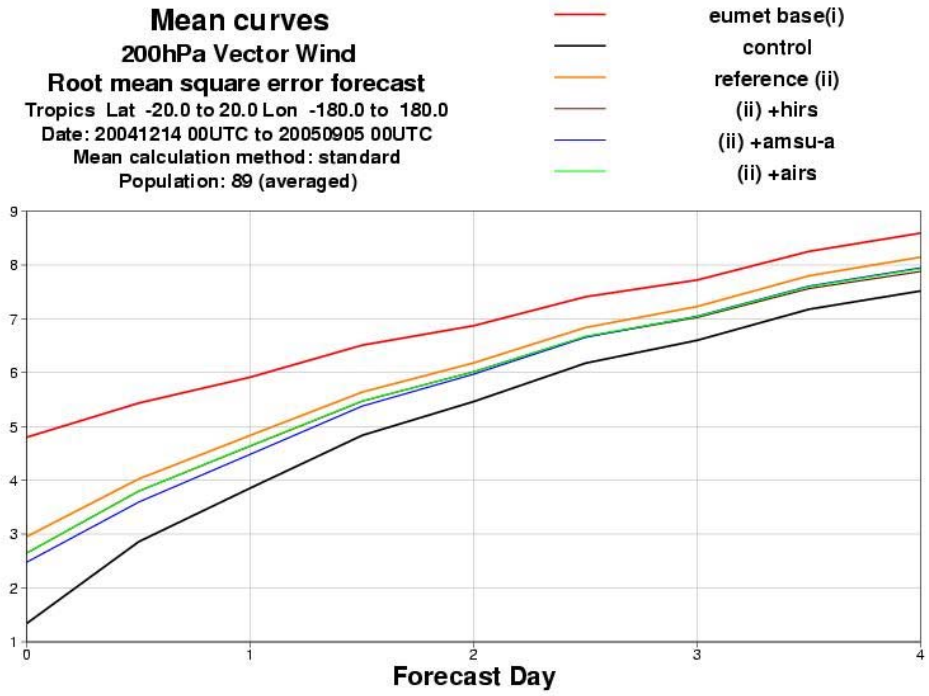

Figure D-19: Impact of three sensors (based on AMV(REF)) on 200 hPa wind for (AMV(REF)+HIRS), (AMV(REF)+AMSUA) and (AMV(REF)+AIRS) for the tropics.

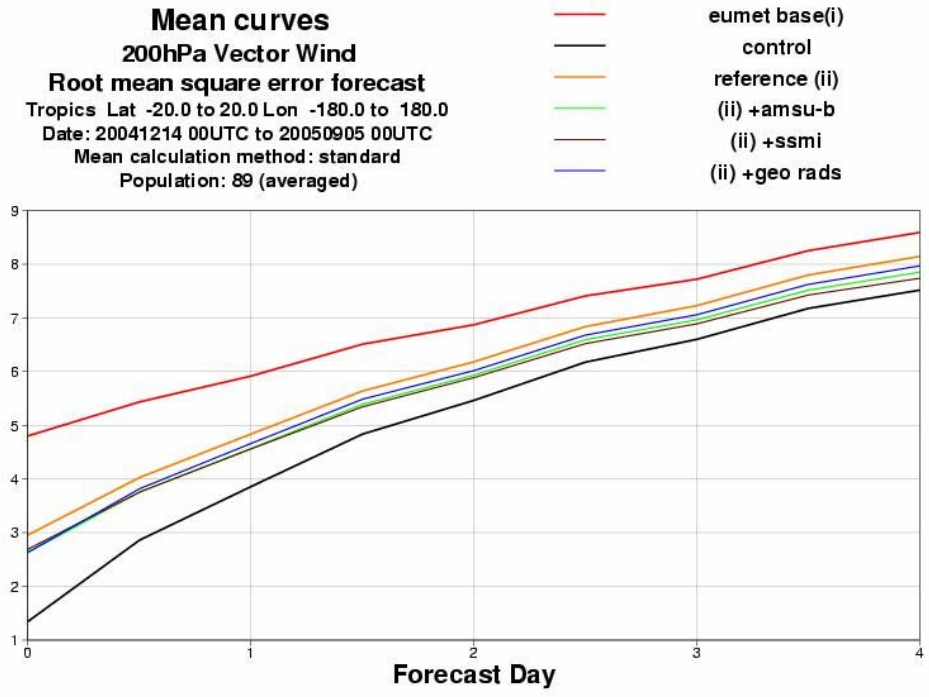

Figure D-20: Impact of three sensors (based on AMV(REF)) on 200 hPa wind for (AMV(REF)+ AMSUB), (AMV(REF)+SSMI) and (AMV(REF)+CSRs) for the tropics.

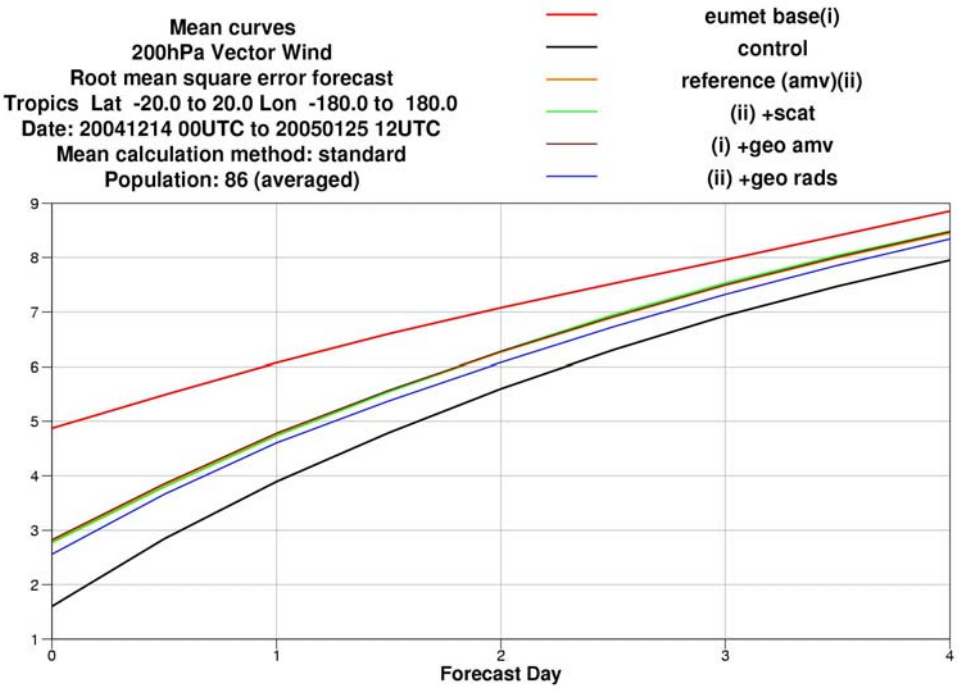

Figure D-21: Impact of three sensors (based on AMV(REF)) on 200 hPa wind for (AMV(REF)+SCAT), (Baseline+AMVs(GEO)) and (AMV(REF)+CSRs) for the tropics.

Impact of adding HIRS to the *AMV(REF)*

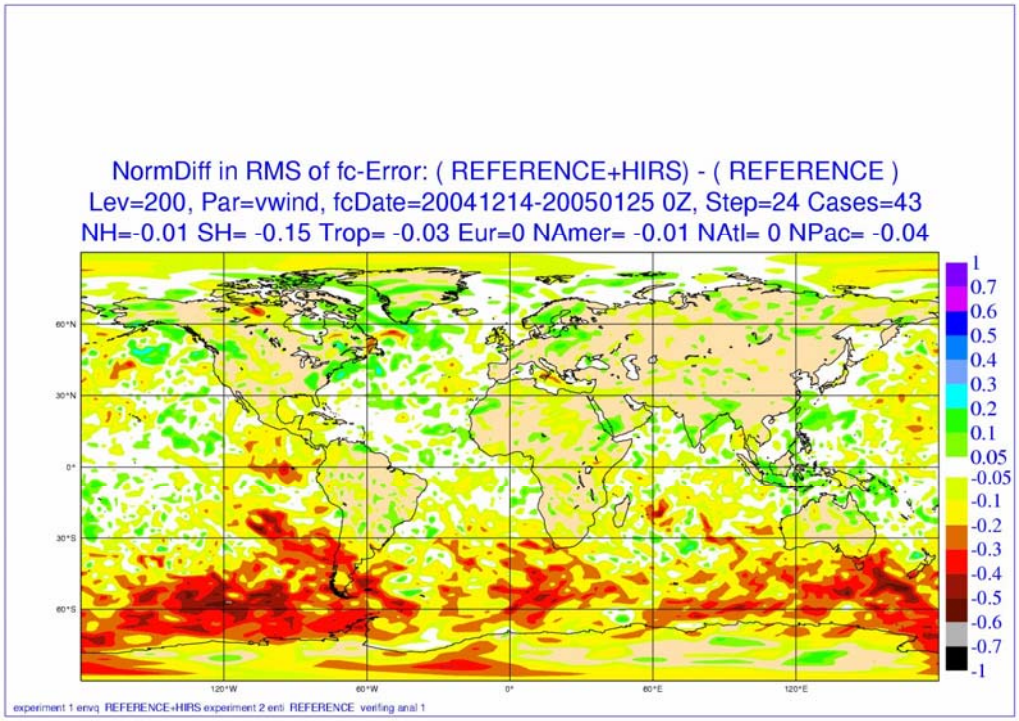

Figure D-22: Mean normalized 48-hour forecast error difference between AMV(REF)+HIRS and AMV(REF) for the 200 hPa wind.

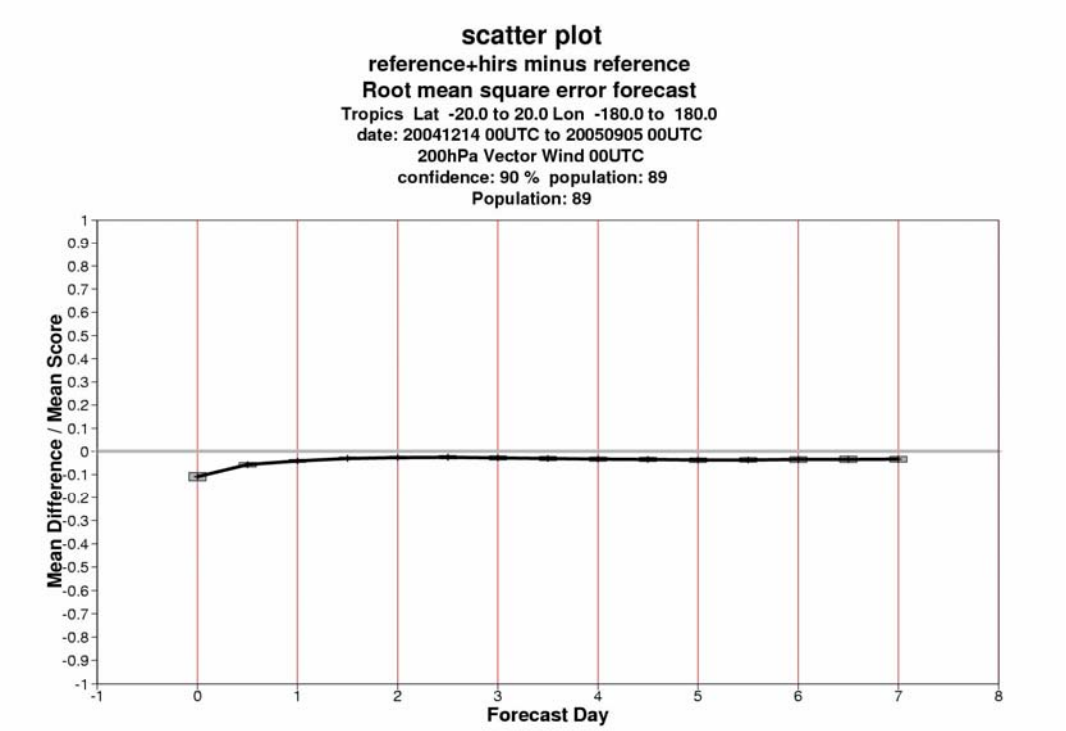

Figure D-23: Time series of normalized 200 hPa wind rmse differences between AMV(REF)+ HIRS and AMV(REF) for forecast errors up to day 7 in the Tropics. Negative values indicate positive impact for the AMV(REF)+HIRS.

Impact of adding AMSUA to the*AMV(REF)*

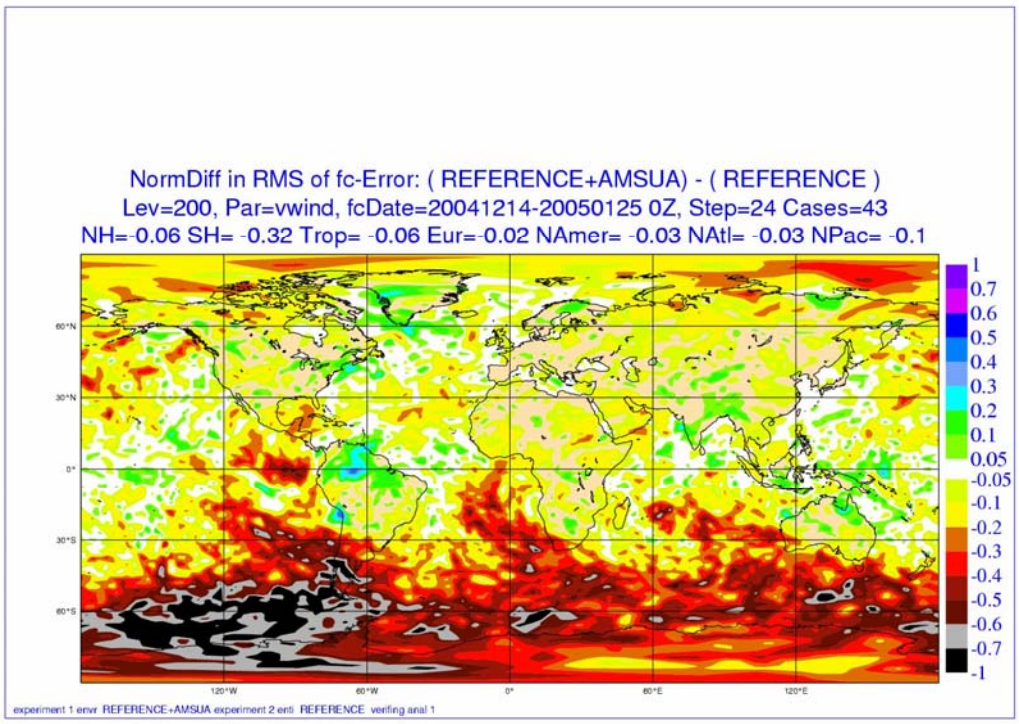

Figure D-24: Mean normalized 48-hour forecast error difference between AMV(REF)+AMSUA and AMV(REF) for the 200 hPa wind.

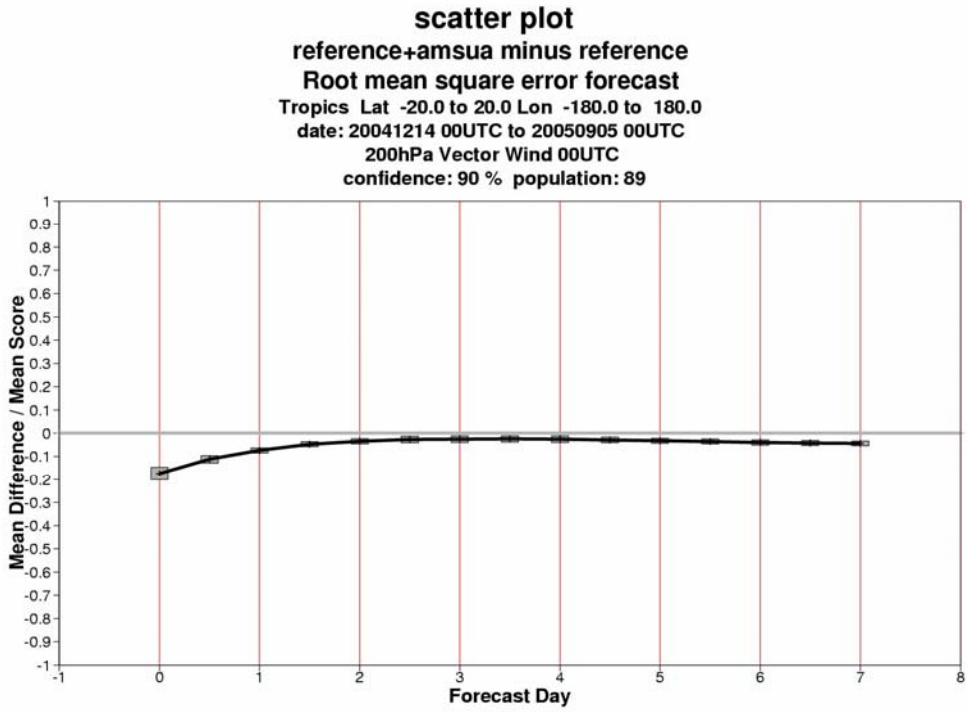

Figure D-25: Time series of normalized 200 hPa wind rmse differences between AMV(REF)+ AMSUA and AMV(REF) for forecast errors up to day 7 in the Tropics. Negative values indicate positive impact for the AMV(REF)+AMSUA.

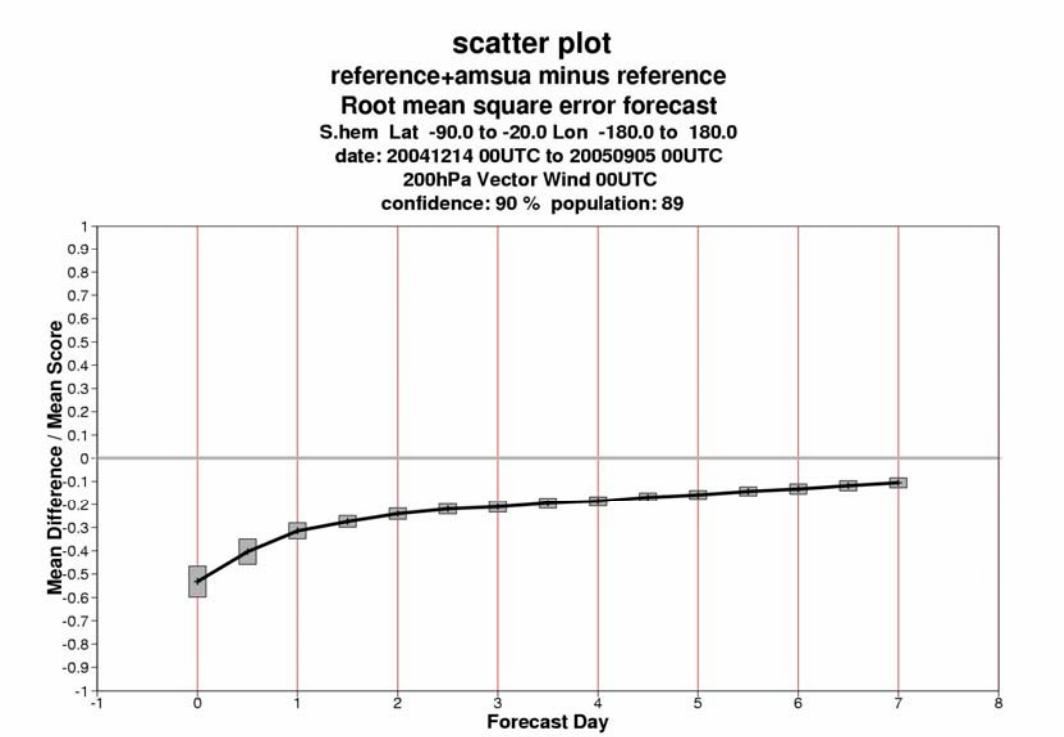

Figure D-26: Time series of normalized 200 hPa wind rmse differences between AMV(REF)+ AMSUA and AMV(REF) for forecast errors up to day 7 in the Southern Hemisphere. Negative values indicate positive impact for the AMV(REF)+AMSUA.

Impact of adding AIRS to the *AMV(REF)*

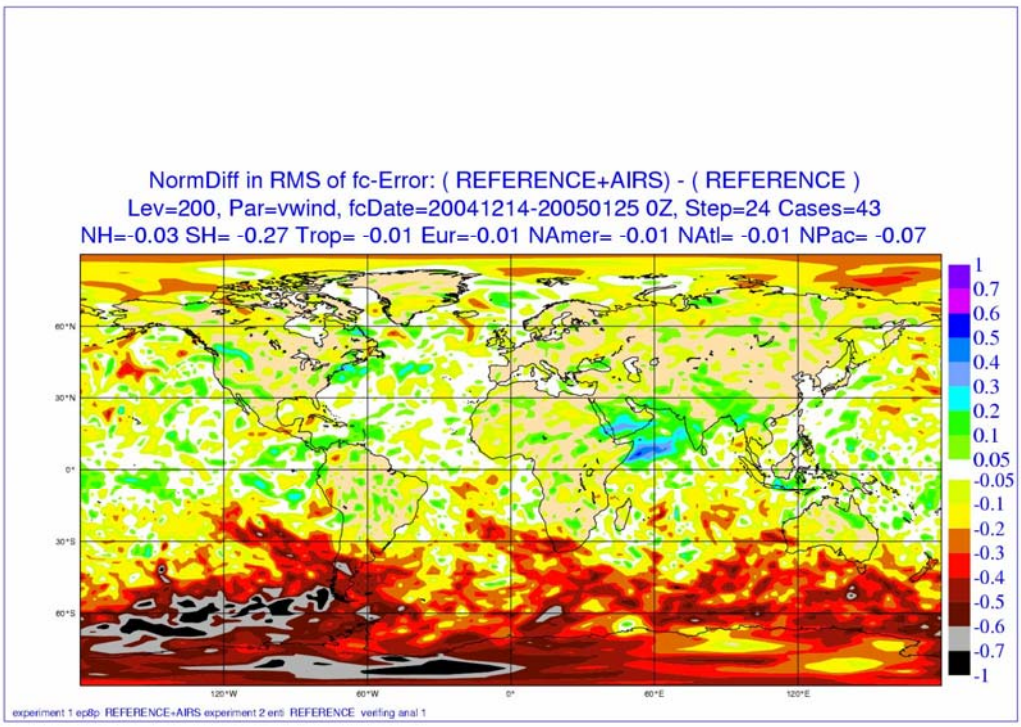

Figure D-27: Mean normalized 48-hour forecast error difference between AMV(REF)+AIRS and AMV(REF) for the 200 hPa wind.

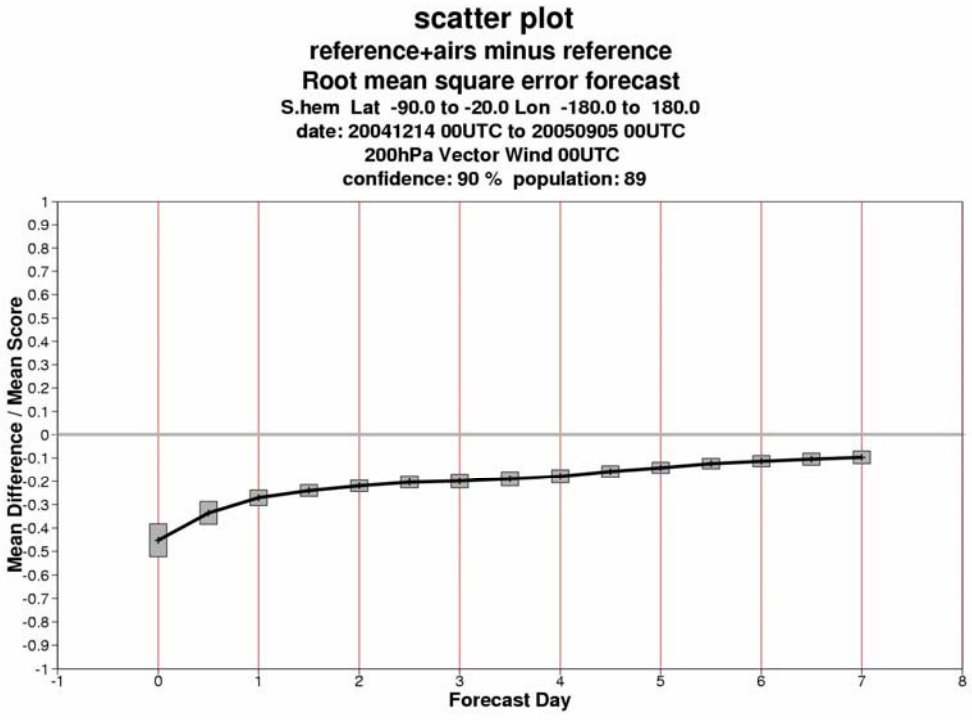

Figure D-28: Time series of normalized 200 hPa wind rmse differences between AMV(REF)+ AIRS and AMV(REF) for forecast errors up to day 7 in the Southern Hemisphere. Negative values indicate positive impact for the AMV(REF)+AIRS.

Impact of adding CSRs to the *AMV(REF)*

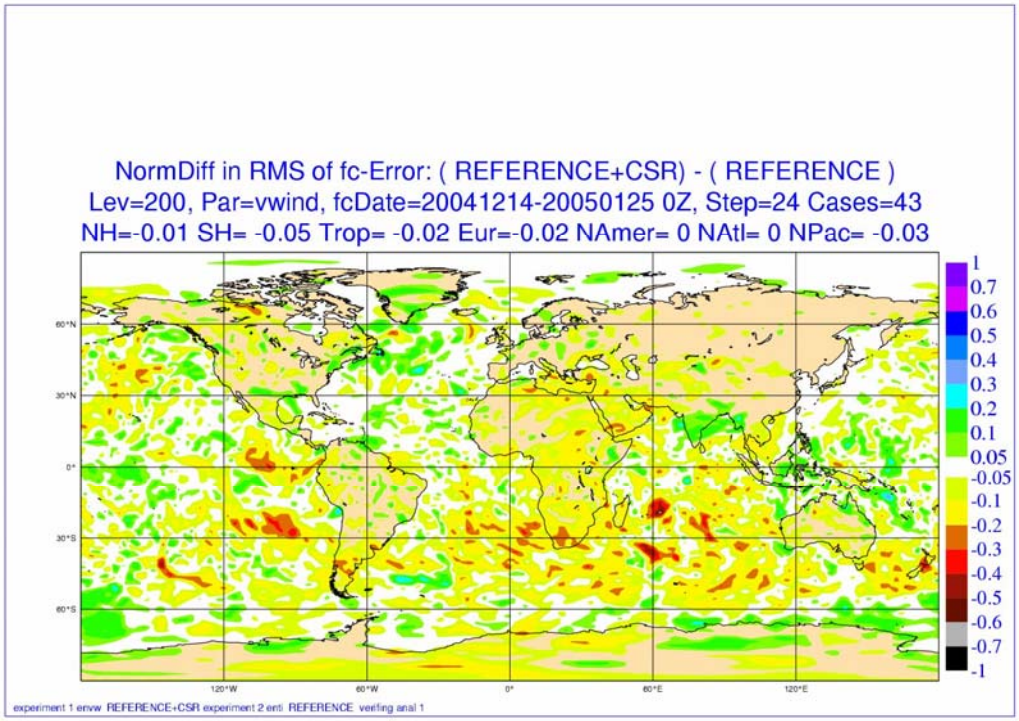

Figure D-29: Mean normalized 48-hour forecast error difference between AMV(REF)+CSRs and AMV(REF) for the 200 hPa wind.

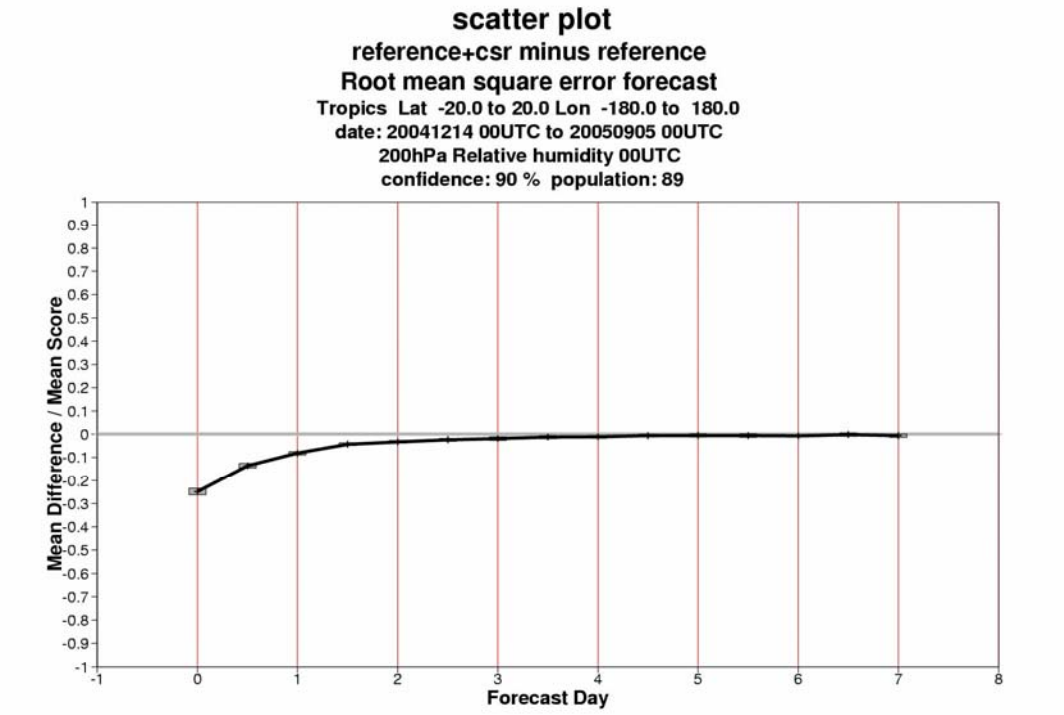

Figure D-30: Time series of normalized 200 hPa relative humidity rmse differences between AMV(REF)+ CSRs and AMV(REF) for forecast errors up to day 7 in the Tropics. Negative values indicate positive impact for the AMV(REF)+CSRs.

Upper level wind (200hPa AMSUA(REF)

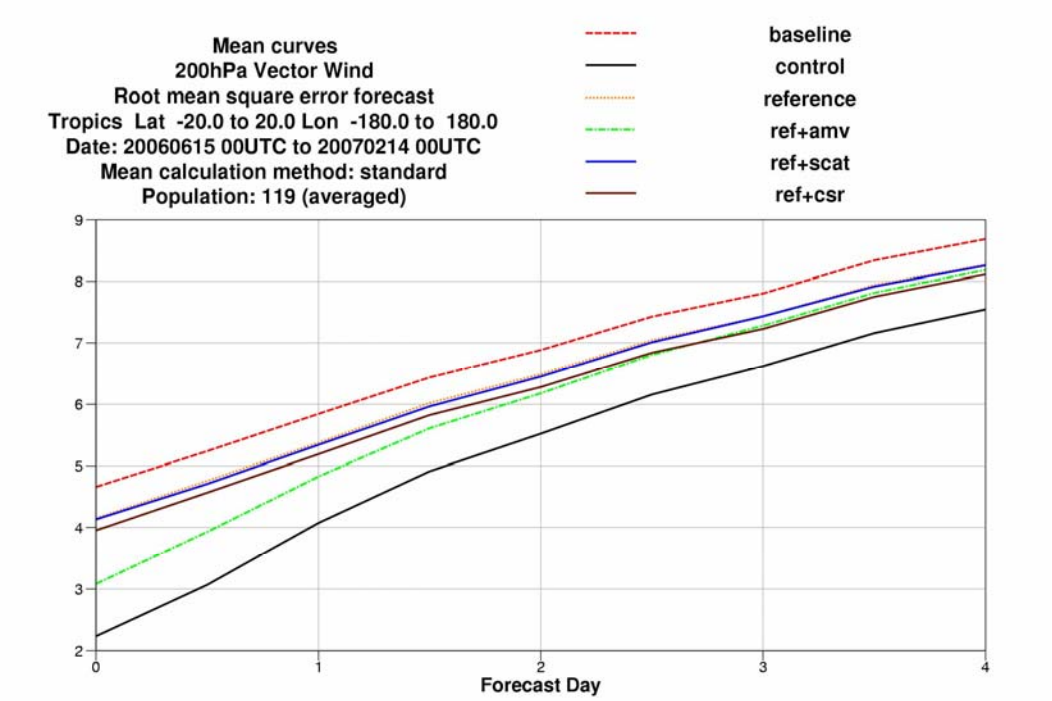

Figure D-31: Impact of three sensors (based on AMV(REF)) on 200 hPa wind for (AMV(REF)+ AMVs), (AMV(REF)+SCAT) and (AMV(REF)+CSRs) for the tropics.

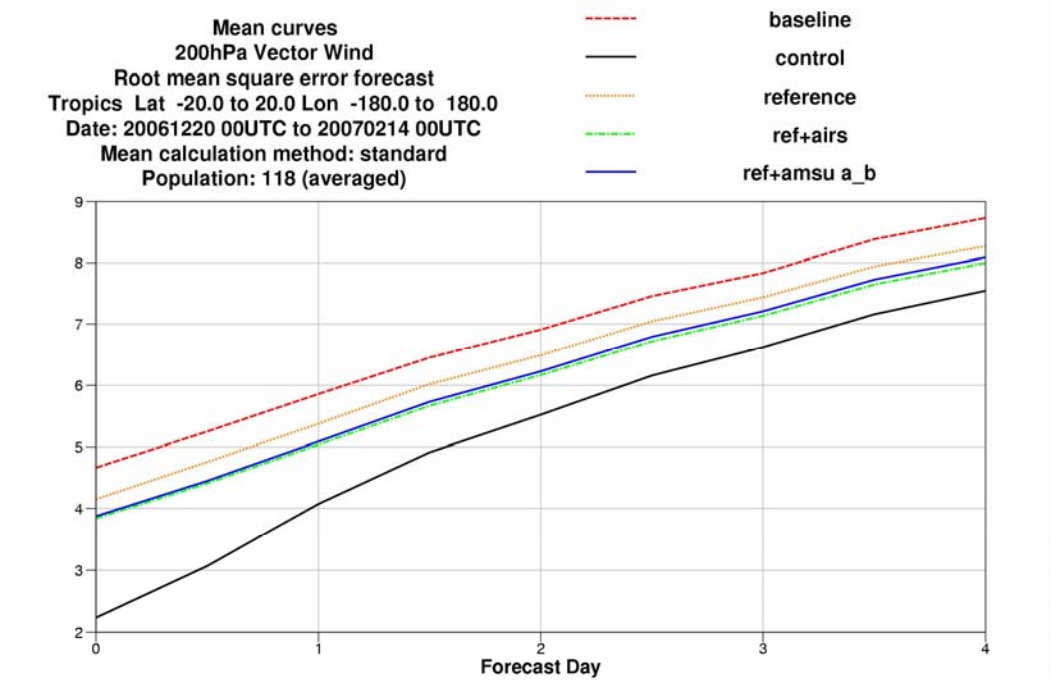

Figure D-32: Impact of three sensors (based on AMV(REF)) on 200 hPa wind for (AMV(REF)+ AIRS) and (AMV(REF)+AMSUA/B) for the Tropics.

Appendix E

MODIS AMVs

Impact of removing MODIS from the *AMV(REF)*

Significant impact comes from the removal of the MODIS winds from the AMV(REF) system.

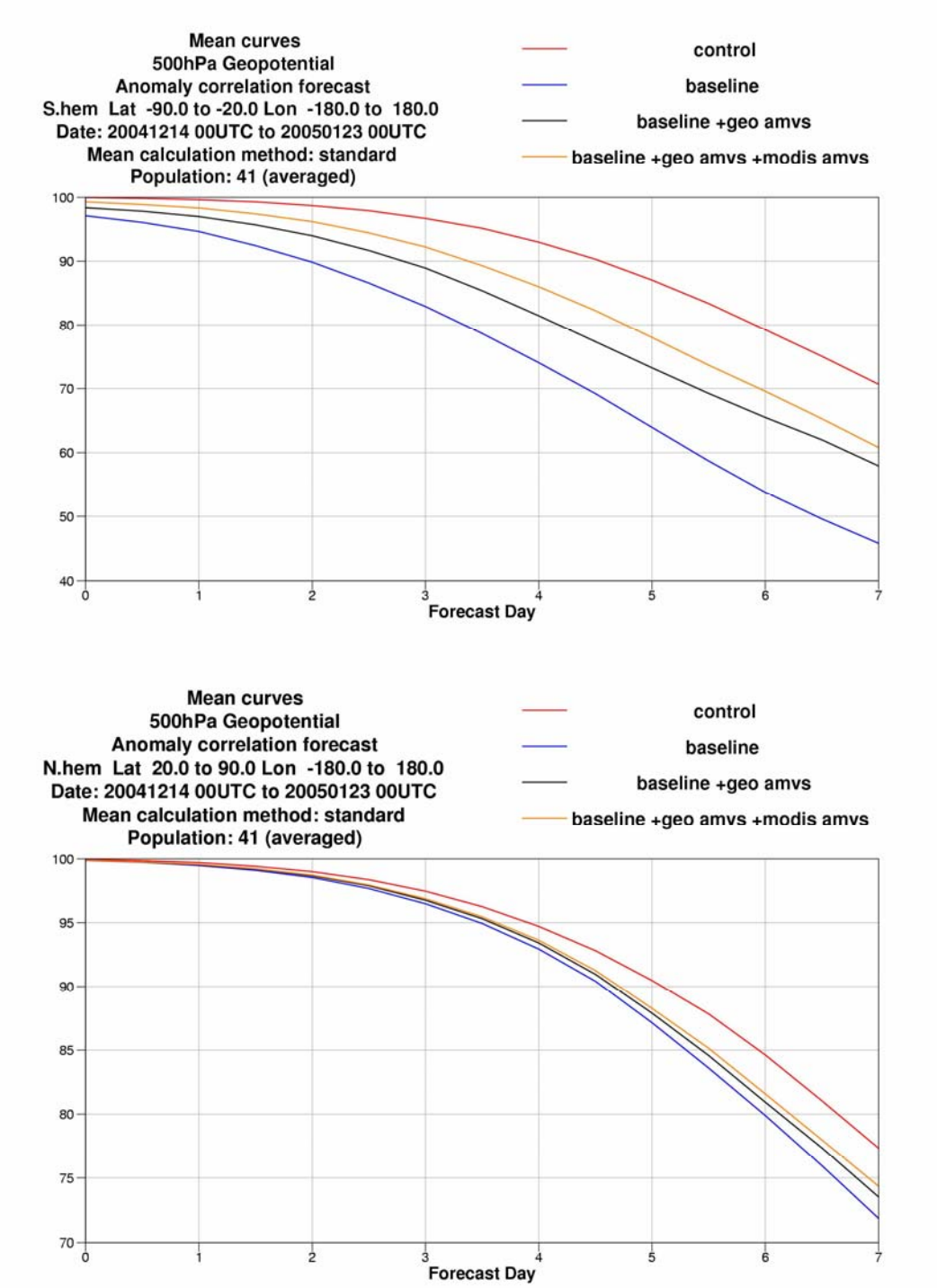

Figure E-1: Impact of modis AMVs on 500 hPa geopotential for (Baseline + AMVs(GEO)) and (Baseline + AMVs (GEO_Modis) for the Southern hemisphere(top) and the Northern hemisphere(bottom).

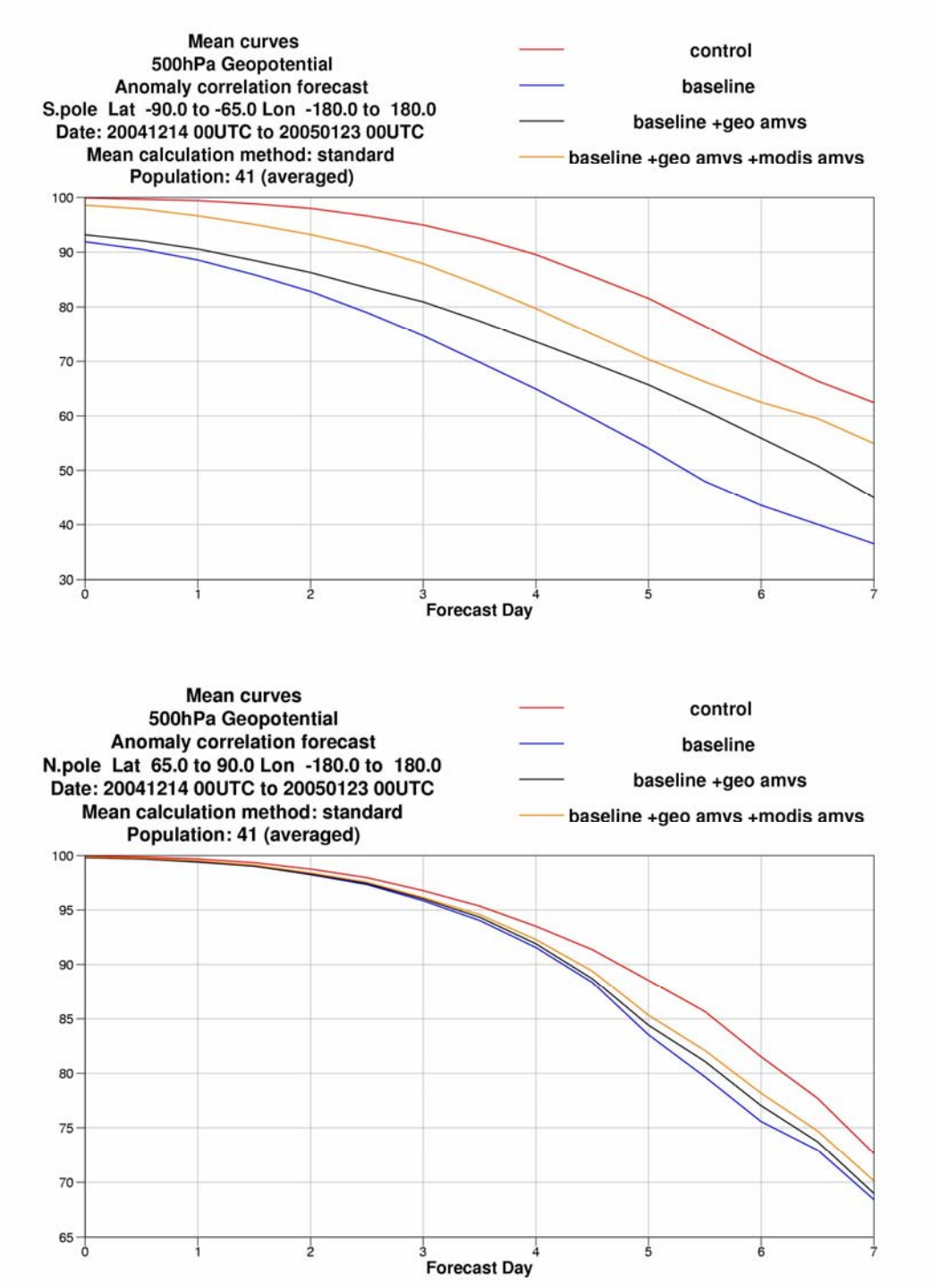

Figure E-2: Impact of modis AMVs on 500 hPa geopotential for (Baseline + AMVs(GEO)) and (Baseline + AMVs (GEO_Modis) for the Southern pole(top) and the Northern pole(bottom).

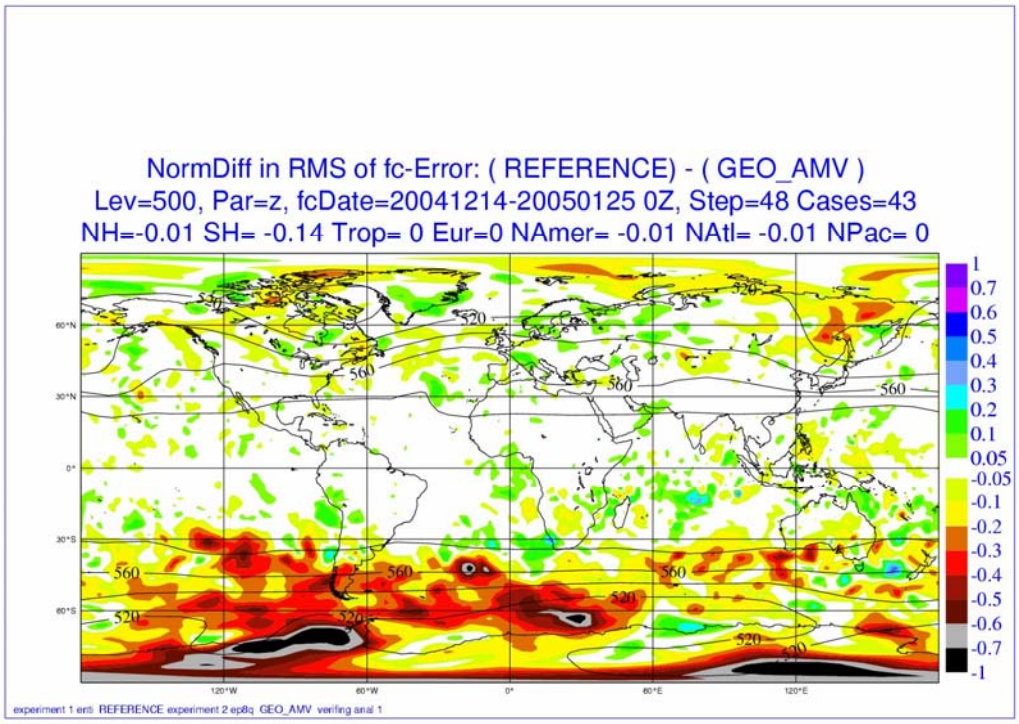

Figure E-3: Mean normalized 48-hour forecast error difference between AMV(REF) and AMV(REF)-GEO(AMV) for the 500 hPa geopotential.

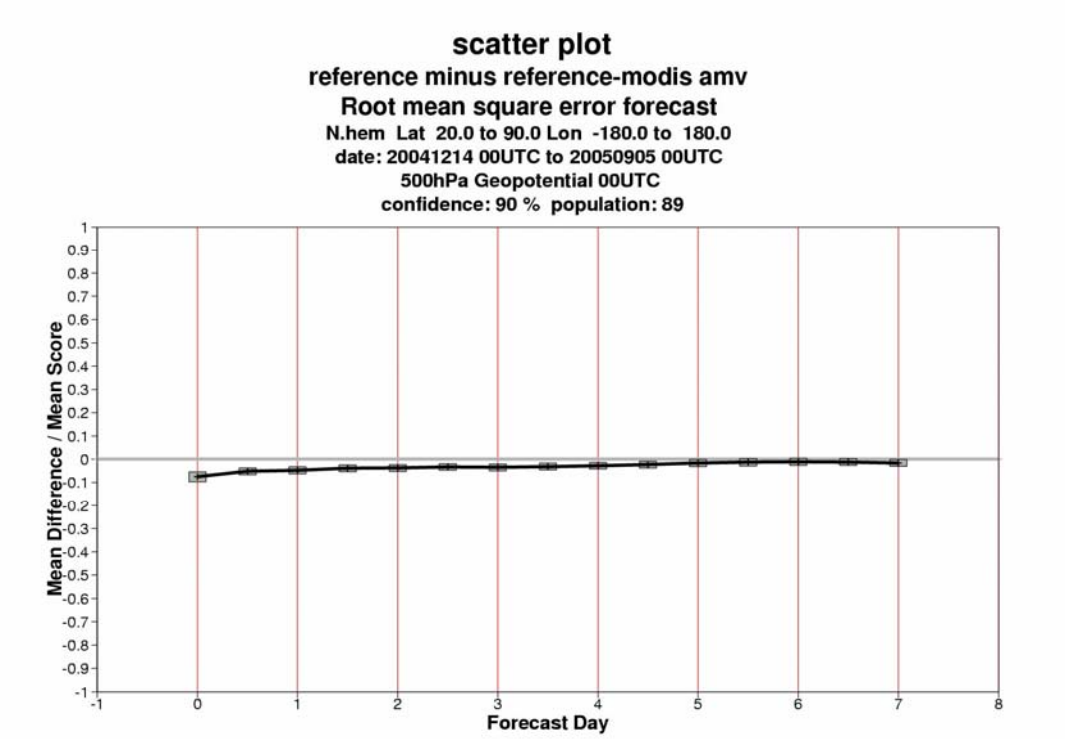

Figure E-4: Impact of modis AMVs on 500 hPa geopotential rmse for (Reference) and (Reference - AMVs (Modis) for the Northern Hemisphere

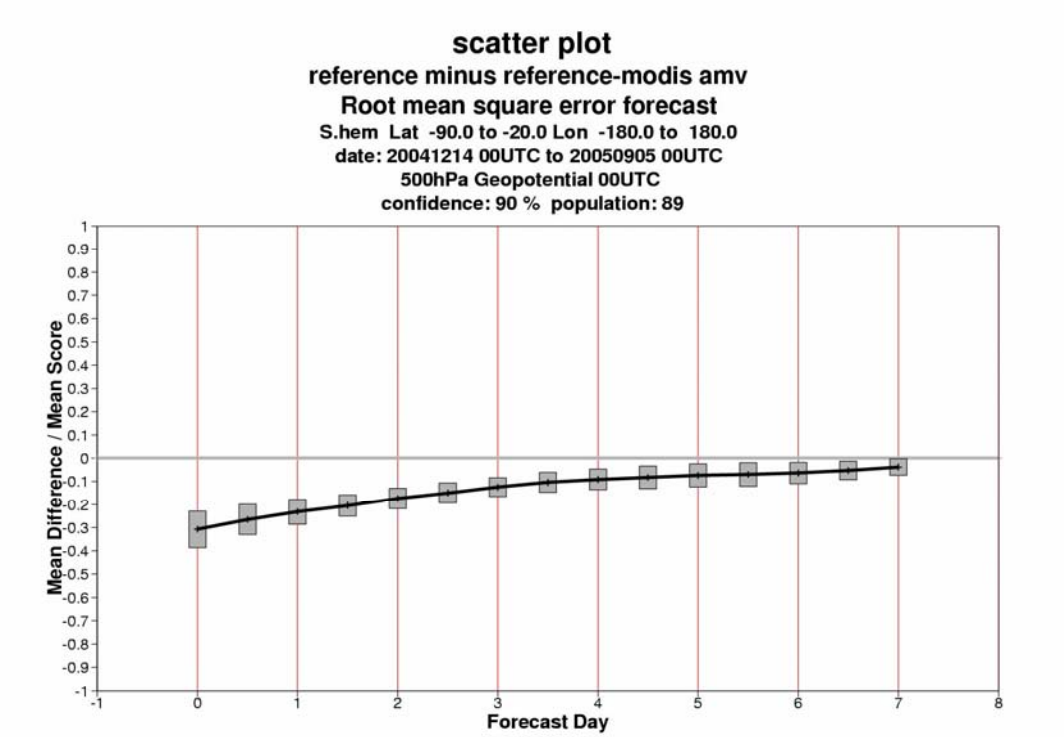

Figure E-5: Impact of modis AMVs on 500 hPa rmse geopotential for (Reference) and (Reference - AMVs (Modis) for the Southern Hemisphere

Appendix F

(ii) Comparsion of *AMV(REF)*+AIRS with *AMV(REF)*+(AMSUA and AMSUB).

An extra data assimilation experiment has been run for a summer and winter period. This experiment enables a more realistic comparison of microwave and infrared. AMSUA is mostly sensitive to temperature and AMSUB mostly humidity whereas AIRS is sensitive to both humidity and temperature. In this data assimilation experiment only used NOAA 16 AMSU A and AMSUB added to the ***AMV(REF)***.

The evaluation of forecasts has also been done using two variables and at various levels

500 hPa Geopotential impact of adding AMSUA/B and AIRS to the *AMV(REF)* in the Northern Hemisphere

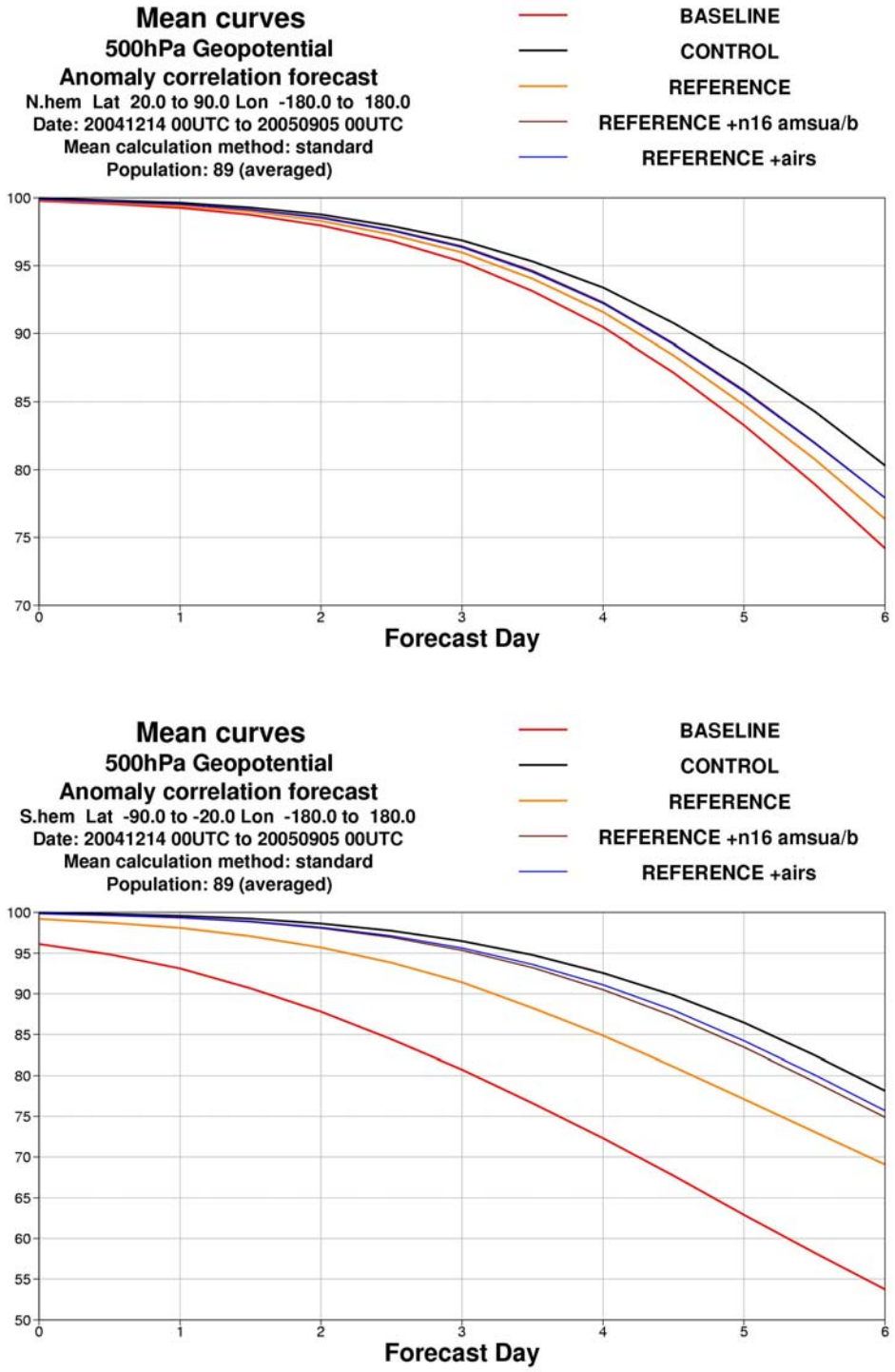

Figure F-1: Impact of all sensors (based on AMSUA(REF)) on 500 hPa geopotential height for (top) (AMSU(REF)+AMSUA+AMSUB) and (AMSU(REF)+AIRS) (20°–90°S) and (bottom) for the northern hemisphere (20°–90°N).

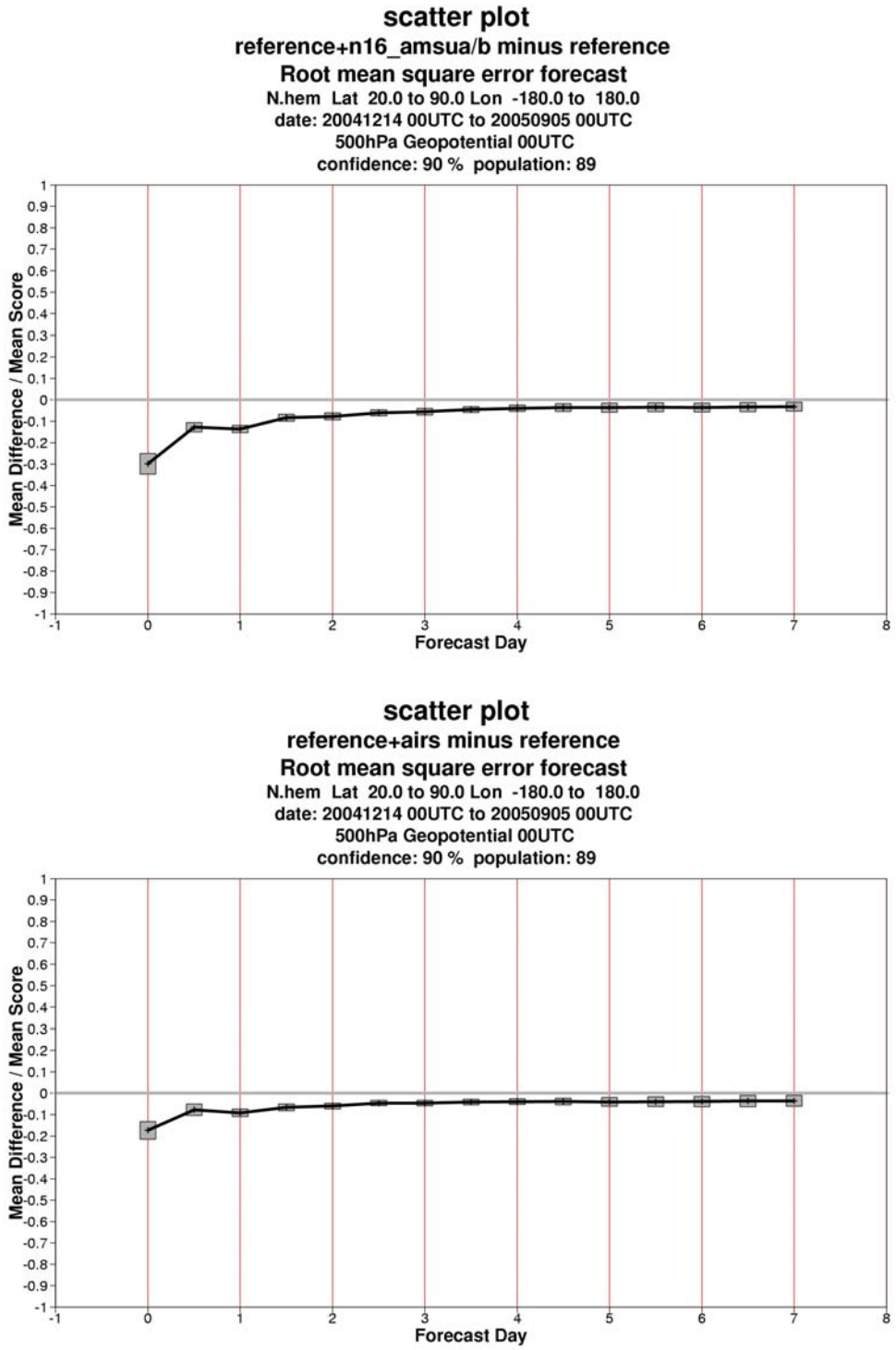

Figure F-2: Time series of normalized 500 hPa geopotential rmse differences between AMV(REF)+ AMSUA+B and AMV(REF) for forecast errors up to day 7 in the Northern Hemisphere(top) and AMV(REF)+ AIRS and AMV(REF) (bottom). Negative values indicate positive impact.

500 hPa Geopotential impact of adding AMSUA/B and AIRS to the *AMV(REF)* in the Southern Hemisphere

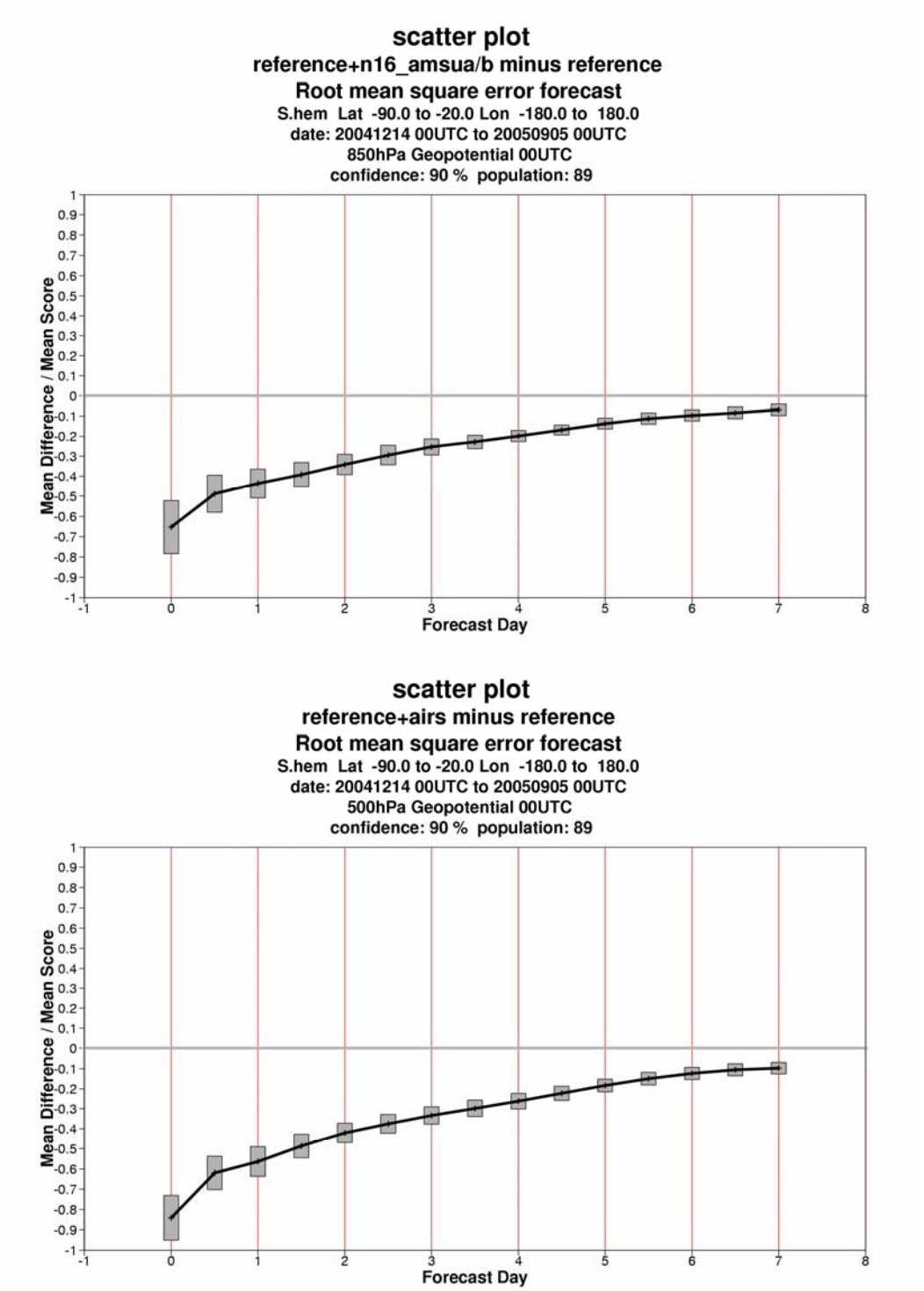

Figure F-3: Time series of normalized 500 hPa geopotential rmse differences between AMV(REF)+ AMSUA+B and AMV(REF) for forecast errors up to day 7 in the Southern Hemisphere(top) and AMV(REF)+ AIRS and AMV(REF) (bottom). Negative values indicate positive impact.

500 hPa Geopotential impact of adding AMSUA/B and AIRS to the *AMV(REF)*

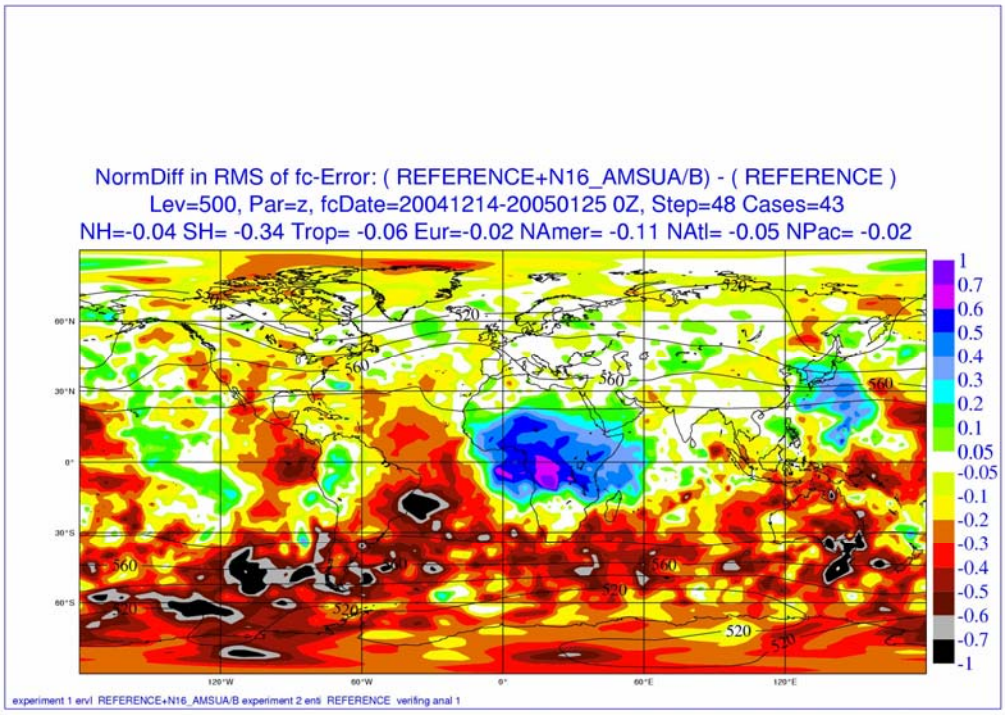

Figure F-4: Mean normalized 48-hour forecast error difference between AMV(REF)+AMSUA/B and AMV(REF) for the 500hPa geopotential height.

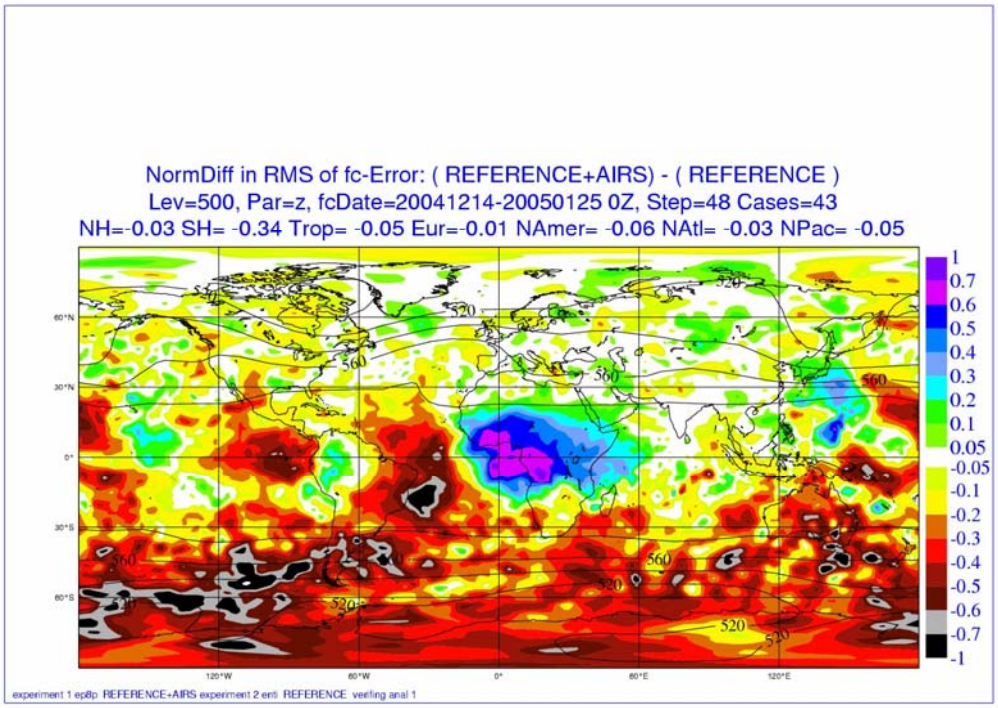

Figure F-5: Mean normalized 48-hour forecast error difference between AMV(REF)+AIRS and AMV(REF) for the 500hPa geopotential height.

Humidity impact of adding AMSUA/B and AIRS to the *AMV(REF)*

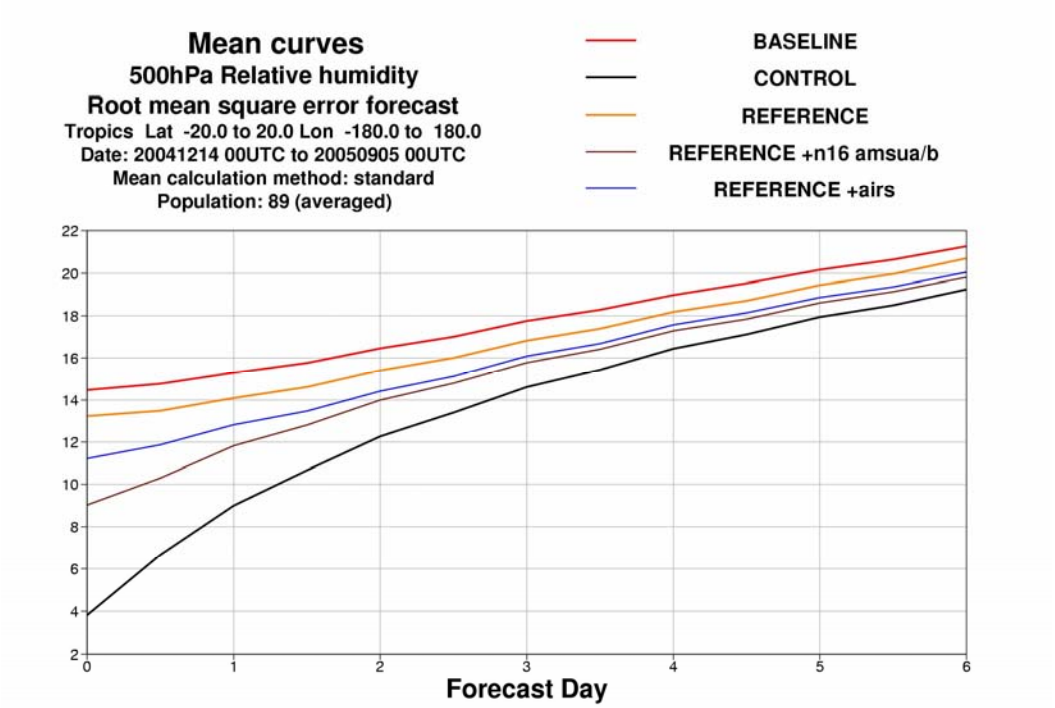

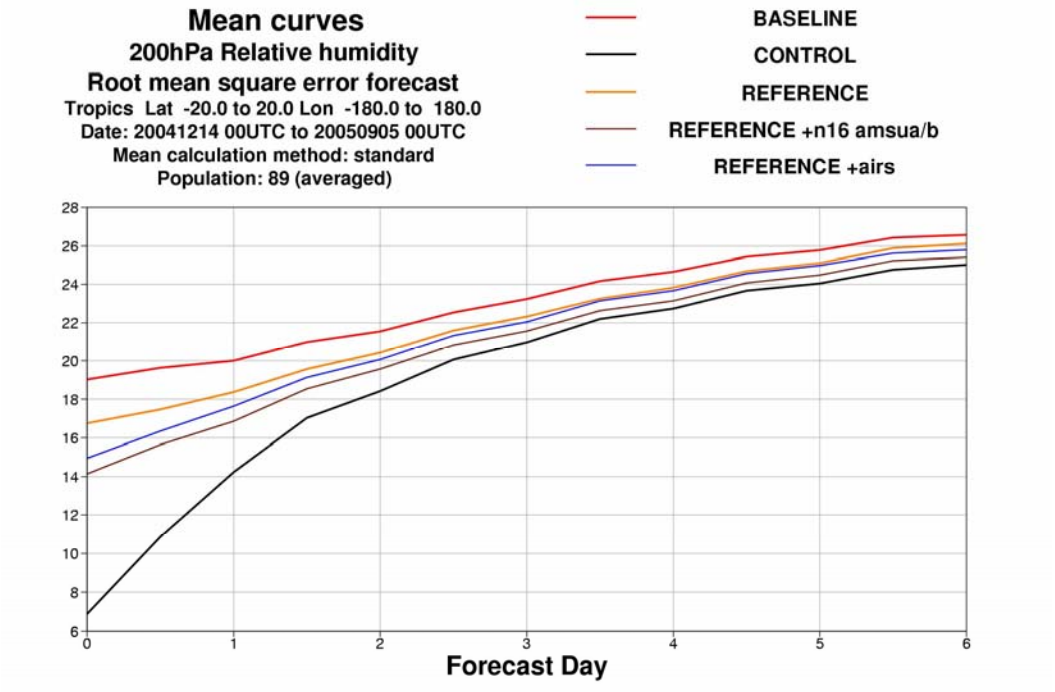

Figure F-6: Impact of all sensors (based on AMSUA(REF)) on relative humidity for (AMSU(REF)+AMSUA+AMSUB) and (AMSU(REF)+AIRS) for 500 hPa (top) and 200 hPa(bottom) for the tropics.

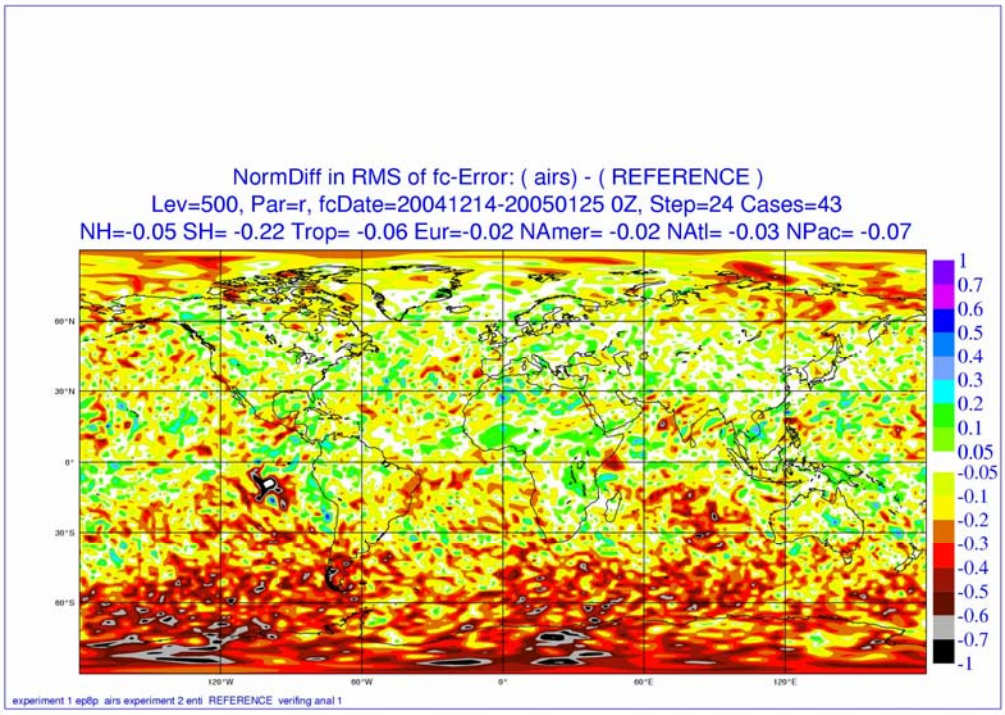

Figure F-7: Mean normalized 48-hour forecast error difference between AMV(REF)+AIRS and AMV(REF) for the 500hPa relative humidity.

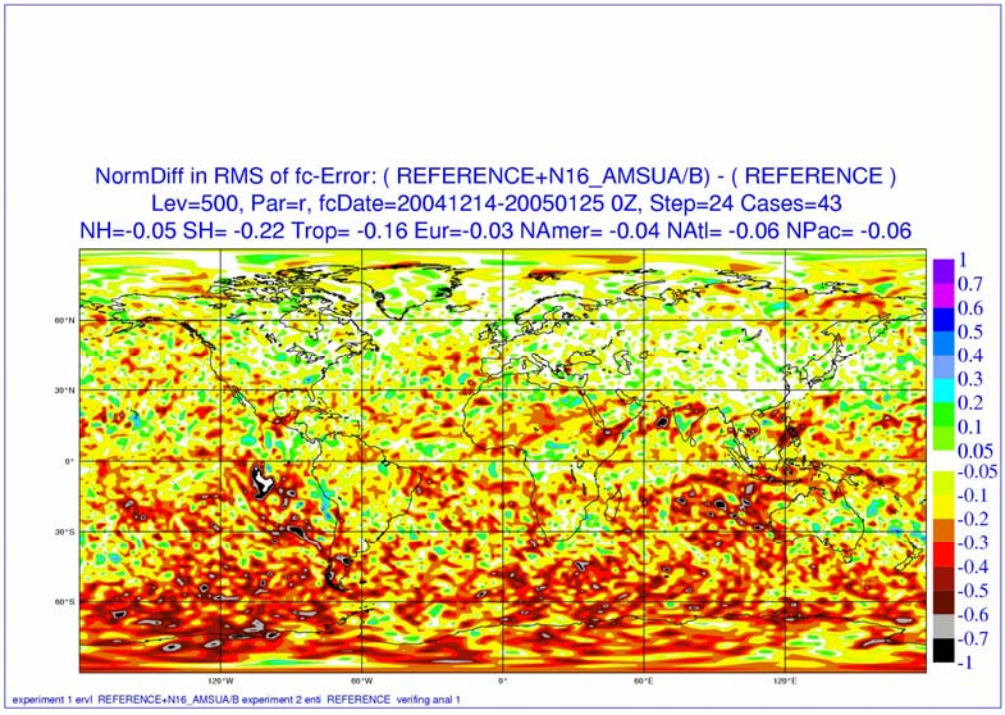

Figure F-8: Mean normalized 48-hour forecast error difference between AMV(REF)+AMSUA/B and AMV(REF) for the 500hPa relative humidity.

Appendix G

(iii) AIRS channels combinations:

Experiments were run (summer only) adding various AIRS channel combinations to the AMSUA(REF). In additional AIRS CONTROL denial experiment was all run.

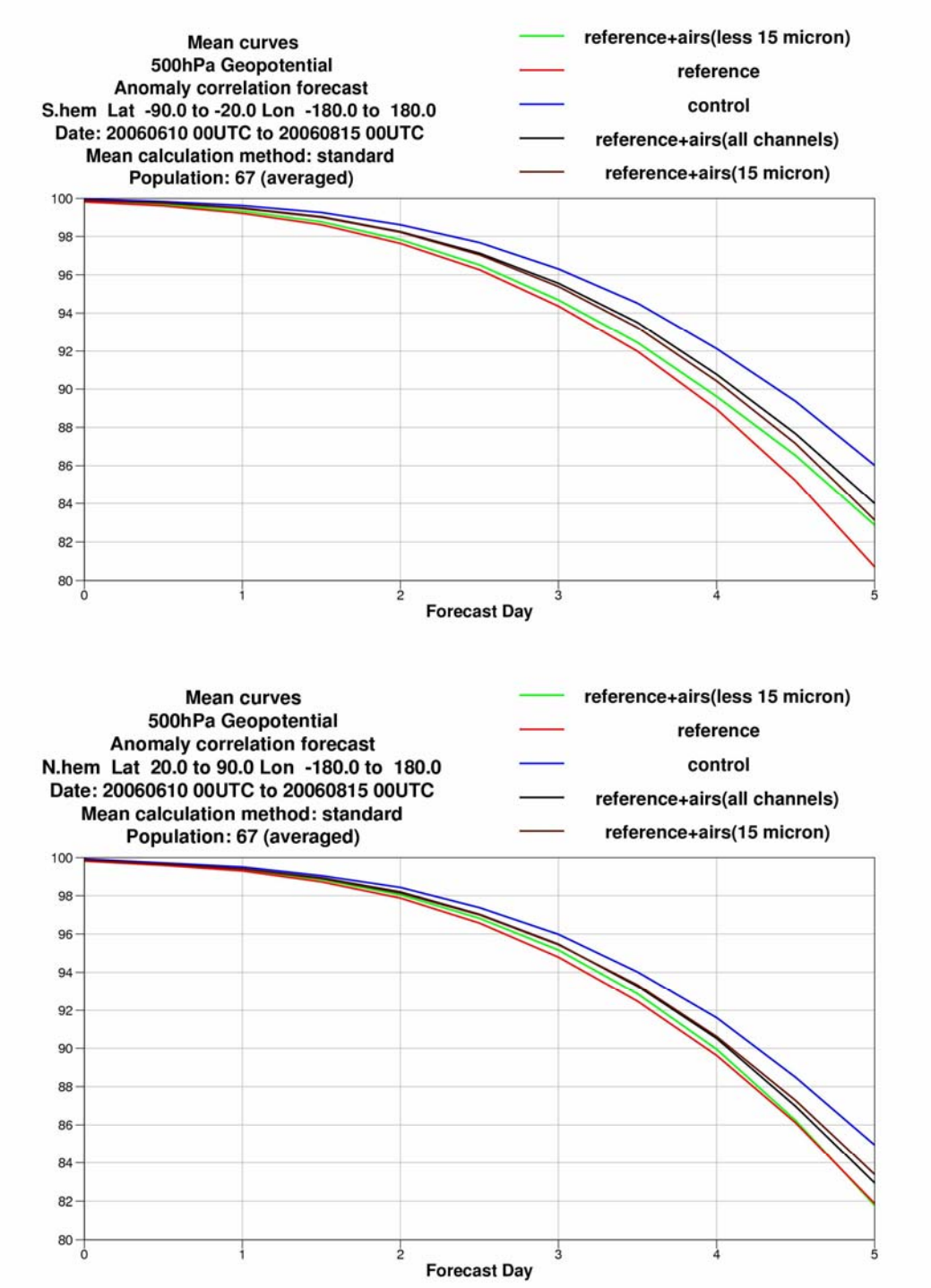

Figure G-1: Impact of AIRS (based on AMSUA(REF)) on 500 hPa geopotential height for (top) (AMSU(REF)+AIRS(all channels), (AMSU(REF)+AIRS(less 15 micron cannels) and (AMSU(REF)+AIRS(15 micron cannels) (20°–90°S) and (bottom) for the northern hemisphere (20°–90°N).

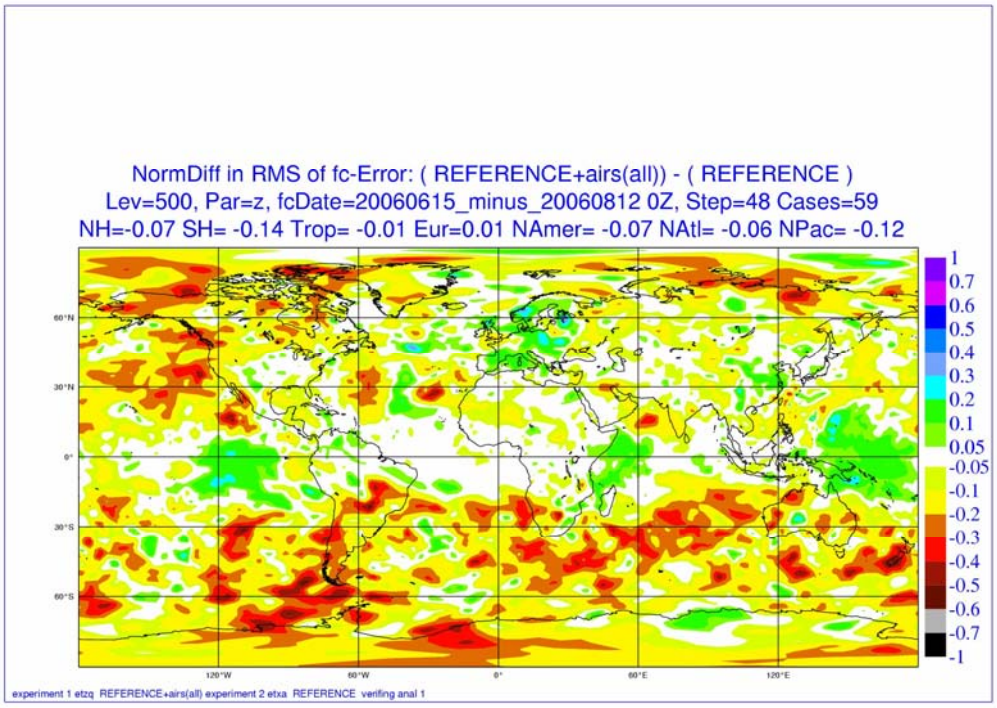

Figure G-2: Mean normalized 48-hour forecast error difference between AMV(REF)+AIRS(all) and AMV(REF) for the 500hPa geopotential height.

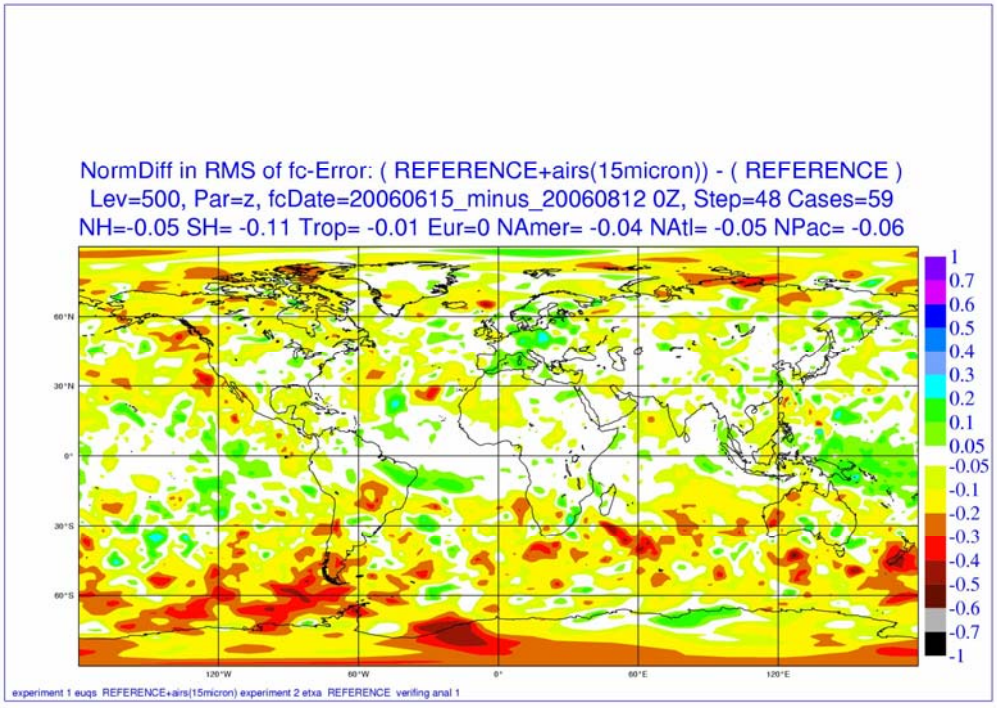

Figure G- 3: Mean normalized 48-hour forecast error difference between AMV(REF)+AIRS(15 micron) and AMV(REF) for the 500hPa geopotential height.

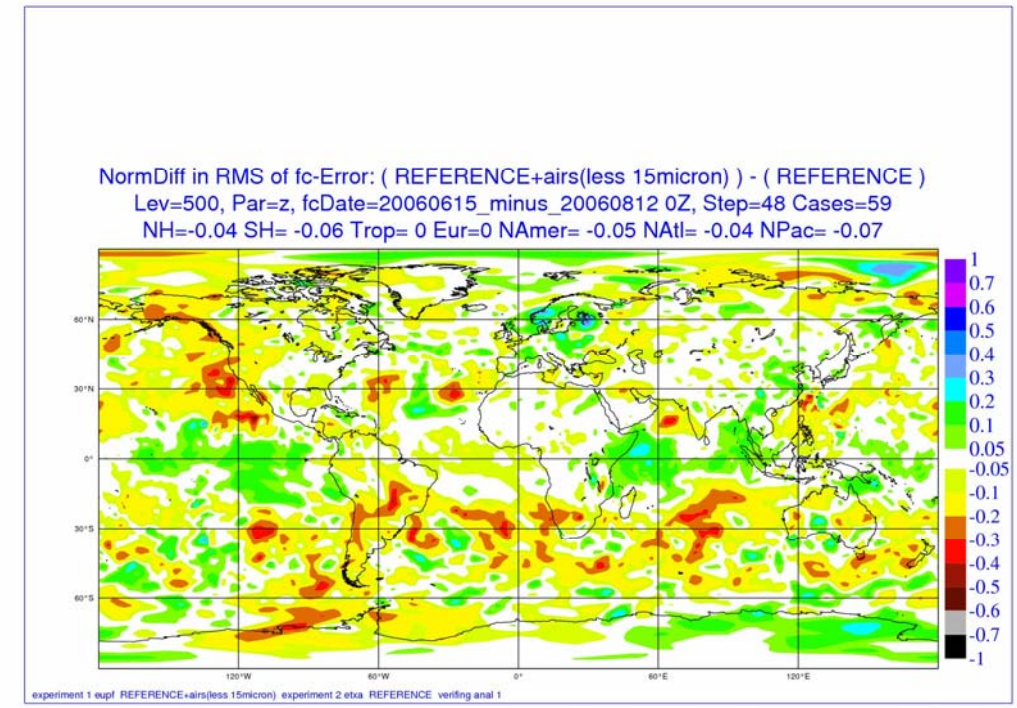

Figure G- 4: Mean normalized 48-hour forecast error difference between AMV(REF)+AIRS(less 15miron) and AMV(REF) for the 500hPa geopotential height.

Appendix H

(iv) SSMI clear and rainy impact AMSUA(REF):

Experiments were run (summer only) adding SSMI clear sky, SSMI rainy and SSMI (clear + rainy) to the AMSUA(REF). In additional two SSMI CONTROL denial experiments (SSMI rainy and SSMI clear) were run.

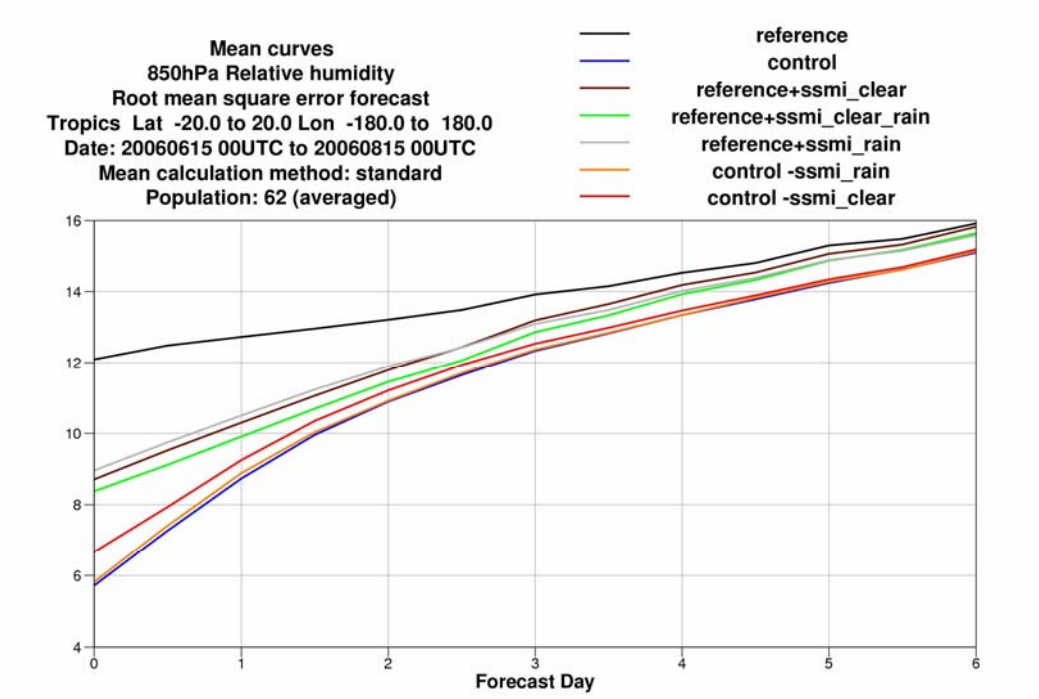

Figure H- 1: Impact of SSMI radiances (based on AMSUA(REF)) on 850 hPa relative humidity

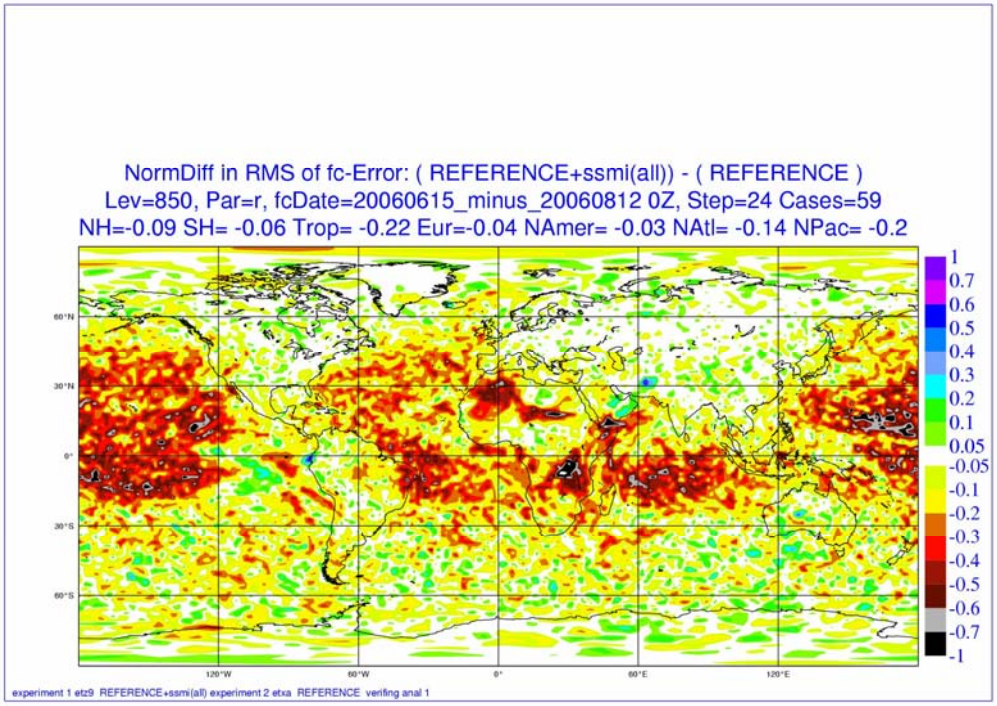

Figure H-2: Mean normalized 48-hour forecast error difference between AMSUA(REF)+SSMI(all) and AMSUA(REF) for the 500hPa geopotential height.

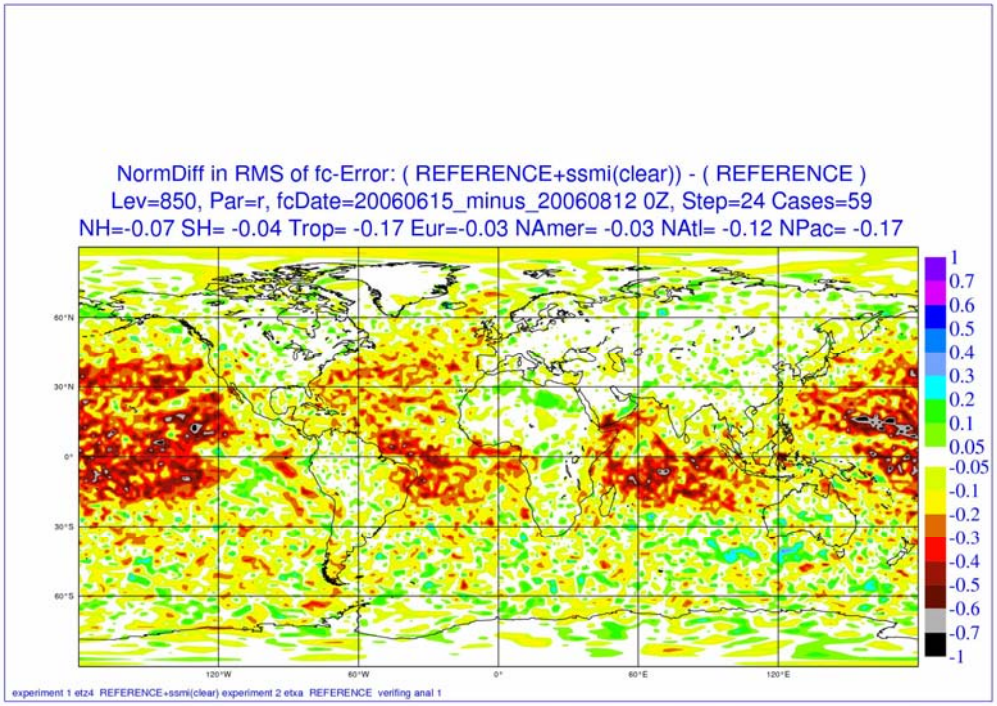

Figure H-3: Mean normalized 48-hour forecast error difference between AMSUA(REF)+SSMI(clear) and AMSUA(REF) for the 500hPa geopotential height.

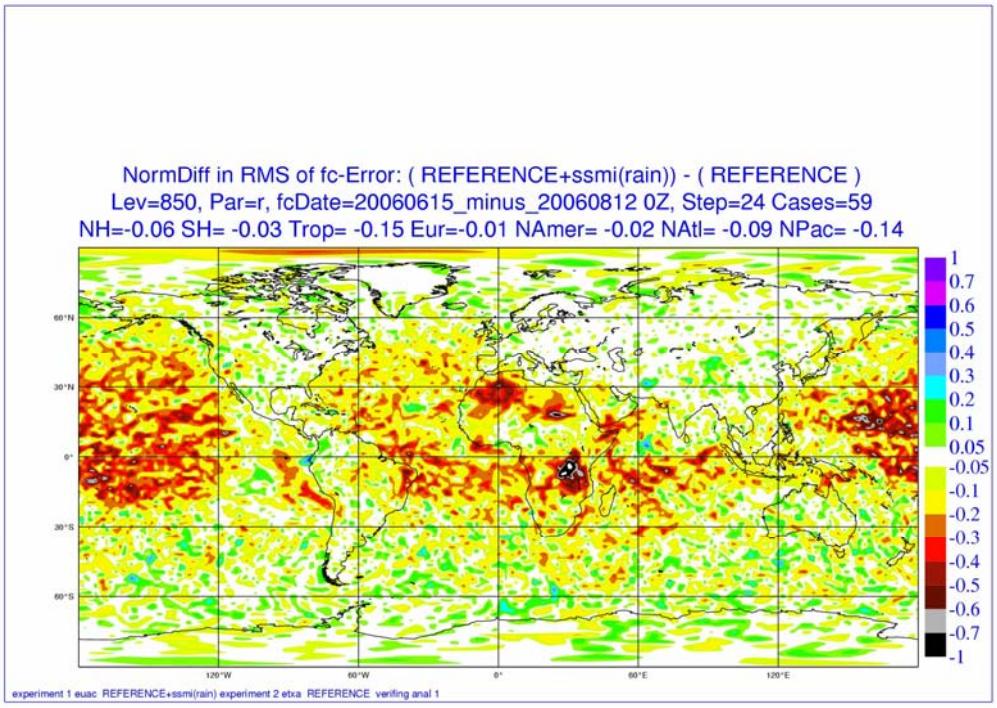

Figure H-4: Mean normalized 48-hour forecast error difference between AMSUA(REF)+SSMI(rain) and AMSUA(REF) for 850hPa relative humidity.

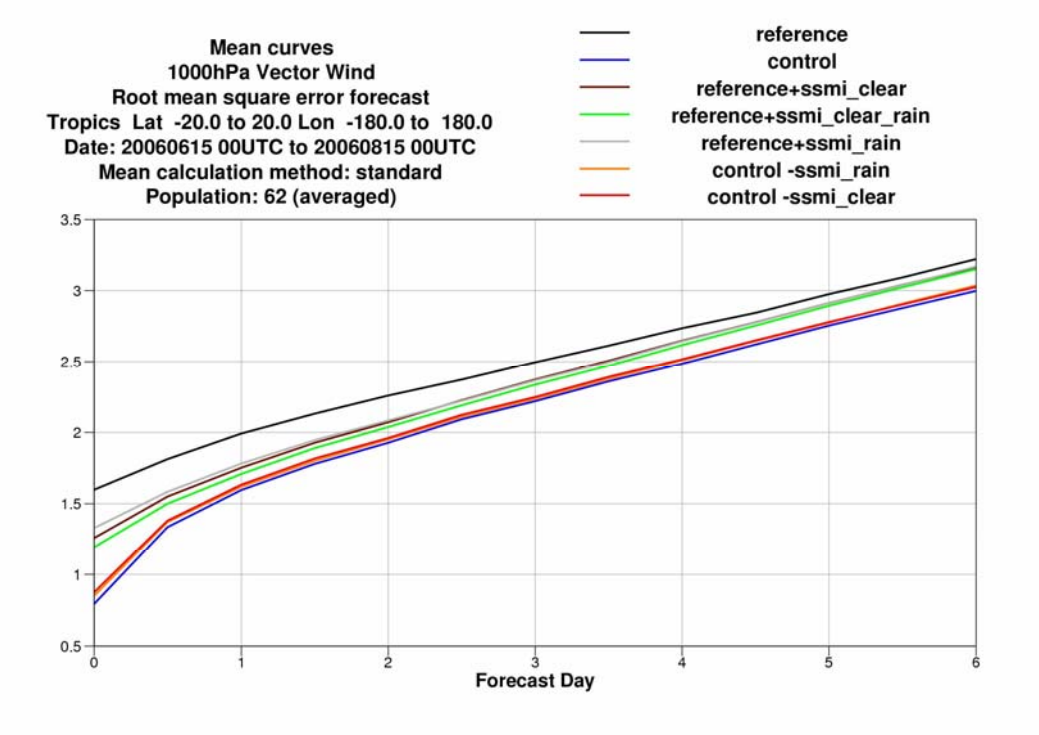

Figure H-5: Tropical impact of SSMI radiances (based on AMSUA(REF)) on 1000 hPa wind.

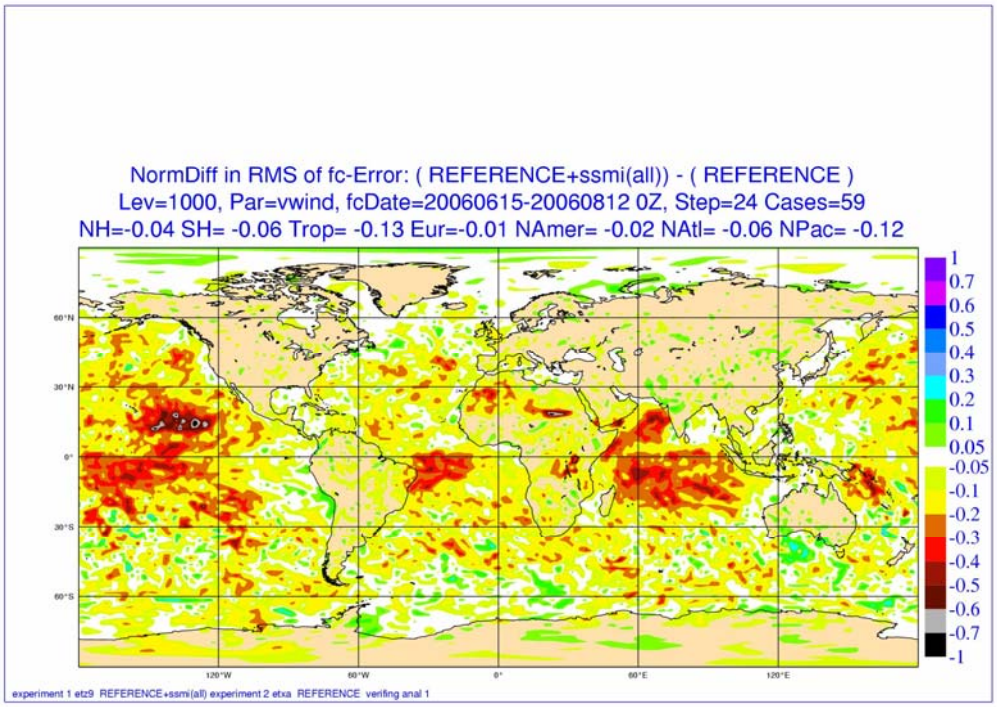

Figure H-6: Mean normalized 48-hour forecast error difference between AMSUA(REF)+SSMI(all) and AMSUA(REF) for 1000hPa wind.

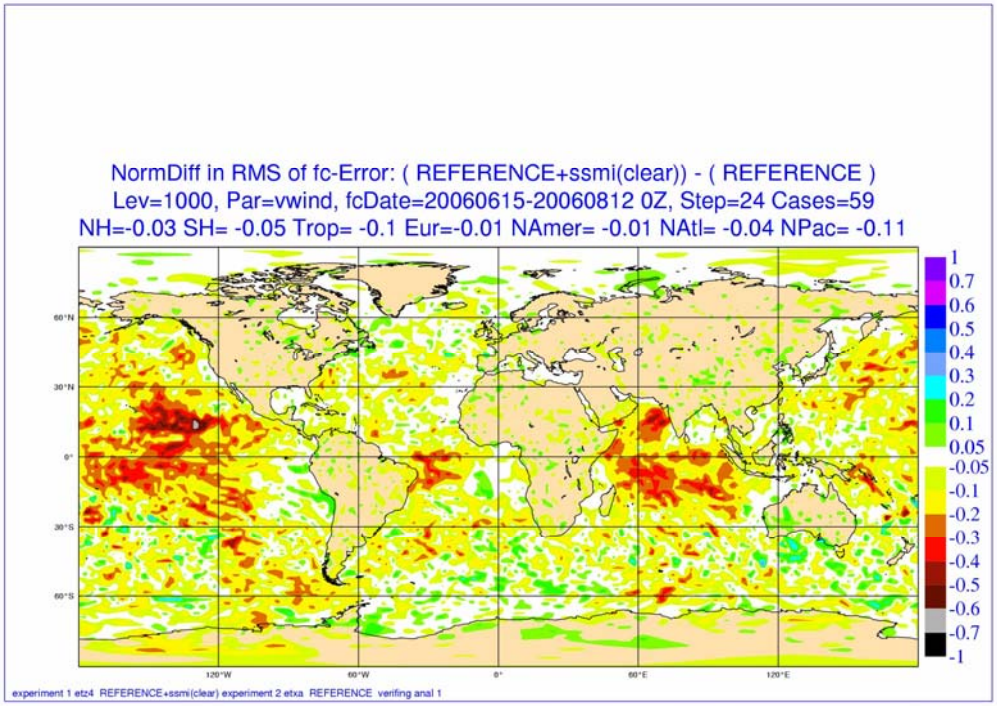

Figure H-7: Mean normalized 48-hour forecast error difference between AMSUA(REF)+SSMI(clear) and AMSUA(REF) for 1000hPa wind.

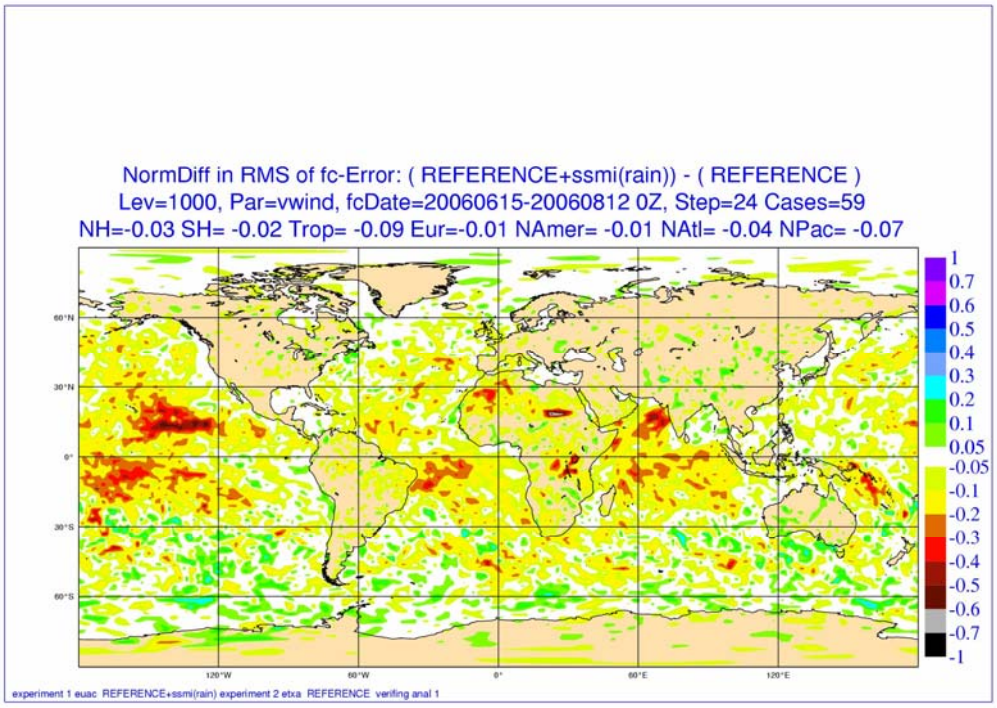

Figure H-8: Mean normalized 48-hour forecast error difference between AMSUA(REF)+SSMI(rain) and AMSUA(REF) for 1000hPa wind

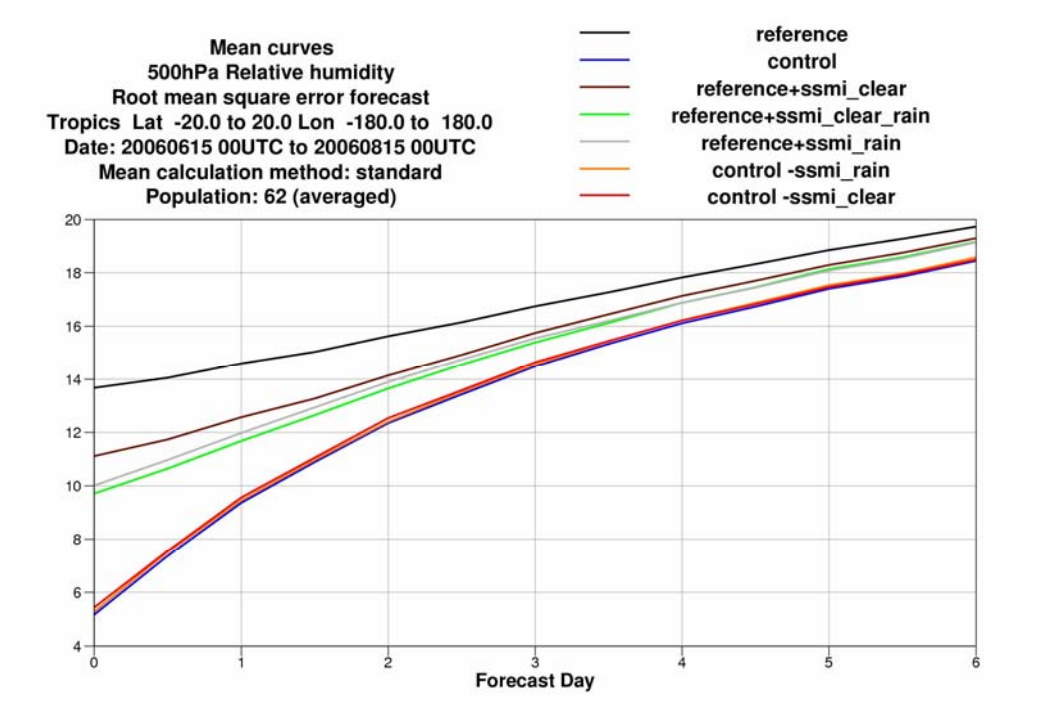

Figure H-9: Tropical impact of SSMI radiances (based on AMSUA(REF)) on 500 hPa relative humidity.

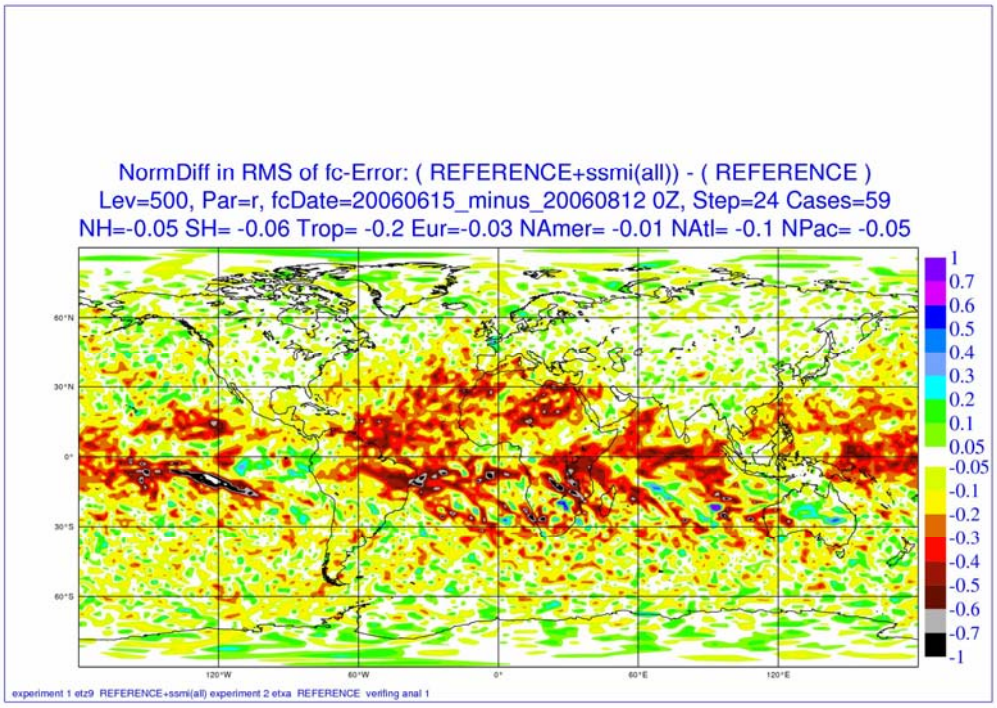

Figure H-10: Mean normalized 48-hour forecast error difference between AMSUA(REF)+SSMI(all) and AMSUA(REF) for 500hPa relative humidity.

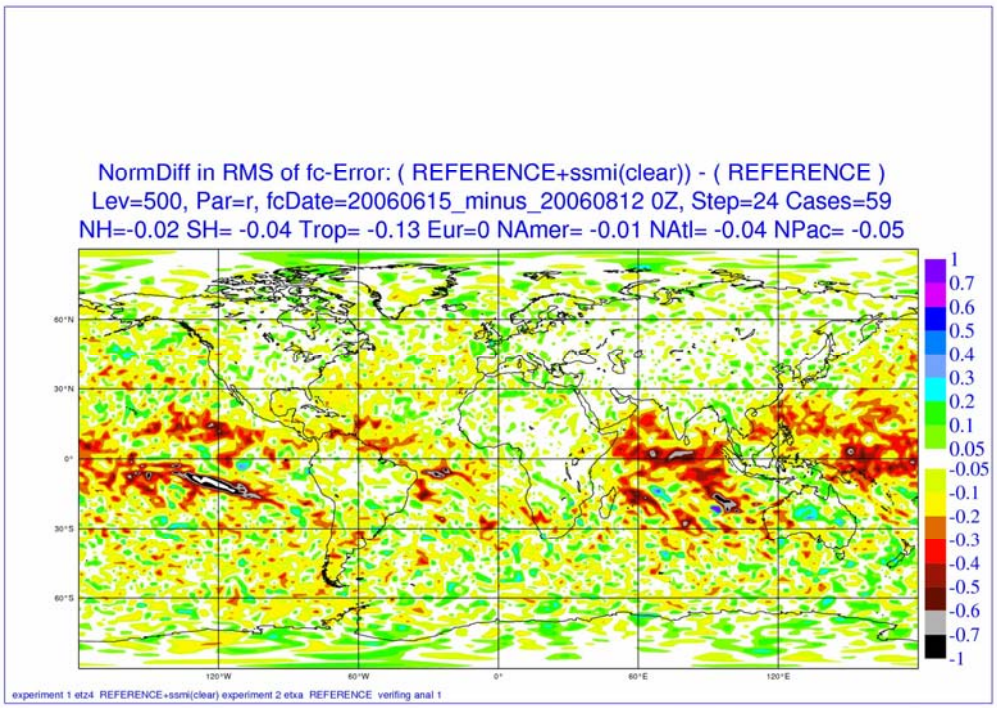

Figure H-11: Mean normalized 48-hour forecast error difference between AMSUA(REF)+SSMI(clear) and AMSUA(REF) for 500hPa relative humidity.

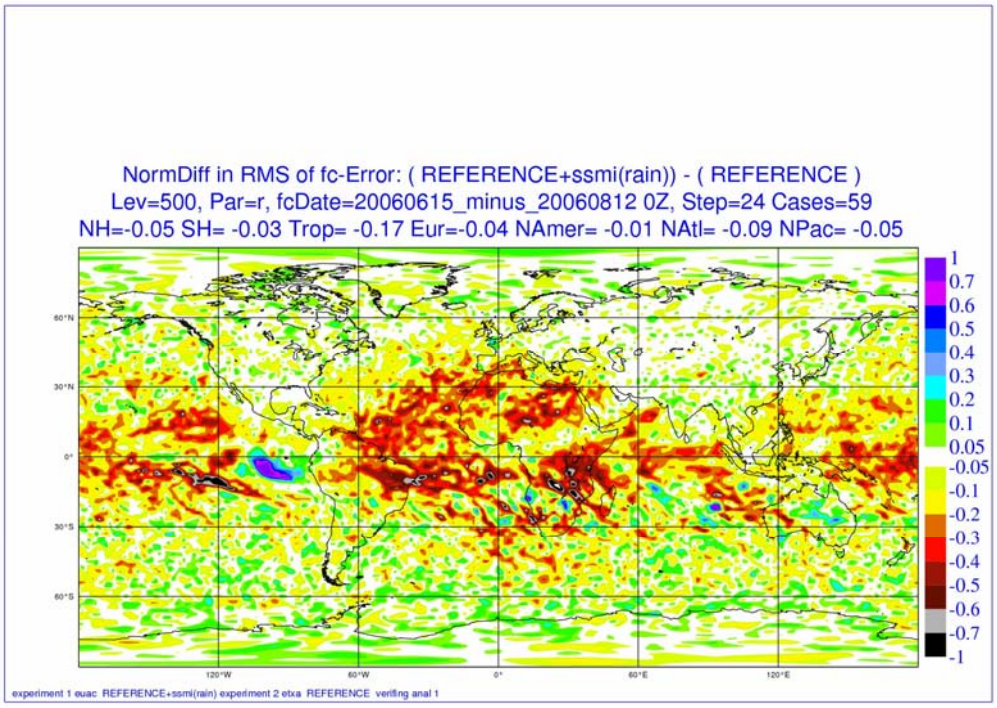

Figure H-12: Mean normalized 48-hour forecast error difference between AMSUA(REF)+SSMI(rain) and AMSUA(REF) for 500hPa relative humidity.

Appendix I

(v) AVHRR AMVs

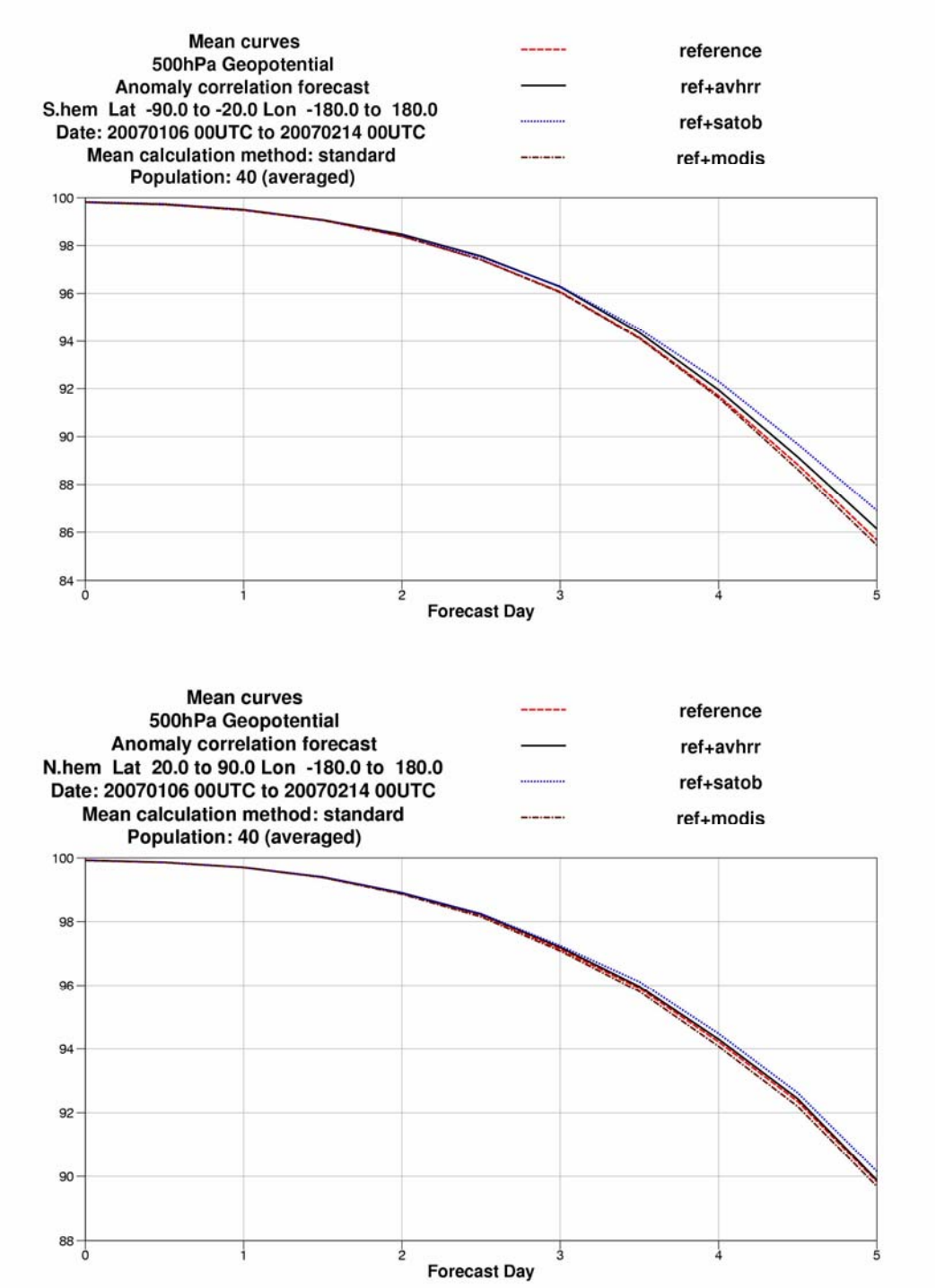

Figure I-1: Impact of AMVs (AVHRR,MODIS and GEO) (based on AMSUA(REF)) on 500 hPa geopotential height for southern hemisphere (top) (20°–90°S) and for the northern hemisphere (20°–90°N) (bottom).